Zeitschrift: IABSE reports = Rapports AIPC = IVBH Berichte
Band: 37 (1982)

Rubrik: Theme 6: Case studies of steel structures

THEME 6

Case Studies of Steel Structures

Etudes de cas de constructions en acier

Fallstudien von Stahlbauten

Leere Seite
Blank page
Page vide

Fatigue Design of the Honshu-Shikoku Bridges in Japan

Dimensionnement à la fatigue des ponts de Honshu-Shikoku au Japon

Ermüdungsfestigkeitsnachweis der Honshu-Shikoku Brücken in Japan

Y. MATSUZAKI
Director
Honshu-Shikoku Bridge Authority
Tokyo, Japan

H. SHIMOKAWA
Director
Honshu-Shikoku Bridge Authority
Tokyo, Japan

K. MURAKAMI
Chief of Design Division
Honshu-Shikoku Bridge Authority
Tokyo, Japan

SUMMARY
This report describes the fatigue design concepts used for the Honshu-Shikoku steel bridges. In particular, design load conditions, fatigue strength of welded joints and welding conditions in fabrication are discussed.

RESUME
Cet article décrit les bases du calcul à la fatigue utilisées pour le dimensionnement des ponts métalliques de Honshu-Shikoku. Il commente en particulier les charges de calcul admises, la résistance à la fatigue des assemblages soudés ainsi que les conditions de soudure lors de la fabrication.

ZUSAMMENFASSUNG
Der Beitrag beschreibt die Bemessungskonzepte, die bei den Honshu-Shikoku Stahlbrücken angewendet wurden. Insbesondere werden die Lastannahmen und die Ermüdungsfestigkeit geschweisster Verbindungen sowie die Schweissbedingungen während der Herstellung beschrieben.

1. INTRODUCTION

Of the Honshu-Shikoku bridges on the three routes, the bridges on the Kojima-Sakaide route are designed to be of the highway and railway combination type, and the total number of trains within 100 years of the service life is expected to be 9.5×10^6. And as the quenched and tempered high strength steel of 58 ~ 80 kg/mm^2 class which is rarely used for bridges will be used in the Honshu-Shikoku bridges considerably, the fatigue design is one of the important problems.

Therefore, Honshu-Shikoku Bridge Authority has conducted fatigue tests on many small specimens made with quenched and tempered high strength steel, furthermore, the Authority has conducted fatigue tests on large scale specimens of truss models and various kinds of welded joints made with quenched and tempered steel since 1975, by using a large scale fatigue testing machine specially provided which has a capacity of 400 tons dynamic loading.

This report describes the basic idea of the fatigue design of the Honshu-Shikoku bridges which has been decided as a result of consideration of such tests.

2. TRAIN LOAD

Construction of highway with four lanes and railway with four tracks (two for ordinary line cars and two for Shinkansen cars) are planned on the bridge on the Kojima-Sakaide route (Fig. 1), but the limit of simultaneous passage of two trains has been considered on the design of a suspension bridge in point of view of economy. The train load adopted is the same with the one provided in the design standards of the Japanese National Railways as shown in Fig. 2. As the loaded length of the influence line of the stiffning truss, tower and cable of suspension bridge is comparatively long, only the load of the pulled cars needs to be considered. Therefore, for simplification of calculation, it has been decided to design by the use of equivalent uniform loads.

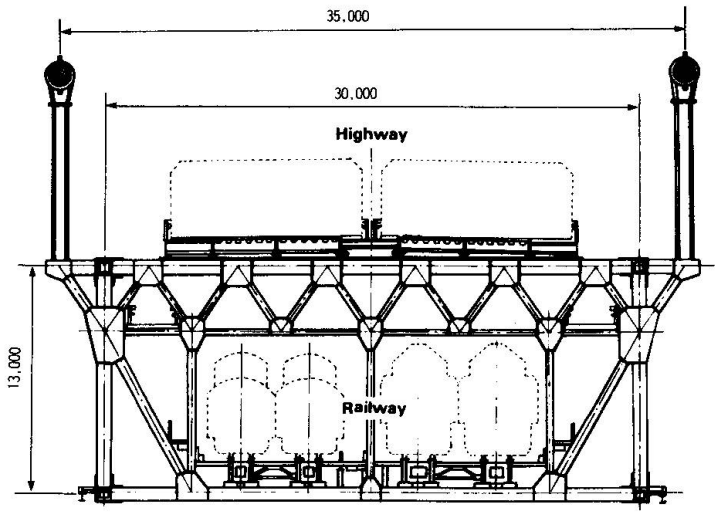

Fig1. Cross-Section of suspension bridge (Kojima-Sakaide Route)

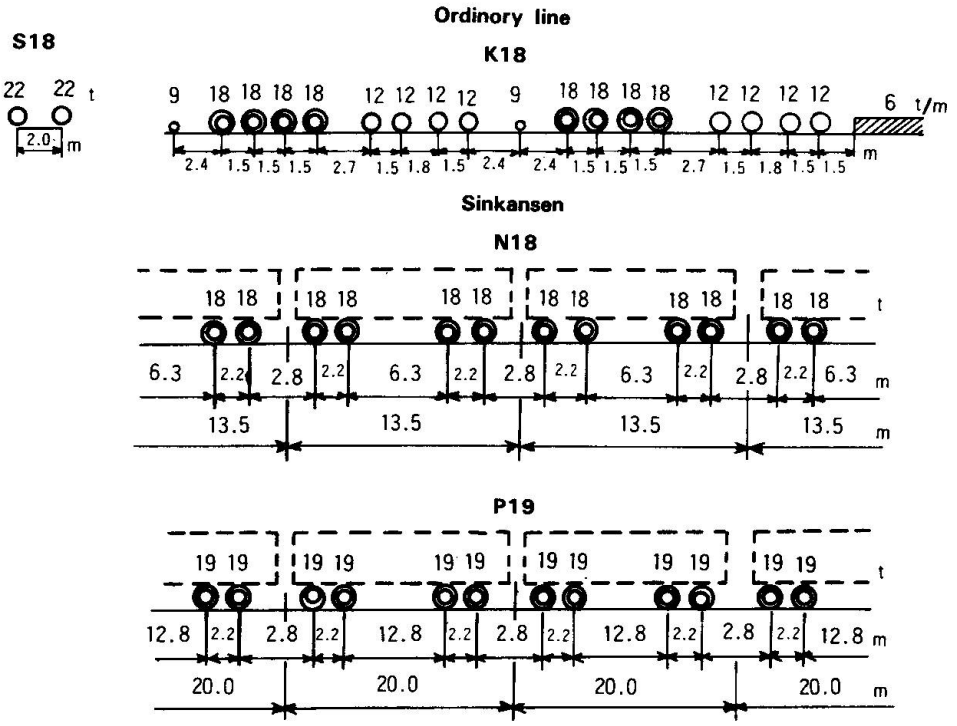

Fig. 2. Train load

2.1 TRAIN LOAD FOR STATIC DESIGN

The load of the Shinkansen has been set at an average load intensity of 3.8 t/m of a passenger train P19 (300 per cent of the passenger capacity) and the maximum loaded length at 320 m (train of 16 cars). The load intensity of the ordinary line has been set at 3.8 t/m, same as that of the Shinkansen line in consideration of real weights and wheel distance of cars etc., and the maximum loaded length at 370 m in consideration of the tractive force of locomotive engines.

2.2 TRAIN LOAD USED FOR FATIGUE DESIGN

It has been decided that 2.7 t/m per one track (maximum loaded length 400 m), average load intensity obtained by the modified Miner's rule, is to be used as the train load used for fatigue design in consideration of frequency distribution and the simultaneous passage of trains to be limited to a single track. And it has also been decided that, in order that the cumulative effects of the passage of various kinds of trains on a single and double tracks may be considered, allowable fatigue stress is to be modified according to the degree of cumulative effects.

3. ALLOWABLE FATIGUE STRESS

The joint details have been classified into four grades with respect to the normal stress and three grades with respect to the shearing stress based on many test data and the fatigue strength, and the allowable fatigue stress at 2×10^6 loading cycles has been fixed for each of grades.

Furthermore, in order that the cumulative effects of various trains within 100 years of the service life may be considered, the S-N curve of each grade has been fixed and modified coefficients of allowable fatigue stress have also been fixed by using the modified Miner's rule.

3.1 CLASSIFICATION OF JOINTS

Table 1 shows the classification of grades of representative joints and Table 2 the allowable fatigue stresses.

Table1 Classification of joint details

Joint details	Category	
	41~53kg/mm² Class Steels	58~80 kg/mm² Class Steels
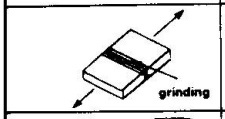	A	
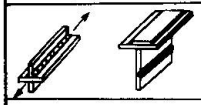	A	B
	C	C * / D
	C	

* Regular bead shape of fillet weld

Table2. Fatigue allowable stress (R=0)

Category	Fatigue allowable stress
A	15.3 kg/mm²
B	12.75 kg/mm²
C	10.5 kg/mm²
D	8.0 kg/mm²

The test results of longitudinal groove welded joints made with quenched and tempered steel indicated that the fatigue strength of the large scale truss model specimens was considerably low due to welding defects (blowholes etc.) at the corner welding of truss chord member. And the tests of longitudinal groove welded and box section specimens revealed that the fatigue strength of the box section specimens was considerably lower than that of the longitudinal groove welded specimens. The limits of defects of longitudinal groove welded joints have been fixed by these test results and the longitudinal groove welded joints made with quenched and tempered steel has been classified as the category "B" shown in Table 2.

With respect to transverse fillet welded joint, the results of tests indicated that the fatigue strength with large specimens tends to be lower than small ones. In the case of quenched and tempered steel, since the use of low hydrogen electrodes for welding makes bead convex and reduces the fatigue strength, the category has been classified as "C" same as mild steel on condition of use of improved electrodes to make good bead shape of fillet weld.

3.2 S-N CURVE

The fatigue tests of large specimens revealed that fatigue cracks are formed at an extremely early stage of the repeated load and nearly all their lives until failure are spent for the growth of fatigue-cracks. The curve of the S-N line to be used for design will be assumed $-1/m$ (m means the fixed number of the Paris's rule). Judging from the many test data in Japan, the value of m was fixed at 4 to mild steel (41 ~ 53 kg/mm^2 grade) and 3 to quenched and tempered steel (58 ~ 80 kg/mm^2 grade). Then, the S-N curve (Fig. 3) of each grade has been fixed on the assumption that the value of ΔK_{th} (the threshold stress intensity factor for fatigue-crack propagation) is zero.

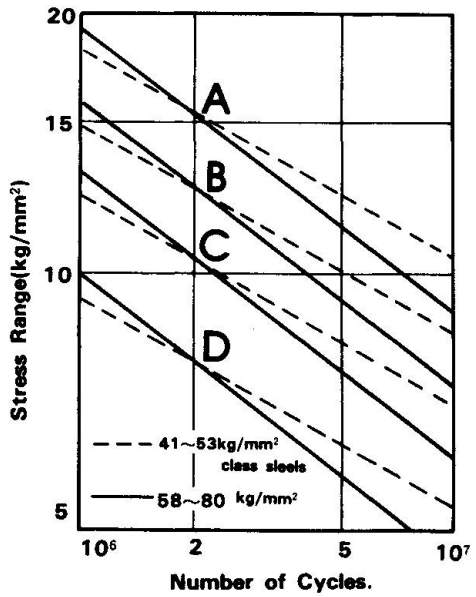

Fig.3. SN curves

4. STANDARDS FOR FABRICATION OF STEEL BRIDGES

Results of fatigue tests of large specimens have been reflected on the standards for fabrication of bridge members. On these standards, the accuracy and cleanness of the groove and the limits of welding defects have been fixed, furthermore the welding tests on the chord members having two panels with actual scale of bridge should be obliged prior to the fabrication of bridge. With respect to the longitudinal groove welding, it has been introduced that defects in the root section are to be inspected by splitting and exposing the section, and with respect to the fillet welding to install diaphragms, it has been introduced that the shapes should be examined. And also welding conditions must be determined by each fabrication plant.

5. POSTSCRIPT

This report is a summary of studies and discussions by the committee for structural problems of Honshu-Shikoku bridges in Japan Society of Civil Engineers. The authors wish to express their appreciation to each member of the committee.

References

(1) Japan Society of Civil Engineers: Fatigue Design for Honshu-Shikoku Bridges, 1974, 1980 and 1981 (written by Japanese)

(2) Tajima J., Okukawa A. and Tanaka Y.: Fatigue Design Criteria on Honshu-Shikoku Bridges, 10th Congress of IABSE, Sept. 1976.

(3) Japan Society of Civil Engineers: The Specification of Steel Railway Bridge, 1974 (written by Japanese)

(4) Design Standard for Superstructures, June 1980, Honshu-Shikoku Bridge Authority (written by Japanese)

Fatigue Evaluation of Existing Steel Highway Bridges

Evaluation de la fatigue dans les ponts-routes existants en acier

Abschätzung der Ermüdungsfestigkeit bestehender Strassenbrücken aus Stahl

IVAN J. DVORAK
Chief Bridge Engineer
Teng and Associates, Inc.
Chicago, IL, USA

DONALD C. ZIMMER
Chief Engineer
IL State Toll Highway Auth.
Oak Brook, IL, USA

SUMMARY
In 1978 numerous fatigue cracks were found in various components of a major interchange structure carrying expressway traffic in the Metropolitan Chicago Area. As a result of these findings, a project dealing with an evaluation of accumulated fatigue damage and predictions of fatigue life expectancy of all steel bridges within this system was initiated.

RESUME
En 1978 de nombreuses fissures de fatigue furent trouvées dans différents éléments de la structure d'un important échangeur de trafic de la région de Chicago. Conséquence de ces découvertes, une étude fut entreprise afin de permettre l'évaluation des dommages cumulés de fatigue ainsi que l'espérance de vie de tous les ponts réalisés selon ce système.

ZUSAMMENFASSUNG
Im Jahre1978 wurden an verschiedenen Teilen einer wichtigen Brückenkonstruktion über eine Autobahn im Gebiet von Chicago Ermüdungsrisse festgestellt. Diese Feststellung führte zu einem Forschungsprojekt, welches den akkumulierten Schaden und die zu erwartende Lebensdauer aller Stahlbrücken des Autobahnsystems Illinois untersucht.

INTRODUCTION

Thirty-three cracks in bent connection plates and brackets supporting expansion bearings were found during inspection of Bridge Structures No. 209 and 210, carrying the Tri-State over the East-West Illinois State Toll Highway. The useful life of these original components was exhausted after 20 years in service, and the safety of these structures was questioned.

Detailed analysis and field testing have identified most of the cracks as having been caused by fatigue.

As a result of these findings, a project dealing with evaluation of accumulated fatigue damage and prediction of fatigue life expectancy of all steel bridges owned and maintained by Illinois State Toll Highway Authority was initiated.

This project consisted of the following: review of drawings, preparation of inventory sheets for each structure, design stress range calculation, research of loading history of these structures, instrumentation of selected details, evaluation of actual stress ranges, calculations of accumulated fatigue damage and fatigue life expectancy, field inspection of selected details, and recommendations of retrofitting methods.

Relatively inexpensive retrofitting is possible when the early discovery of fatigue cracks is made.

2. FATIGUE EVALUATION OF 82 STEEL HIGHWAY BRIDGE

2.1 Preliminary Review

The 82 steel bridges at 50 different sites on the Tollroad System were reviewed and analyzed according to current AASHTO Specifications. The findings were presented in one or two-page reports called "Fatigue Location Inventory."

The fatigue stress category and its allowable stress range for each location were determined according to the design detail and the applicable repetitive loading and compared with the design stress range determined by preliminary analysis.

As a final step in this phase, a table was prepared which summarizes the findings of the "Fatigue Location Inventory" and which lists all reviewed steel bridges with the following information:

a) Structure number and location of structure;
b) Loading case - number of cycles;
c) Stress range due to the design load;
d) Category of allowable fatigue stress range at the section where the stress range was calculated;
e) Allowable stress range for the particular category;
f) Overstress, based on the design load, expressed in percentage of allowable stress range; and
g) Remarks.

2.2 Detailed Analysis of Ten Structures

Only ten structures were selected for detailed analysis due to the limited scope of this project. Overstress based on the design load, expressed in percentage of allowable unit stress, and a location of the details in respect to the positive or negative moment region were the only criteria used in selection of these structures. It is known that continuous span structures, consisting of steel stringers and concrete decks which were designed as non-composite, do actually act as a composite section provided the bond between concrete and steel beam is not destroyed. Therefore, the structures with details susceptible to fatigue crack located in negative moment region were not selected for further detailed analysis because the actual stresses would be only a fraction of design stresses calculated on assumption of non-composite section.

Only the structures with highest overstress and with the details susceptible to fatigue cracks located in positive moment region were selected (Table 1).

STR. NO.	LOADING CASE	DESIGN STRESS RANGE N/mm2	FATIGUE STRESS CATEGORY	ALLOWABLE STRESS RANGE N/mm2	% OVERSTRESS	REMARKS
1147, 1148	I	131 80	D E'	48 18	272 444	Low Traffic Volume
367, 368	I	83 80	D E'	48 18	172 444	(+) Moment Region
355, 356	I	84 46 61	D E E'	48 34 18	175 135 339	Intermittent Fillet Welds
209, 210	I	52	E'	18	289	(+) Moment Region
191, 192	I	102 50 83	D E' E'	48 18 18	212 277 461	(+) Moment Region (-) Moment Region

TABLE 1

All of these bridges were built between the years 1958 and 1971. The typical cross section is shown in Figure 1. The stringers were from wide flange rolled sections. The simple or continuous spans were from 18.9 m to 31.4 m.

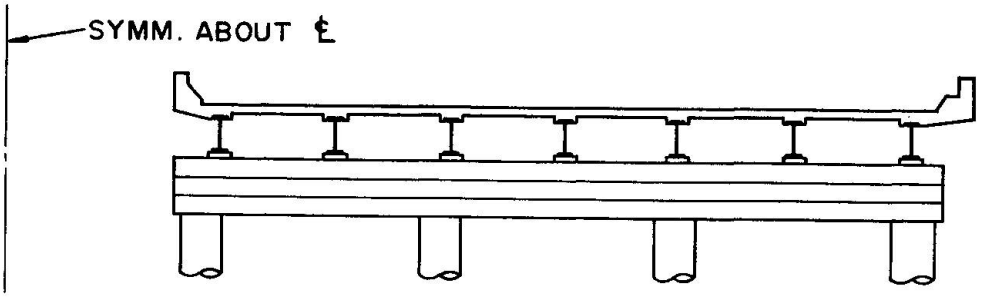

Figure 1 -- Typical Section

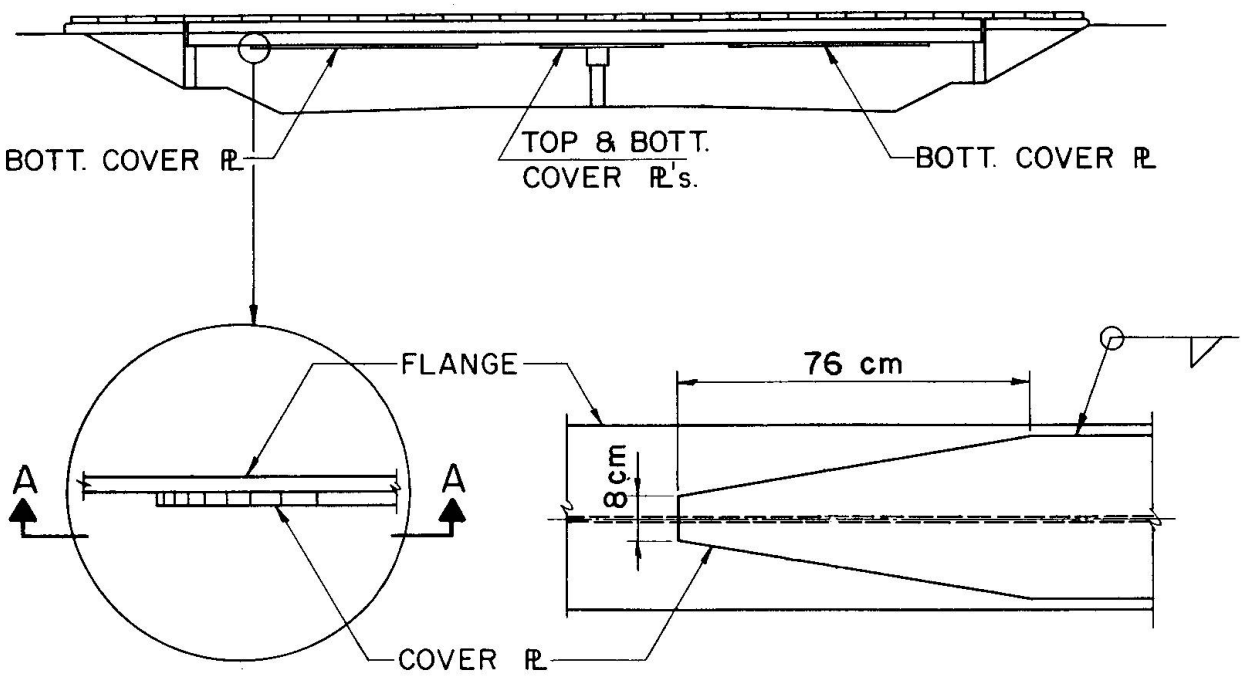

Figure 2 -- Typical End Detail of Welded Cover Plate

All structures selected for detailed analysis have welded cover plates. Their end details belong to Category E' with allowable 18 N/mm^2 stress range for over 2,000,000 cycles.

The typical end detail of welded cover plate is shown on the Figure 2.

Stress ranges for these structures were analyzed by the computer at various desired locations. The overstress, based on the design load and expressed in percentage of allowable unit stress, ranges from 444 percent on structures No. 1147 and 1148 to 277 percent on structures No. 191 and 192.

2.3 Strain Measurement

Based on the detailed analysis, structures No. 355, 356, 367, and 368 were selected for instrumentation. The purpose of such testing was to measure strains due to the actual live load and to determine actual stress ranges in the detail under investigation. These actual stress ranges and estimated number of their occurrences were used to determine the cumulative fatigue damage of these structures and to estimate their useful life expectancy. The strains were recorded continuously for 24 hours; field data from the gages was conditioned and recorded on a Sangamo 3500 magnetic tape recorder. The recorded analog data was replayed on an Analog-to-Digital conversion system.

During processing time, the time history data of the strains which enter as analog values is converted to digital values and written on a digital magnetic tape. At the start of processing of any given vehicle traversal, a special identifying data block is written which includes, among other parameters, a count of the particular vehicle. This block labels and separates the data representing individual vehicle crossings. Thus, a compressed reel of data written in digital form is produced which contains only the crossing information and which has been stripped of the vast amount of zero traffic time.

This data is then further processed by Peak-to-Peak Method. The individual groups of data for each specific crossing are checked to obtain the strain range values. The initial values of all gages are used as an arbitrary zero, and succeeding strain values are checked for the maximum and minimum values which are retained. The strain range is then the algebraic difference of these two values.

The range of strain so determined for each gage then is used to add one count to a table of the number of occurrences at given levels of strain for each gage.

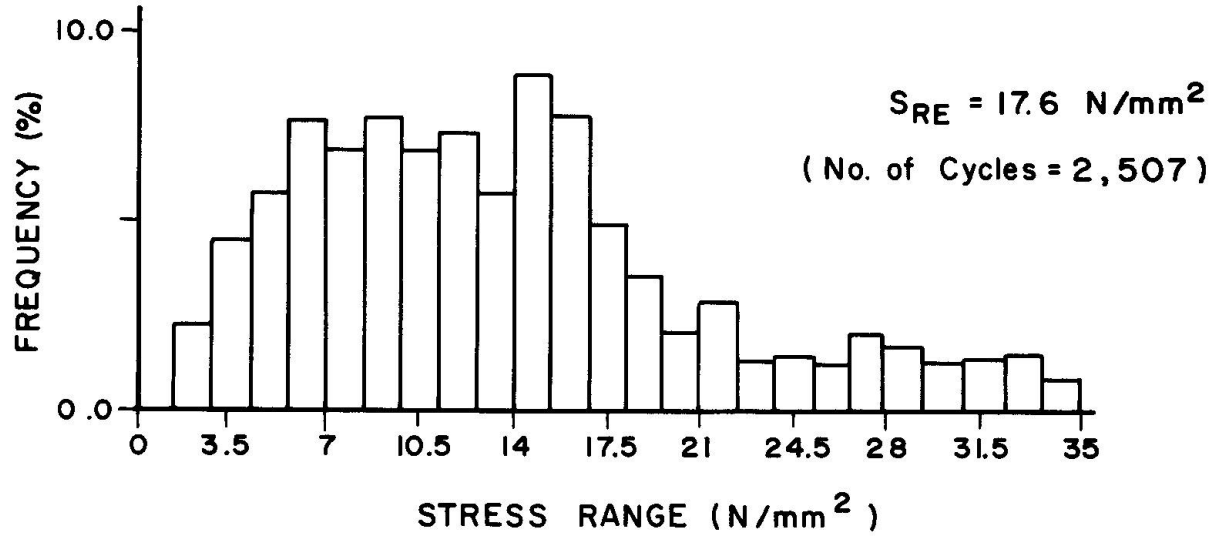

Figure 3 -- Histogram of Stress Range Spectrum for Gage No. 6

The processed strain data was used in preparation of stress range histograms. Figure 3 shows the stress range histogram for stresses recorded at gage No. 6, recorded on the Bridge No. 367.

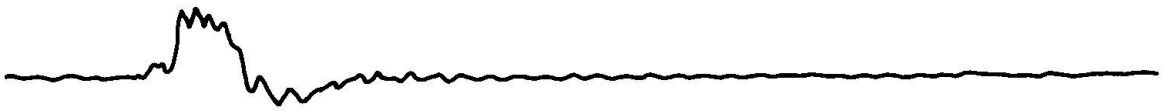

Figure 4 -- Typical Strain Response at Gage No. 6

Figure 4 shows a typical record of strain measured on gage No. 6. A certain percentage of the recorded strains on gage No. 6 were observed to look like those shown on Figure 5.

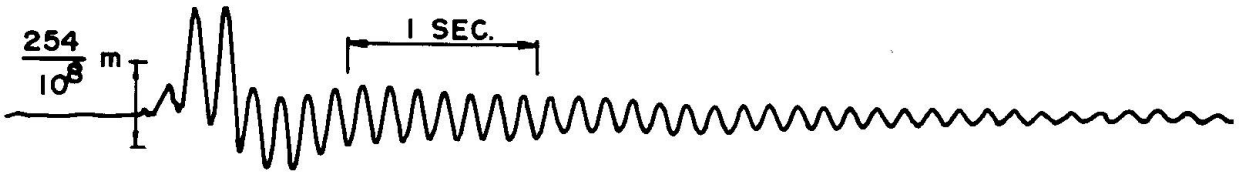

Figure 5 -- Strain Response on Gage No. 6

Additional field inspection revealed that the open expansion joint at the south end of the bridge has the following deficiencies:

a) excessive opening;
b) vertical misalignment; and
c) depression at the adjacent approach slab.

These deficiencies cause a truck's axles to become airborne, landing with considerable impact at various points of the span, depending on the speed of the truck. Such type of loading causes the structure to get excited and to be stressed approximately 40 percent more than the adjacent structure whose expansion joint is in good condition and, therefore, does not experience such loading.

Once the structure becomes excited with a relatively low damping, it is possible for one passing truck to cause approximately 15 cycles of relatively high stress ranges as shown in Figure 5. Thus, the fatigue life expectancy of such structures is dramatically reduced due to the higher stress and additional stress range cycles.

It is obvious that maintenance of the bridge and approach slab surfaces as well as the alignment of expansion joints are extremely important factors in the determination of the structure's fatigue life expectancy.

2.4 Traffic Data

The next step in this project was to determine the traffic volume and the axle loadings which have occurred on the sections of the tollway system since its opening to the traffic and to predict the future traffic magnitude to which the bridges in these sections will be subjected. This data is then used to calculate accumulated fatigue damage and predict fatigue life expectancy off steel bridges under investigation. Traffic volume figures were obtained from the study based on traffic data obtained from the Illinois Tollway's annual traffic reports. This data was used to prepare a table of actual traffic growth of commercial vehicles using Illinois Tollway system between the years 1959 and 1990.

Of next importance was to find statistics on cross vehicle weight and axle load. Weight measurements were conducted on over 10,000 vehicles of rural interstate truck traffic in the state of Illinois during the period 1968 through 1976 by the University of Illinois.

This data of traffic volume and axle load was used to determine fatigue life expectancy of any tollroad bridge.

2.5 Accumulation of Fatigue Damage

The accumulated damage to any structure could be determined if the loading history and spectrum of actual stress ranges these loads are inducing into this structure are known.

The spectrum of stress ranges caused by the actual traffic was measured on four structures. The measurements were taken in the vicinity of the details which are susceptible to fatigue cracks. These measurements and loading history data were used in the detailed evaluation of accumulated fatigue damage and prediction of fatigue life expectancy of these structures.

As a final result of this evaluation, the number of trucks required to cross the bridge in order to initiate a fatigue crack at the end of welded cover plate has been calculated. This calculated number of trucks was then compared with the table of annual and accumulated transactions, and the year during which the first fatigue cracks on this detail will appear was provided.

2.6 Field Inspections

All ten structures which were selected for detailed analysis have the critical areas susceptible for fatigue cracking at toes of welds of cover plate termination. Thus, the areas needing examination are relatively small.

Two methods were used during the course of this field inspection to detect cracks, the visual examination with a 10X magnifying glass and the dye penetration examinations.

According to accumlation of fatigue damage calculations, the fatigue cracks alaready should have started at the end of cover plates on structures No. 367 and 368. All those details were sandblasted and examined by 10X magnifying glass. Approximately 2 mm long fatigue cracks were found on every one of them.

2.7 Suggested Repair Procedure

The following three methods were considered for improving the fatigue life and for arresting the progress of fatigue damage:

a) Grinding the weld toe to remove the slag intrusions and reduce the stress concentration;

b) Air-hammer peening the weld toe to introduce compression residual stresses; and

c) Remelting the weld toe using the gas tungsten arc process (GTA), also commonly referred to as the TIG or tungsten inert gas process.

Out of these three methods, only peening is considered an effective retrofitting method which improves the fatigue life expectancy of the detail. The other effective method of retrofitting is splicing with A-490 high strength bolt.

3. SUMMARY AND CONCLUSION

Findings of serious fatigue cracks in structures, described in the INTRODUCTION of this paper, were instrumental factors in the initiation of the fatigue evaluation program of all steel bridges owned and maintained by Illinois State Toll Highway Authority. There are 82 steel bridges within this system, all of which were built between the years 1958 and 1971.

Required fatigue inventory documentation for all these bridges was prepared based on the review of drawings, calculations, and field inspection.

Ten structures with E' category detail were selected for detailed fatigue evaluation.

Preliminary field inspection did not uncover any fatigue cracks of such magnitude as those described in the INTRODUCTION of this paper.

The actual stress ranges were obtained from the measured strains. The existing traffic studies were used to determine the loading history of each structure.

The fatigue life expectancy for each structure was calculated based on the actual stress ranges and loading history of the structure.

The analysis of structures No. 367 and 368 revealed that the fatigue cracks already should have started at the end of welded cover plates.

During the detailed field inspection of these structures, approximately 2 mm long fatigue cracks were found at the weld toes of the cover plate ends. This confirmed the theoretical findings.

As a final step on this project, repair procedures were proposed to arrest the progress of fatigue damage and to improve the fatigue life of the structure.

4. ACKNOWLEDGEMENT

This project was made possible by the financial support of the Illinois State Toll Highway Authority. The project was initiated by the authors and was conducted by Envirodyne Engineers (former employer of I. J. Dvorak). The authors wish to express their gratitude to all persons and organizations who made this work possible, particularly to Dr. John W. Fisher, who served as a special advisor on this project, and to Prof. Vincent McDonald who provided assistance for field measurements and evaluation of recorded stress.

5. REFERENCES

1. AASHTO: Standard Specifications for Highway Bridges, 1977.
2. FISHER, J.W. HAUSAMMANN, H. SULLIVAN, M.D. AND PENSE, A.W.: Detection and Repair of Fatigue Damage in Welded Highway Bridges, 1979.
3. SHILLING, C.G., KLIPPSTEIN, K.H., BARSON, J.M. AND BLAKE G.T.: Fatigue of Welded Steel Bridge Members under Variable-Amplitude Loadings, 1979.
4. FISHER, J.W.: Bridge Fatigue Guide, Design and Details, 1977.
5. WOODWARD, H.M. AND FISHER, J.W.: Prediction of Fatigue Failure in Steel Bridges, 1980.
6. NCHRP: Nondestructive Methods of Fatigue Crack Detection in Steel Bridge Members, 1975.
7. WALKER, W.H.: Stress History Studies and the Fatigue Life Expectancy of Highway Bridges, 1980.
8. ISTHA: Annual Traffic Report, Illinois State Toll Highway Authority.
9. WILBER SMITH AND ASSOC.: Comprehensive Travel Patterns and Characteristics Studies, 1979.

Prediction of Fatigue Life in a Steel Bridge

Prédiction de la durée de vie dans un pont métallique

Voraussage der Lebensdauer einer Stahlbrücke

P. MAREK
Assoc. Prof.
Czech Technical University
Praha, CSSR

SUMMARY
The paper presents the fatigue life investigation of a temporary, high strength steel bridge for tram traffic. The loading as well as response history was considered and a fatigue criterion, based on the stress-range concept, was applied. In agreement with the safe service life estimate supported by a simple fracture mechanics study, fatigue cracks were observed in the bottom flange after about three and a half years of use. The bridge was removed.

RESUME
L'article présente l'examen de la durée de vie d'un pont temporaire en acier à haute résistance soumis au trafic de trams. Les charges aussi bien que leurs évolutions ont été considérées et un critère de fatigue, basé sur le concept amplitude de contraintes, a été appliqué. Des fissures ont été observées dans l'aile inférieure après environ trois ans et demi de service, et ceci en accord avec l'estimation de la durée de service fiable et avec une étude simple de mécanique de la rupture. Le pont a été enlevé.

ZUSAMMENFASSUNG
Dieser Artikel beschreibt eine Lebensdauerberechnung einer provisorischen Brücke aus hochfestem Stahl, welche von Strassenbahnen befahren wird. Die Lasten sowie das Tragverhalten und ein Ermüdungskonzept, welches die Spannungsdifferenz berücksichtigt, wurden in Betracht gezogen. In Übereinstimmung mit einer Lebensdauerabschätzung, welche sich auf bruchmechanische Überlegungen abstützt, wurde nach einer Betriebsdauer von 3 1/2 Jahren ein Ermüdungsriss im unteren Flansch gefunden. Die Brücke wurde für den Verkehr gesperrt.

1. INTRODUCTION

In order to solve a local public transportation problems a temporary four-span tramway steel bridge was built over Vltava river in Prague.Simple supported plate girders - see Fig.1 - made of high strength steel were exposed to heavy traffic.While the theoretical data (design according the current specifications) and experimental results (loading test of a completed bidge) proved the required safety with respect to the strength criterion, the prediction of fatigue life had to be prepared considering the actual loading and response history.

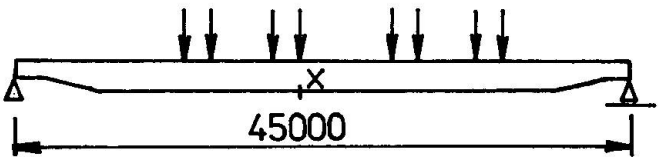

Fig.1 Scheme of the 1824 mm high plate girder (X - the location investigated with respect to fatigue)

This paper presents a brief review of the investigation and of the obtained results.

2. FATIGUE STRENGTH CRITERION

In czechoslovak specifications /1/ the fatigue criterion is based on the stress range concept(since 1976-/3/).Recently the bi-linear S-n curves were proposed for steel bridges /5/ - see Fig.2.The investigation of the fatigue life in the case of the tramway bridge was based on the actuel stress spectrum related to the location X (see Fig.1),on the application of Palmgren-Miner rule and S-n curves shown in Fig. 2.The main attamtion was focused on the end zones of cover plates (lower flange of the girder),on the end zones of vertical stiffeners and on the errection joints. (Yield strength 500 MPa - steel grade ČSN 15222) The results were compared with results according ISO and SIA specs.

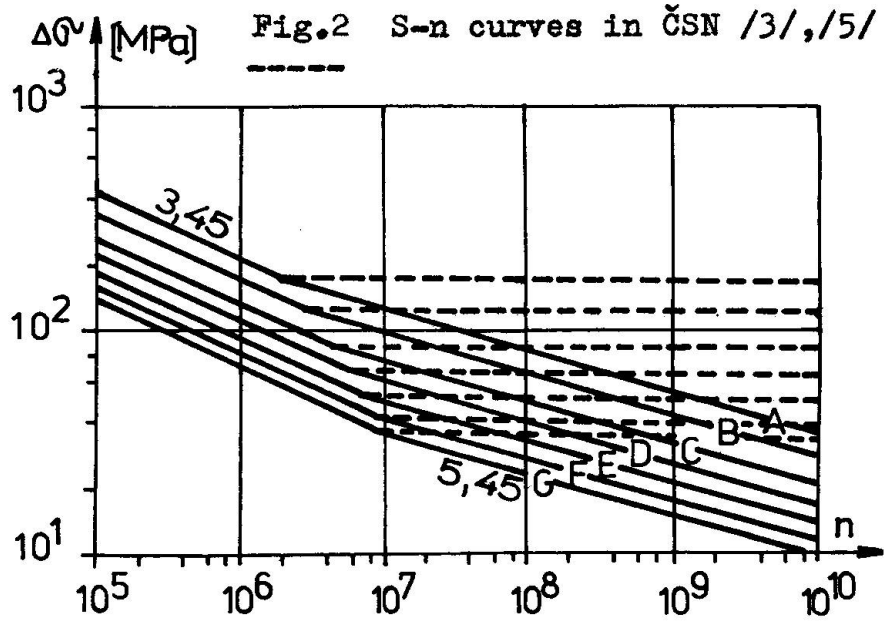

Fig.2 S-n curves in ČSN /3/,/5/

3. STRESS HISTORY

According to the traffic rules just one train was allowed to move on the bridge at one time - the mass of the train was about 16,5 t (empty) resp. 30,5 t (full loaded).The speed was limited to 20 km/h.

The investigation of loading and respose history was conducted in following parts :

a - full scale loading test of the bridge allowed the comparison of the stress ranges in selected locations obtained from theoretical analysis and from actual measurements,

b - the dynamic test (train mouving 20 km/h) allowed to estimate the dynamic response,

c - the 24 hours stress recording(using strain gages in selected locations) allowed to estimate a "typical" working day stress-range spectrum - see Fig.3 and Fig.4,

d - considering tramway time schedule,traffic forecast,etc. the one year stress range spectrum was estimated - see Fig.5

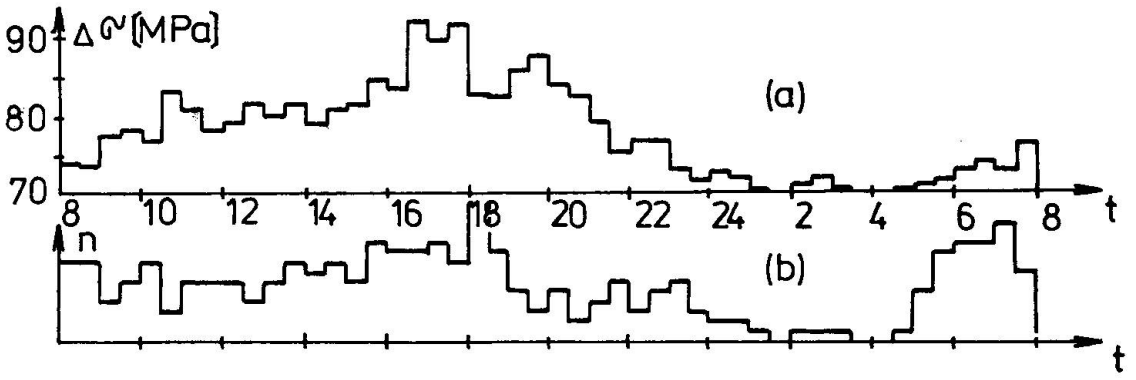

Fig.3 Results of 24 hour stress range recording in location X :
----- (a)- average stress range (half hour intervals)
(b)- number of cycles in half hour intervals

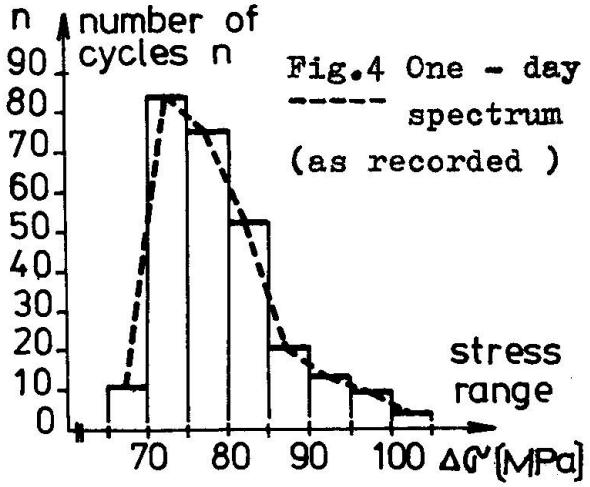

Fig.4 One - day spectrum (as recorded)

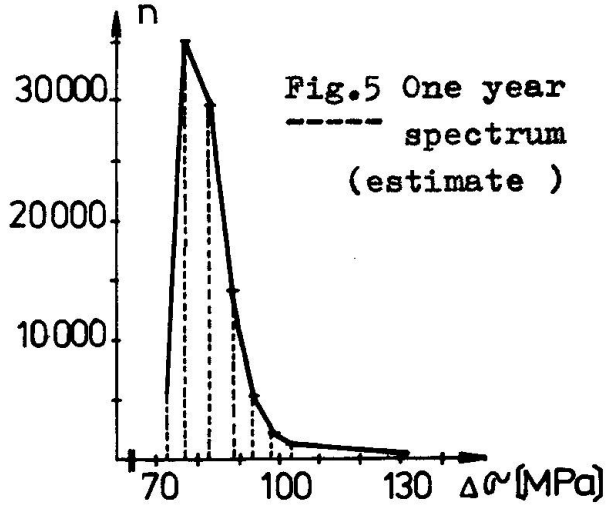

Fig.5 One year spectrum (estimate)

4. FATIGUE LIFE

Using one-year spectrum, Palmgren-Miner rule and S-n curves according to czechoslovak specifications /1/ the fatigue life was derived for individual notch categories - see Fig. 6(a). Considering the notch category "G" the four years limitation corresponds to the spectrum as shown on Fig.5.
Assuming the same stress range spectrum as above, a comparison was made using SIA /6/ and ISO /2/ specifications - see Fig. 6 (b),(c).

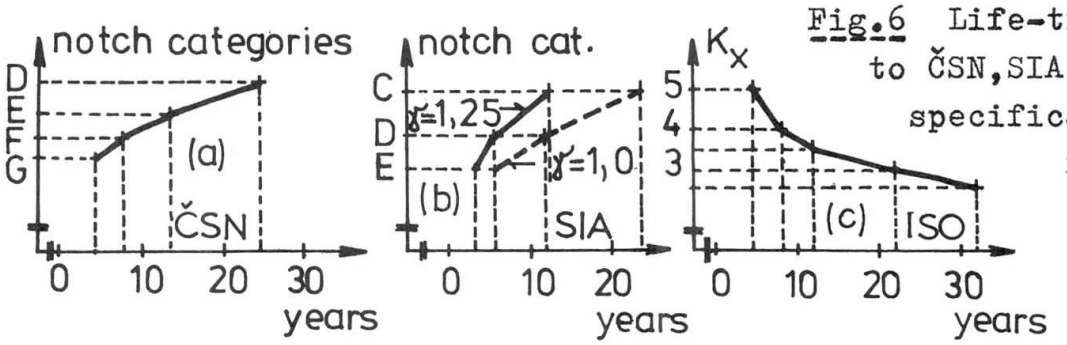

Fig.6 Life-time according to ČSN, SIA and ISO specifications ref./1/, /6/, /2/.

Due to rather low predicted fatigue life a periodic checking of the lower flange and some other locations was proposed after three years of service. Using a simplyfied fracture mechanics model /4/ an adequate interval for checking - six months - was suggested.

5. CRACKS OBSERVATION

After about three and half service years cracks were detected on several locations in the end zones of cover plates (lower flange) e.g. see Fig.7. A slow crack propagation was observed in some cases. After some complementary material tests (K_{IC}, crack propagation rate, /7/) and with respect to the coming winter season it was

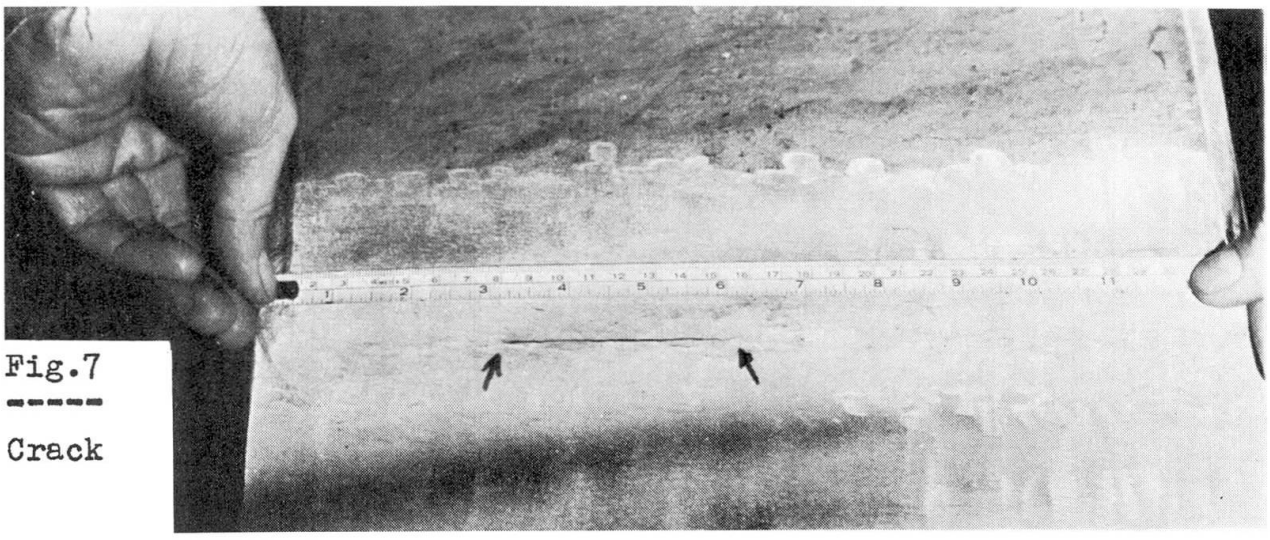

Fig.7 Crack

decided to interrupt the traffic on the tramway bridge and to replace it by different bridge system.
After a necessairy checking,the removed bridge girders may be used again as supporting parts of structural systems which are not subjected to fatigue loads (e.g. roof systems).

6. SUMMARY

The application of current specifications based on stress range concept and fracture mechanics study allowed to predict the fatigue life of a steel tramway bridge with sufficient accuracy. Attention was paid to the investigation of the actual loading and response history in order to estimate the stress range spectrum for important locations of the welded high strength plate girder.

REFERENCES

1. ČSN 73 1401 Design of Steel Structures (in Czech).Specifications. ÚNM Praha,1976,ČSSR
2. ISO - Tentative proposal for first draft of chapter on fatigue. 19.7.1979
3. MAREK P.: Fatigue Strength in revised Specifications ČSN 73 1401 (in Czech).Inženýrské stavby 1976/4,Alfa,Bratislava
4. MAREK P.,HÁŠA P.,and KOTTOVÁ J.: On the durability of steel bridge from the viewpoint of its fatigue strength (in Czech). Inženýrské stavby,1981/2,Alfa,Bratislava,ČSSR
5. MAREK P.,KROUSKÝ J.: Fatigue Strength of Steel Bridges (in Czech),Inženýrské stavby,1981/2,Alfa,Bratislava,ČSSR
6. SIA 161/1979, Stahlbauten,Schweizer Norm SN,Zürich
7. ZMRHAL V.: Experimental Investigation of a Bridge with respect to the Fatigue Life (in Czech). In: Proceedings of the Conference " Limit States Design of Metal Structures".ČSVTS (DT Plzeň),Karlovy Vary, April 1981,ČSSR

Leere Seite
Blank page
Page vide

Fatigue Failures of Steel Railway Bridges in China

Ruptures de fatigue dans les ponts-rails en acier, en Chine

Ermüdungsbrüche an Eisenbahnbrücken aus Stahl in China

SHI YONGJI
Eng., Group Leader
China Academy of Railway Sciences
Beijing, China

YANG YENMAN
Eng.
China Academy of Railway Sciences
Beijing, China

CHEN ZEGAN
Eng.
China Academy of Railway Sciences
Beijing, China

SUMMARY
This paper briefly describes the basic conditions of steel bridges on Chinese railway lines including their date of construction and the materials, technology and specifications used. Fatigue cracks are classified according to the age of the bridge at the time of their detection and then their causes analysed. Finally, examples are given of fatigue failure in bridges from every period of construction.

RESUME
Cet article donne un aperçu des ponts-rails en acier réalisés en Chine, en mentionnant leur date de construction ainsi que les matériaux, les techniques et les spécifications utilisés. Les fissures de fatigue constatées sont classées d'après l'âge de la construction au moment de leur apparition, et leurs causes sont analysées. Enfin, des exemples de rupture de fatigue de ponts sont donnés pour chacune des périodes de construction.

ZUSAMMENFASSUNG
Die technischen Bedingungen und Bauzeiten der Eisenbahn-Stahlbrücken in China (Baustoffe, Technologien und Entwurfsvorschriften) werden kurz beschrieben. Entsprechend dem Alter der Brücken und dem Zeitpunkt der Entdeckung der Ermüdungsrisse werden die Ermüdungsrisse klassifiziert und deren Ursache analysiert. Im weiteren werden Beispiele von Ermüdungsbrüchen verschiedener Altersstufen nach Charakter, Rissstellen und Ursachen untersucht.

1. The seriousness of fatigue failures

Failure accidents in the predicted service life of steel railway bridges may be attributed to the following reasons: excessive deformation, bulking, fatigue, fracture, vibration and other natural disasters. It is roughly estimated that more than 70% of the failures are due to fatigue. So fatigue is a more dangerous factor in the safety of steel bridges. According to investigations carried out by Beijing Railway Administration on 851 steel girder spans over 115 railway bridges along the Beijing-Handan Line, as many as 65 spans were found to have cracks. That is 7.6% of the total number of girders investigated (Table 1).

Table 1

Period of Construction	Spans investigated	Spans with cracks	Percentage	Percentage against the total number of cracked spans
- 1937	177	29	16.4	44.6
1937 - 1945	190	22	11.6	33.8
1946 - 1949	72	2	2.8	3.1
1950 -	412	12	2.9	18.5
Total	851	65	7.6	

To make studies of discovered fatigue cracks provides a great help to the devising of repair methods, the accumulating of experiences, the revision of fatigue design specifications and technological procedures in preventing possible future failures of fatigue. It is especially important that many Chinese old girders, which have been in use 30-40 years, were fabricated in time when fatigue concept was not yet sufficiently understood, os the fatigue problems could not be fully considered in their designs. Under the circumstances that traffic density and weight have increased by wide margins, it is no wonder that fatigue problems of various types should have appeared. Therefore it is high time to pay attention to the investigation of fatigue failures and push on the research work in calculating the fatigue life of existing bridges.

2. Basic conditions about steel railway bridges in China

In reference to construction date, the steel railway bridges may be classified into two groups:

(1) Bridge built before 1949
Most of the steel bridges erected during this period are basically steel girders from Europe, America, Russia and Japan. All of them are reveted structures of variegated low carbon steel materials including rimmed, semikilled and killed steel or even wrought iron used in earlier years. Though the majority of these bridges are still in service, some of them were strengthened, and a few were altered as a result of insufficient loading capacity or serious fatigue cracks.

(2) Bridges built after 1950
Between 1950 and 1957, China was running short of steel. Emphasis was given to the development of prestressed concrete bridges. Exceptions were a few very long span bridges which were made of imported low carbon steel, with rivet connections. The typical example for these is the Wuhan Yantze River Bridge constructed in 1957.

Since 1958 or so, our steel bridge industry has advanced on our own road. Step by step, we use home-made low carbon steel (σ_b = 412 N/mm^2), and 16Mn. low alloy steel (σ_b = 510 N/mm^2) in place of imported materials. Rivet connection has gradually given way to weld connection and bolt-and-weld connection. This transition began in 1966 when the Chengdu-Kunming Railway Line was constructed. During this period, new specifications were established. The typical examples are the Nanking Yangtze River Bridge and Ying Shuicun tied arch bridge on Chengdu-Kunming Railway Line. The latter is a large bolt-weld bridge with the span-length 112 M. In the course of developing railway bridges of longer span and lighter weight, 15 MnVN high strength low alloy steel (σ_b = 588 N/mm^2) was produced and used in conbination with 16 Mn steel on Baihe Bridge on the Shacheng-Tongliao Railway Line in 1976. This bridge is a 3 x 128^m bolt-weld connected continuous truss.

3. Classification and formation of fatigue cracks of steel railway bridges

Fatigue cracks of steel railway bridges are caused mainly by structural stress concentration as well as defects formed in manufacturing and welding. In principle, fatigue cracks due to stress concentration can be avoided, since design specifications for fatigue have prescribed allowable fatigue stresses for different types of structural joints. It takes a long time for crack to propagate, even if the crack has appeared. But manufacturing and welding defects are difficult to predicte in fatigue design. The cracks of this kind generally appear in a short time after the structure is built. Hence, in order to explain the causes of their formations, the paper assumes to identify fatigue cracks according to the time of their appearance.

3.1 Cracks occurred in the early stage

The cracks occurred in the early stage are meant by that they are found within a few months, up to 3-5 years at most, after the structure is put in service. These cracks mostly occur at weld joints of various members in a short span beam (or members having short loaded length of influence lines). They often take place at these places where welding cracks or serious manufacturing and welding defects have already existed.

It is known to all that the most important factors causing fatigue cracks are the number of stress cycles and the distribution mode of stress frequency. The former is related to the type of train load and calculated girder span or loaded length of influence line of the member concerned.The latter is influenced by the magnitude of the wheel load, in addition to the above mentioned factors. Field measurements show that, in case of long span girders (> 30 M), the girder is subjected only to a single stress cycle during the passage of a train. As for short span girders, under the loading action of a passing train, the number of stress cycles varies with the number of axles and the number of bogies the shorter the span, the greater the number of stress cycles. It is clear from the above statement that though the stress level in short span girders caused by the axle load of a train is generally low, even lower than the fatigue limit of the joint, and has little consequence upon the formation of fatigue crack, but it plays an active part in the propagation of an existing weld crack. What is more, the greatly increased number of stress cycles speeds up the propagation of the crack. This is the major cause which accounts for crack propagation taking place in a very short period of time in the case of short span girders with weld cracks.

3.2 Fatigue cracks occurred after a long service period

This form of cracks is referred to those which occur after the structure has been used for ten years to several decades. The causes of formation of such

cracks may be mentioned as follow:
— The train density and train load have greatly outpaced the original design loading.
— The design of certain structural details has not been considered comprehensively.
— The manufacturing technology and machining precision are not up to the design requirements.
— There are out-of-plane deformations which have not been considered in the design, and secondary stresses generated as a result of restraint imposed upon the deformations.
— Fairly high auxiliary stresses are generated at certain locations due to abnormal displacement of bridge bearings.

These fatigue cracks generally go through a complete formation process (metallurgical crystal lattice slide — microscopic crack — macroscopic crack --crack propagation). The time traversed under such circumstances will be much longer than that with weld cracks.

4. Case study of fatigue failures of steel railway bridges in China

The following are some typical examples of different kinds of cracks on steel railway bridges constructed in different historical periods.

4.1 Brittle fractures caused by repair welding

Bridge No. 248 on the Beijing-Baotou Railway Line was a rolled I-beam bridge which was manufactured in Britain in 1898 and erected in 1903. Its original length was 7 M and was cut down to 4.6 M in 1947 to be used as a simple span. There were four drilled holes of Ø19 on the webs and two on the bottom flanges. These holes were filled later by gas welding when it was cut. It so happened that at about 11 o'clock in the mroning of November 30, 1967, after a heavy snow fall, a large piece of flange metal broke off together with a portion of the web. Fig 1 is a sketch of the girder and the failure location. Photo 1 is the fallen off piece. From the fracture surface, we could find that the weld quality was very poor. Under repeated action of train load through a long period of time, fatigue crack was initiated at the notch (Photo 2).

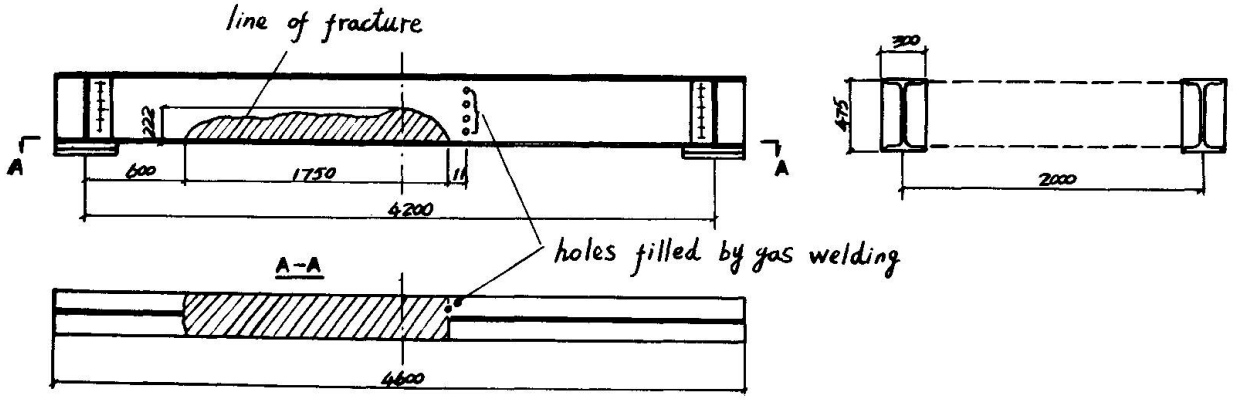

Fig 1 Sketch of the girder bridge No. 248 and its failure location

Samples were taken from the girder for chemical analysis and mechanical test. The steel strength was equivalent to that of the carbon steel but was high in S, P and N content which made it difficult for welding. The ductility of the material at low temperature was rather poor and the ageing effect tendency was quite strong. U-notch impact test showed that the brittleness transition temperature was about +15°C - 0°C.

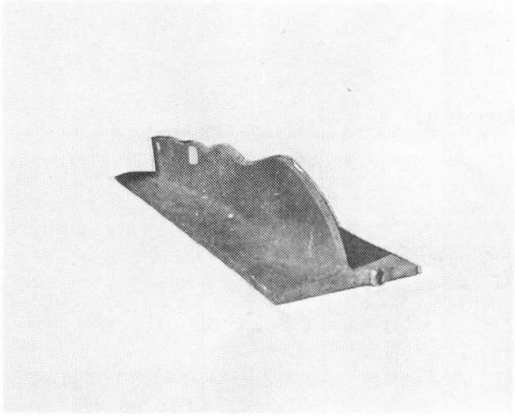

Photo 1 The fallen off metal of bridge No. 248

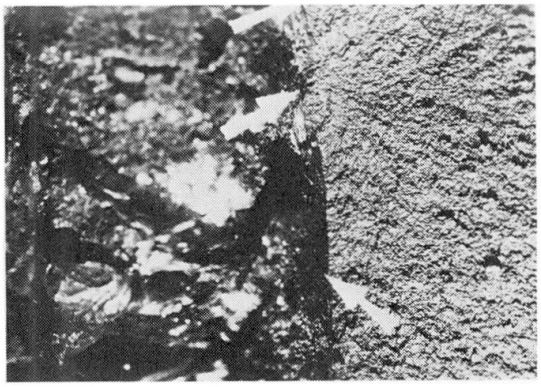

Photo 2 Fatigue crack at the notch of bridge No. 248

This accident once more teaches that direct repair welding on steel girders must be strictly forbidden. Otherwise it would be very much likely that weld defects or weld cracks should appear and deterioration, a decrease in ductility in particular of the weld metal and the heat affected zone would happen. And these would certainly give rise for the formation of fatigue crack and brittle fracture. This is an important problem we must pay attention to in the reconstruction and maintenance of bridge in the future.

4.2 Fatigue failures at riveted joint

One accident of this kind took place on Taizi River Bridge on the down line of the Changchun-Dalian Railway. It was a 17 span simple through truss bridge.

On March 23, 1973, the fracture occured at the upper panel point of the first diagonal of the 16th truss built in 1930, with a span length of 33.54 M. Photo 3 show the location of the fracture.

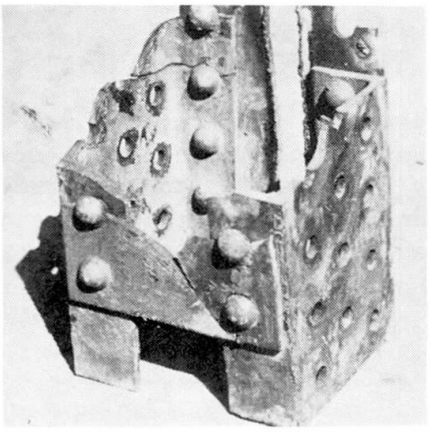

Photo 3 The form of the fracture member of Taizi River Bridge

Field investigation revealed that fatigue crack took place at an early stage in one of the diagonal channels. The other channel was pulled to break with obvious appearance of a bottleneck. The causes of the formation of the fatigue cracks are as follows:

At the time of design 50 years ago, the fatigue behaviour of the riveted joints was not clearly understood. The present train load and train load and train density (about 80 trains per day) on the bridge were much greater than those when the bridge was first constructed. The lateral bracings were too weak, so the passing trains caused the truss to produce great vibration in the horizontal direction.

4.3 Fatigue cracks caused by improper detailing

In Fig 2 is indicated the fatigue cracks occuring at the angles connecting the end cross beam and the main truss. In the original design, the bottom flange of the end cross beam was placed directly against the bearing plate so that the reaction force might be partly transmitted through the plate. However, after many years of operation, a gap of 2-3 MM was formed between the bottom flange of the cross beam and the top of the bearing plate, which had deformed and worn out. As a result, the line of transmission of the reaction force was so

altered that the stresses in the connecting angles were greatly increased. This was the major cause of the fatigue cracks.

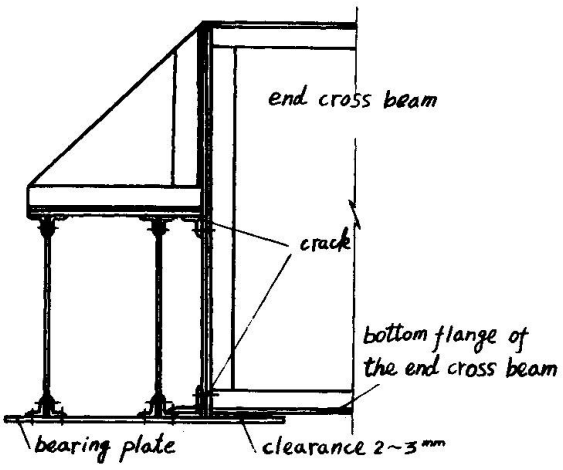

Fig 2 Fatigue cracks occuring at the connecting angles

4.4 Longitudinal fatigue cracks on the upper flanges of plate girders directly supporting wheel load

In some old-type riveted girders, both the upper and lower flange cover plates were provided in conformity to the moment diagram. Some of them often stopped at a distance from the bridge support. The flange plate between the support and stopped point was rather thin (8 MM only), but it cantilevered out as many as 110 MM (Fig 3). This was why longitudinal fatigue cracks often took place at this location. The two major causes of the formation of this longitudinal fatigue cracks are: (1) high impact forces under the direct train wheel load. (2) Transverse deflection of the upper flange induced by the vertical deforation of sleeper under train load. The beam action of sleepers on D.P.G. Bridges arose from a difference that existed between the center to center distance of the main girders which was 2 M and the gauge distance of the rails which was 1.435 M.

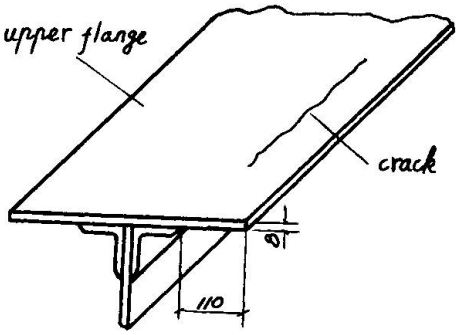

Fig 3 Crack on the upper flange

4.5 Cracks at the toe of fillet weld of vertical stiffeners of stringer of truss bridges

Langjiang Bridge on the Changsha - Liuzhou Railway Line, which was completed and opened to traffic on November 28, 1964, was the first bolt-weld railway through truss bridge using 16 Mn steel, with a span length of 61.44 M. One hundred days later, a horizontal crack was observed right beneath the manual weld, which connected the semi-automatic welds on both sides of stiffener, at the end of the center stiffener of stringers on March 8, 1965 (Fig 4).

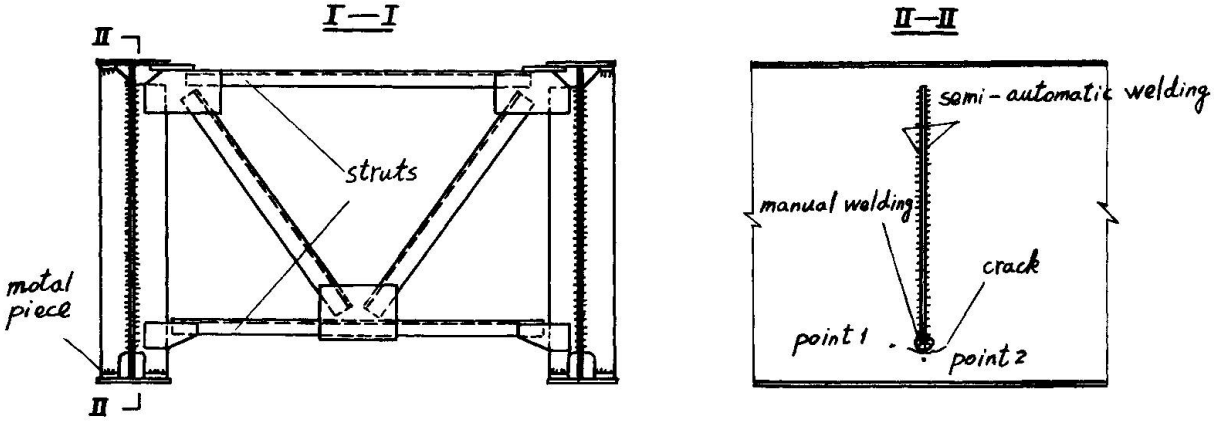

Fig 4 Crack at the end of the center stiffener

After the crack was revealed, the stringer was subjected to a test. Test result showed that, under the long-term action of train load, the metal pieces, which

were inserted in the gaps between the stiffener ends and flange, could hardly keep bearing tight against the flanges. It was obvious that this type of structural detail would not meet the design requirements. In such a case, the vibration frequency measured on point 1 and 2, near the lower end of the center stiffener, was about 30 HZ, this location produced great vibration as the train passed. The maximum alternate stress at point 1 was observed to be +45.6 and -31.0 N/mm^2. However, when the bottom flange of the stringer and the bottom lateral bracing of the truss were held rigidly together, the vibration frequencies at point 1 and 2 were measured to be 40-50 HZ and the alternate stress reduced to less than ±4.9 N/mm^2.

Furthermore, out-of-plane deformation and angle of rotation are produced in the stringer under the action of train load. The additional flexural stresses were induced at the lower end of the vertical stiffener.

In addition to the above considerations, the welding technologies used for the vertical stiffeners of the stringers were unfit. Employing manual welding to connect the semi-automatic welds on both sides of the stiffener was apt to produce welding defects instead of any favourable effect. It may be concluded that the horizontal crack or under cut (even it was very fine) at the lower end of the vertical stiffener welds would propagate very fast under the action of the above-mentioned additional stresses.

Since the Langjiang Bridge accident, the constructional detail of the stiffener and the strut hastbeen modified. The lower strut of cross brace, instead of being connected to the lower end of the vertical stiffener, was made to connect to the bottom flange of the stringer through gussest plate. Furthermore, 16Mn low alloy steel was used to make the stringers, the height of which was thus reduced from 1,450 to 1,290 MM. After these modifications, no fatigue problem has been encountered at this location.

4.6 Welding cracks on the fillet welds of stringer flanges of girder bridges

The Puyanjiang Bridge on the Hangzhou-Nanchang Railway Line is a half-through girder bridge with a total length of 166.9 M. The third span is 34.75 M in length. The girder was made in September, 1975 and opened to traffic in 1976. In July, 1979, the first crack was found at the toe of fillet weld of a stringer. Eleven cracks at similar locations of the bridge were found in latter inspection. The most serious one appeared at the fillet weld near the end of the upper flange of the stringer in the 8th panel. The crack ran 25 MM along the toe line and then turned an angle of 30° into the web 17 MM (See Fig 5).

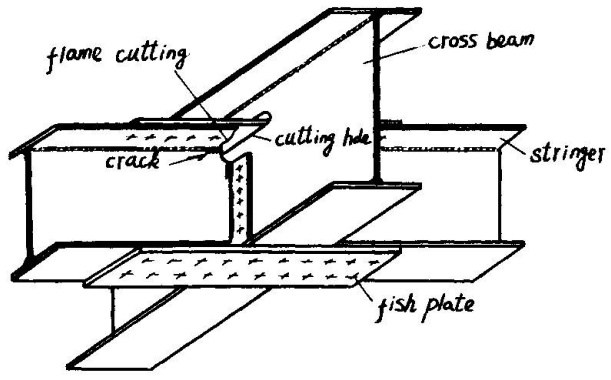

Fig 5 Cracks at the toe of filled welds of stringer flange and connecting plate between cross beam and stringer.

During manufacture, flame cutting of the flanges and the web was done in one operation. The cut face was not machined nor ground with disk sander. Its zigzagged outlook showed that the cutting quality was very poor and did not meet the need of design. Considering the location of the crack, its tendency and course of propagation, and the length of service time, it is quite possible that crack(1) owes its origin from the toe crack which developed under the effect of thermal stress during flame cutting accompanied by a complicated state of residual stresses induced around the crack. As a result, under the train load, first of

all developed into the web plate, and then extended along the direction normal to the principal stress in the web.

4.7 Cracks at the toe of fillet weld connecting horizontal bracing with gusset plate

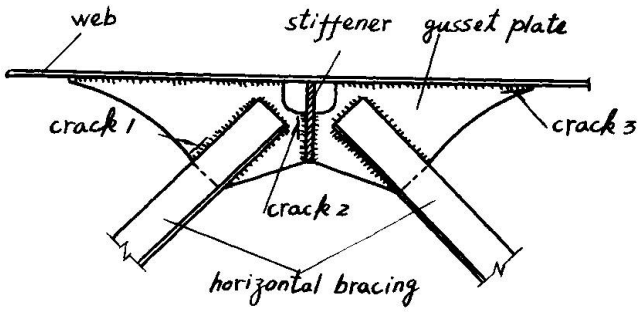

Fig 6 Cracks at the toes of fillet welds of the gusset plate of horizontal bracing

Fig 6 shows the cracks found at the welds of the gusset plates of the horizontal bracing on the deck girder bridges of 22.0 M span in the Shenyang Railway Administration. These bridges were erected after being fabricated in 1974-1975. Very soon thereafter, the cracks were generally found. During an overall inspection in April, 1976, cracks of this kind were found at as many as 29 places on five of the 22.0 M span girders on the No.3 Anshanhe Bridge on the Changchun-Dalian Railway Line. It was more than four years from the cracks found up to now, they did not propagate. These cracks, in the main, were essentially welding cracks at the toe of weld.

4.8 Cracks in the weld connecting horizontal and vertical stiffeners

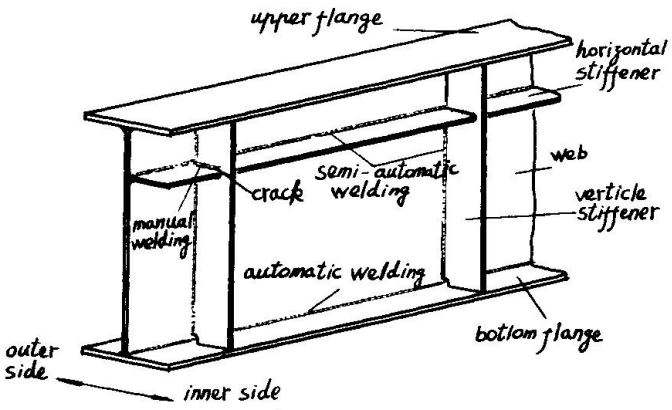

Fig 7 Cracks in the welds connecting horizontal and vertical stiffeners

Fig 7 shows the crack found at the toe of weld connecting the horizontal and vertical stiffeners on welded deck girder bridges. To avoid this kind of welding cracks, aside from that it is essential to select the right type of welding rod, to strictly control the baking temperature of the rod so as to reduce its hydrogen content, to reduce the assembly tolerance as much as possible, and to clear the steel plates of rust, it is also advisable to modify the structural details and to rearrange the welding sequence. The horizontal stiffener can be made with a whole piece of the same length as the web passing through the notches of the vertical stiffeners, and weld up the stiffeners after assembling before other welds are done. An alternative is to leave the horizontal and vertical stiffeners unwelded as arranged in the above-mentioned manner.

5. Conclusion

From the preceeding representative cases of fatigue fractures, it can be seen that the periodical inspections of old bridges become highly necessary. The probability of fatigue crackes occurring within a short period of service time has substantially increased on welded steel bridges with short spans in particular. The fact shows that welding cracks, particularly cracks at the toe of the weld, deserve proper attention even though they exist only in a small amount. For repair of indicated cracks, welding is not preferred. Experience has shown that high strength bolt is a better resort for repair of fatigue cracks and for strengthening of steel girders.

Fatigue Cracking in Two Steel Bridges

Fissures de fatigue dans deux ponts en acier

Ermüdungsrisse in zwei Stahlbrücken

S. CHATTERJEE
Assist. Chief Engineer
Department of Transport
London, UK

P.H. DAWE
Principal Engineer
Department of Transport
London, UK

SUMMARY
A survey of welded details in some revealed fatigue cracking in load bearing stiffeners in two major structures. In both cases analytical investigations were undertaken to identify the causes of the fatigue damage and to determine suitable repair procedures. In-situ static load tests were also carried out and the measured strains compared with the analytical results. The work has highlighted the difficulties in predicting the behaviour of structures and in determining the actual stresses in welded details, and has led the authors to question the current method of fatigue design and assessment.

RESUME
Dans le cadre d'un relevé de l'état de détails soudés de ponts routiers en acier, des fissures de fatigue furent repérées sur des raidisseurs d'appuis dans deux ouvrages importants. Une étude analytique fut entreprise en vue d'identifier les causes des dégâts par fatigue et de déterminer les procédures de réparation appropriées. Des essais de charge statiques in situ furent effectués et les efforts mesurés furent comparés aux valeurs calculées. Ces travaux mettent en évidence la difficulté de prédire le comportement de structures et de déterminer les sollicitations qui s'exercent effectivement sur les détails soudés. Ils amènent les auteurs à mettre en question les méthodes actuelles de calcul et d'évaluation de la fatigue.

ZUSAMMENFASSUNG
Anlässlich einer Untersuchung an geschweissten Teilen einiger Strassenbrücken entdeckte man Ermüdungsrisse in tragenden Versteifungselementen zweier bedeutender Brücken. In beiden Fällen wurden Analysen ausgearbeitet, um die Ursachen der Ermüdungsschäden zu finden, und um geeignete Reparaturmassnahmen zu treffen. An Ort und Stelle wurden statische Belastungsversuche durchgeführt. Die gemessenen Spannungswerte wurden mit den Resultaten der Analysen verglichen. Diese Untersuchung machte wiederum deutlich, dass eine genaue Vorhersage des Ermüdungsverhaltens von Bauwerken schwierig ist. Die Autoren stellen deshalb die derzeitige Methode zur Berechnung des Ermüdungsverhaltens in Frage.

1. INTRODUCTION

1.1 Survey of Welded Steel Bridges

In 1976 the Department of Transport in the UK organised a selective in-situ examination of typical welded joints in a number of steel bridges. The object of the investigation was to see whether cracking or other deterioration was occuring in the welded connections and to get some idea of how welded joints were actually performing in service. Twelve major steel bridges were chosen for the exercise, six being of box-girder and six of plate girder construction, covering different design configurations and severities of traffic loading. The bridges had been in service for from 8 to 20 years at the time of inspection.

For each particular structure critical areas were identified where it was thought that the stresses would be high or that fatigue cracks were likely to occur. The examinations, where possible, concentrated upon typical details within these areas, although the area of inspection depended also on the availability of suitable means of access. The inspections were only intended to cover a representative sample of typical welded joints. The methods used for inspection included careful visual examination and appropriate non-destinctive testing (NDT). The latter methods included magnetic crack detection and ultrasonic testing techniques. In some cases as a result of the initial findings extra inspections were carried out and samples cut from the welds were subjected to metalurgical examination in the laboratory.

1.2 Findings of Survey

Evidence of fatigue cracking was found in four of the bridges but in no case was it considered sufficiently serious to stop traffic on them. In some cases the cracking had been noted previously by the authorities responsible for the maintenance of the structure.

Some examples were also found of cracking which was attributed to defects originated at the time of welding, such as at the stop - start positions on fillet welds. None of these were considered to be of any great significance, but as a precaution it was recommended that they should be monitored from time to time. The fatigue cracking in two of the bridges, and the steps taken to analyse the problems and develop suitable remedial measures, are discussed in this paper.

2. BOSTON MANOR BRIDGE - DESCRIPTION

2.1 History and Description of the Bridge

The bridge forms part of the elevated section of the M4 motorway which runs from the west into London and is very heavily trafficked. It was constructed in 1964 and carries a dual 2 lane carriageway. The bridge consists of 4 eastern and 10 western spans carried by 2 pairs of plate girders and a central section of 3 spans carried by a pair of trusses (Fig 1). Some of the spans are continuous and some are cantilevered with suspended spans. Although sections of the bridge are curved in plan the girders themselves are straight between supports, with the curvature being obtained by laterally displacing the cross-girders relative to the main girder centre lines.

The deck construction is common to all spans and consists of an in-situ reinforced concrete slab cast on precast concrete planks. This is supported on cross-girders at 2.3m centres which bear directly on the top flanges of the main

plate girders or on the top chords of the trusses. The deck is connected to the cross-girders by means of stud shear connectors. The cross-girders are fabricated from plates and have intermediate vertical stiffeners at 1.22m crs. Over the main girders (or chords) there are full depth double bearing stiffeners which are of heavier section and which are welded to both flanges (Fig 2). The intermediate cross-girders are fastened to the main girders by means of threaded studs which are welded to the main girder flanges, while the end cross-girders are fastened by means of high strength bolts.

2.2 Cracking in Cross-Girder Bearing Stiffener Welds

An earlier survey had revealed cracks at the top of many of the cross-girder bearing stiffeners at the extremities of the toe of the fillet weld to the top flange. The report on the inspection attributed the cracks to fatigue and noted that their length and number appeared to be increasing and that they were also present at the bottom flange as well. Following this inspection the maintenance authority conducted a visual survey of all the bearing stiffener welds throughout the structure.

Three modes of structural action were considered as possible sources of stress fluctuation and hence fatigue damage in the cracked components, namely:-

- longitudinal racking of the cross-girders under main girder deflections due to there being no longitudinal shear connection between the concrete deck and the main girders
- rotation of the deck slab under wheel loading
- moment restraint to cross-girders provided by each pair of main girders.

From a study of the cracking pattern it was considered that the first mechanism was the most likely source of cracking and it was decided to examine this hypothesis in more detail using both analytical and experimental methods.

3. BOSTON MANOR BRIDGE - FATIGUE ANALYSIS

3.1 Theoretical Stress Analysis

The object of the main theoretical analysis was to see whether a cracking pattern could be predicted which was consistent with what had been observed. The spans were first of all analysed under live load using a continuous beam program, each main beam being assumed to carry a proportion of the load with no composite deck action, in order to find influence lines for the beam rotations. The next step was to establish the correct relationship between the rotation of the main girder and the rotation of the cross-girder, the relationship being dependant not only on geometry but also on the assumptions made about the relative horizontal movement between the deck and the main girder neutral axes. Three different assumptions were considered and it was found that the one which assumed no relative movement best fitted the cracking pattern.

Further analyses were carried out, one of which considered the rotation of the deck slab under the passage of a vehicle. It was found possible to derive an equivalent beam to represent the slab and to use this to calculate the rotations of the slab and cross-girders under load, but it was not possible, because of the number of unknown parameters involved, to model the bearing stiffener to deck slab joint precisely. The flexibility of this joint is important in determining how rotations of the slab are transmitted into rotations of the cross-girder. Analyses were also carried out to determine any possible contri-

bution to the stiffness of the main girders arising from composite action produced by the shear resistance of the cross-girder bearing stiffeners.

3.2 Static Load Tests

Two commercial vehicles were used for a series of static live load tests on the bridge with the resulting deflections and strains at certain locations on the cross-girders and main girders being measured with deflection gauges and electrical resistance gauges. The gauges not only measured strains in stiffeners and girders but also measured the relative displacements of flanges and stiffeners as a result of the racking movements induced by the applied loading. A large vehicle was used to load the main girder and produce the associated global racking movements while a smaller lorry was used to obtain the local effects due to the deflection of the deck slab itself. The measurements were used to produce influence lines of the strains (or stresses) in the stiffeners and cross-girders and the flange-stiffener separations at the fatigue cracks caused by the racking movements.

3.3 Comparison of Theoretical and Measured Results

Whilst there was fairly good matching between the predicted cross-girder rotations and the observed pattern of cracking throughout the structure, the correlation between predicted and observed measurements in other cases was not so good. For example the measured deflections of the main girders and the racking movements were approximately $\frac{2}{3}$ of the predicted values assuming no composite action, although deflections of the deck slab under wheel loading agreed with the results obtained by simple analysis. The greatest discrepancies were found between the predicted and measured stresses in the bearing stiffeners themselves; there were even differences found between the stresses measured in adjacent stiffeners which would have been expected to have similar stresses.

The normal design calculations assuming rigid joints between the cross-girder and main girder, and between the cross-girder and deck slab considerably overestimated the stresses in the bearing stiffeners. However this is not unexpected since the stresses are very much dependant on the fit-up between the various components, sequence of construction, shrinkage and creep of the deck concrete, prestress in the holding-down bolts and studs and other parameters. Without detailed knowledge of these items it proved impossible to achieve any better correlation between the predicted and measured stresses.

3.4 Prediction of Fatigue Life

In addition to the stress analyses already described, some fatigue life calculations were carried out according to the latest UK fatigue design code, BS 5400: Part 10, and using measured stresses. These calculations gave fatigue lives in the bearing stiffeners which were much shorter than those actually observed, and thus conservative. Part of the differences were thought to be due to the fact that traffic flows were lower than assumed in the code and part due to the difficulty in determining dead load stresses and the change of stresses themselves as a result of cracking. The code also predicted fatigue damage on other stiffeners where no cracking has so far been found. The general indication was that lives predicted by BS 5400 Part 10 were significantly shorter than the actual lives.

3.5 Remedial Measures

Two possible approaches to remedying the fatigue damage to the cross-girders and preventing further occurences were considered. These were:

- to make the deck act compositely with the main girders
- to improve the articulation between the deck, cross-girders and main girders.

Both approaches would involve rewelding the damaged welds where appropriate and necessary. The first solution was considered to be too expensive and so a solution based on the second was devised. Two possible ways of providing better articulation were considered; one was to encourage rocking rather than bending at each end of the bearing stiffener, the other was to brace the cross-girders rigidly to the deck so as to prevent all further racking movements and to provide bearings under each cross-girder to allow sliding movements to take place.

In the event it was decided to carry out trials on some of the spans using the former approach with the results being monitored. The existing fillet welds were cut out and replaced by full penetration butt welds. It was envisaged that the heavier weld would not only improve the fatigue life of the joint but would distort the flanges of the cross-girders sufficiently to pull the edges away from the concrete deck slab and the main girders and thus remove the load path from the stiffener tips. The repairs have been carried out and the resulting strains and differential movements are being monitored so that the effectiveness of the repairs can be assessed.

4. MAIDENHEAD BRIDGE - DESCRIPTION

4.1 History and Description of the Bridge

The Bridge is located on the M4 motorway where it crosses the River Thames. It was constructed in 1961 and originally carried dual 2 lane carriageways with cycle tracks and footpaths but in 1971 the cycle track was removed and the bridge converted to dual 3-lane carriageways. The bridge consists of 8 main shaped plate girders which are continuous over the main piers on the river banks and extend over short spans to abutments at each end (Fig 3). The girders are deeply haunched over the piers and the ends of the side spans are held down at the abutments.

The deck consists of an in-situ reinforced concrete slab which acts compositely with the main girders through inverted 'U' bars welded to tee-shaped sections which are in turn welded to the top flange of the main girder (Fig 4). The main girders are inter-connected not only by the deck slab but also by a series of transverse cross-frames. The main bearing stiffeners are constructed from rectangular trough section and extend from the main bearing blocks to the top flange and are welded to each side of the main girder webs.

4.2 Cracking in Bearing Stiffener Welds

The original sample survey covered 8 out of the 16 bearing stiffeners and in 3 cases revealed cracks at the toe of the fillet weld connecting the bearing stiffener to the top main flange. Some cracks were also discovered lower down the stiffeners where temporary erection cleats had been welded to facilitate the erection of the cross-bracing. A subsequent more comprehensive inspection revealed another 4 cases of toe cracks at the top of the bearing stiffeners. A sample was cut from one of the cracked welds and subjected to microscopic examination; the results indicated that the cracking was due to fatigue and it was considered that it was probably due to rotations of the deck slab over each girder under wheel loading.

5. MAIDENHEAD BRIDGE - FATIGUE ANALYSIS

5.1 Theoretical Stress Analysis

Theoretical stress analyses were carried out to find the stresses in the regions of the toe cracks at the top of the bearing stiffeners. In order to model the interaction of the deck slab, the bearing stiffeners and the transverse bracing, four separate 2D plane frame analyses of the cross-section were carried out to determine the stiffener stresses under wheel loads. The four analyses represented the following assumptions about the rigidity of the moment connection between the slab and the top of the bearing stiffener:

- bearing stiffeners rigidly connected to the deck slab
- stiffeners rotate with the slab but there is no significant resistance to horizontal movement
- shear connectors offer transverse shear resistance but no rotational restraint
- shear connectors offer no tensile or shear resistance.

In these analyses the slab was represented as an equivalent continuous transverse beam whose breadth was determined by further analysis.

A grillage model of a local 3 bay section of the deck slab was used to determine a more precise relationship between longitudinal wheel positions and the rotation of the slab at the bearing stiffener location. The opportunity was also taken to examine the effect of the concrete haunching over the main girder flanges and the lateral bending stiffness of the flange itself. In the analyses upper and lower bound values of stiffness were used based on 2 values of modular ratio.

5.2 Static Load Tests

Two commercial vehicles were used for a series of static live load tests on the bridge with the resulting deflections and strains at various locations being measured by transducers and resistance strain gauges. The strain gauges were used to determine the stresses in the bearing stiffeners while the transducers were used to determine the relative displacements of the girder flanges and the concrete deck slab. The large vehicle was used for the majority of the tests, being driven along a constant tracking position relative to the edge of the carriageway. The smaller vehicle was used to examine the effect of different wheel tracking positions on local stresses.

5.3 Comparison of Theoretical and Measured Results

All 4 plane frame analyses using the lower slab stiffness value predicted deflections which were substantially higher than those measured. However using the analysis which assumed a fully rigid moment connection between the slab and the stiffener and using the higher slab stiffness gave results which agreed reasonably well with those measured. This was considered to indicate that the slab-flange connection transmitted the slab rotations very effectively to the top of the bearing stiffeners.

The peak stresses calculated on the bearing stiffener using the above preferred method of analysis and the higher slab stiffness agreed well with the measured stresses. However it should be noted that the assumed slab stiffness was somewhat higher than would normally be used in design and so the agreement was to some extent rather artificial.

5.4 Prediction of Fatigue Life

In addition to the stress analyses some fatigue life assessments were carried out in accordance with the latest UK fatigue design code BS 5400: Part 10, and using the measured bearing stiffener stresses as a basis for the applied stress spectrum. The vehicle flows and weights were based on census point records from a location fairly close to the bridge. The object of the fatigue assessment was to determine whether the theoretical probability of failure of the welds was greater or less than had actually occurred. It was found that agreement could only be achieved if the stresses in the welds were considerably higher than the values calculated from the measured bearing stiffener stresses. This discrepancy was partly attributed to the uncertainty in determining the true weld throat size which is dependent on fit-up and the degree of root penetration. The general indication was that fatigue lives calculated by BS5400: Part 10 were longer than the actual lives.

5.5 Remedial Measures

Although various remedial measures were considered, including repairing the cracks by replacement welds with increased throat thickness, such a method of repair was rejected in favour of some form of deck stiffening aimed at reducing the deck rotations and consequent bearing stiffener weld stresses. The repair method adopted consisted of providing twin lines of universal beams to support the deck on both sides of the pier supports. These UB were fixed to the webs of the main girders by means of bolted cleats. The beams were fixed to the slab at mid-span by means of anchor bolts set in resin which were bolted to plates welded to the top flange of the beams. Additionally a similar connection was made between the top boom of the existing cross-bracing and the underneath of the deck slab (at the line at the pier supports). No repair was done to the cracked welds due to the risks involved in attempting such an operation on a highly stressed tension flange.

6. DISCUSSION

Although the 2 examples of fatigue damage in existing major steel bridges are of interest in themselves, there are a number of observations which can be made regarding fatigue design and assessment in general.

6.1 Fatigue Behaviour of Existing Structures

In both bridges described the fatigue failures occured due to the structures behaving in ways which had not been foreseen or allowed for in the design. In one case it was the racking movement of the cross-girders and in the other it was the rotation of the main girder top flange due to the deflection of the concrete deck. In both cases the welds affected would not be classed as structural welds since their purpose was to fix the stiffeners in place rather than to carry a direct load or shear force.

The examples described show the difficulties in determining the real stresses occuring in structural details, particularly those arising from secondary causes. In both cases different modes of structural behaviour had to be tried and it was also found that the calculated stresses were very dependant upon the fit-up between the different elements. It was only because in-situ strain gauge measurements were taken on the structures that it was possible to select the most appropriate assumptions regarding the structural behaviour and obtain reasonable agreement between experiment and theory.

The examples underline the importance of understanding the causes of any fatigue failure before undertaking any repairs. By identifying the cause of a failure it is possible to see for instance whether the crack should be rewelded or whether other remedial actions, such as modifying the structural behaviour, should be carried out. If such a study is not done then any repair welding may be ineffective in prolonging the fatigue life of the structure.

Although cracking occured in both bridges, and was fairly extensive in one bridge, it was not considered serious enough to prevent the continued use of the bridges concerned. There is thus a difficult decision in such cases as to whether to carry out repairs, which itself may be a costly and risky operation, particularly if it is undertaken under traffic, or whether to just monitor the cracking to see that it does not spread into a more sensitive part of the structure. In one of the cases quoted the cracks were not repaired and the remedial measures were limited to carrying out strengthening to modify the structural behaviour.

6.2 Implications for Fatigue Design

Unless the designer recognises the potential sources of fatigue damage in his structure then the existence of up-to-date codes of practice or design standards based on the latest fatigue testing data will be of little help in achieving satisfactory structures. There is a need for education to help the designer recognise the unlikely areas where fatigue damage can occur and particularly to make him aware of the effects of displacements in producing secondary stresses in any sort of welded connection.

The case studies have also highlighted the difficulties in deriving the real stresses occuring in structural details, particularly those arising as a result of secondary action. Stress levels have the major influence on fatigue damage and yet at present a relatively small proportion of fatigue research is devoted to the prediction of stresses, although there is some being done in connection with off-shore structures. There is thus a need for a better balance in fatigue research with more resources being devoted to the determination of stresses.

In this connection too there is a case for the testing of larger details which are more truly representative of the details found in actual designs. At present the majority of fatigue information is based on laboratory tests on relatively small scale idealised specimens, and so there are added uncertainties introduced in applying these results to real life structures. In other branches of engineering such as mechanical and aeronautical the testing of full scale prototype design details is common and yet this is hardly ever done in general construction although in the off-shore field large specimens are now being tested. Perhaps this trend for larger scale realistic testing will be taken up by the construction industry.

Finally there is a need to appraise the current approach to fatigue design, as for example set out in the UK code BS 5400: Part 10, to see whether a more pragmatic alternative approach might not be just as effective. There are many uncertainties involved in the present fatigue calculations ranging from stress prediction, loading, stress cycle counting, detail classification and fit-up to Miner's rule itself, so that the reliability of any fatigue calculation is very much in doubt. And yet, as the survey revealed, the fatigue problems that have been discovered have been in areas of secondary structural importance and have not been investigated at all for fatigue in the original design. There is a case therefore for developing a series of standard details or connections which would be shown by large scale tests or otherwise to have satisfactory fatigue performance under given load spectra. The approach would be one based on the adoption of good and proven design practices rather than on detailed calculation and assessment.

7. ACKNOWLEDGEMENTS

The work described in this paper was carried out on behalf of the Bridges Engineering (Design Standards) Division of the Roads and Local Transport Group of the Department of Transport by Messrs Sandberg, Inspecting Engineers, and G Maunsell and Partners, Consulting Engineers. The in-situ static loading tests were carried out by the Transport and Road Research Laboratory of the Department of Transport, and the paper is published by permission of the Deputy Secretary, RLT.

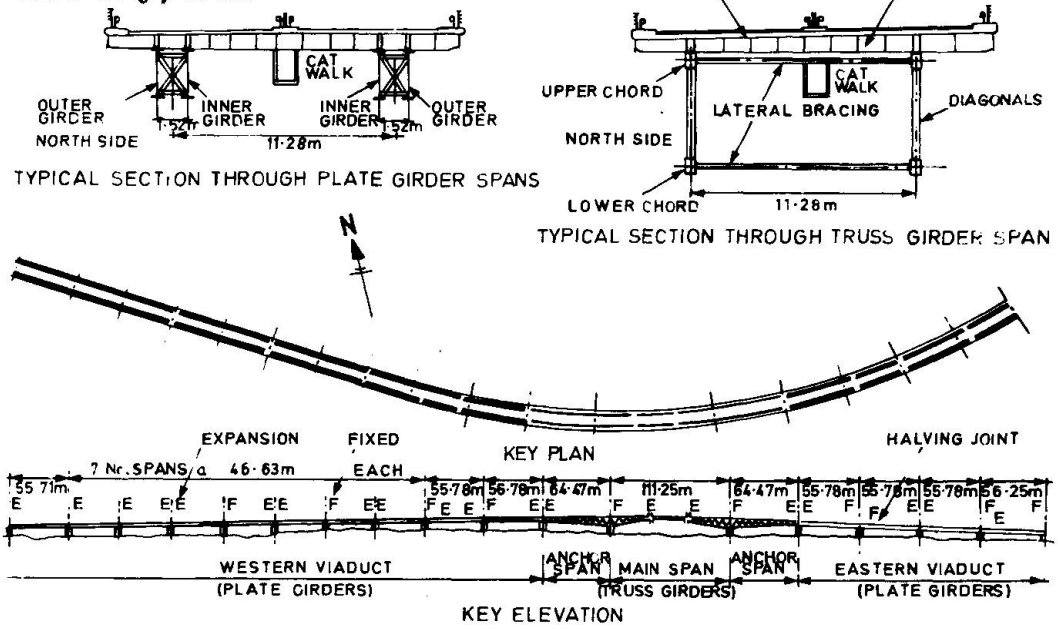

GENERAL ARRANGEMENT OF VIADUCT FIG. 1.

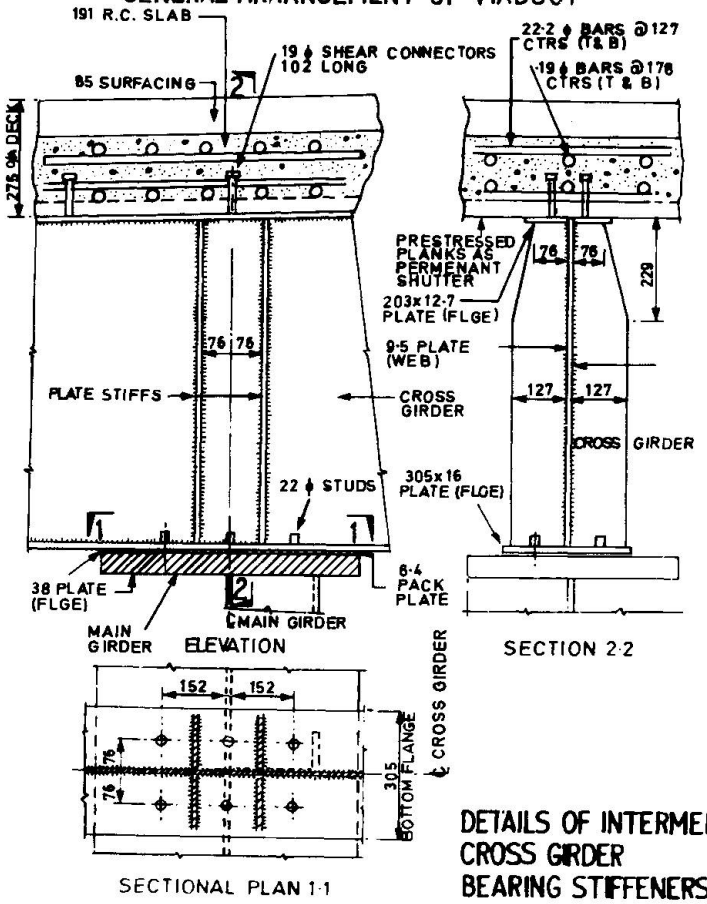

DETAILS OF INTERMEDIATE CROSS GIRDER BEARING STIFFENERS FIG. 2

8F

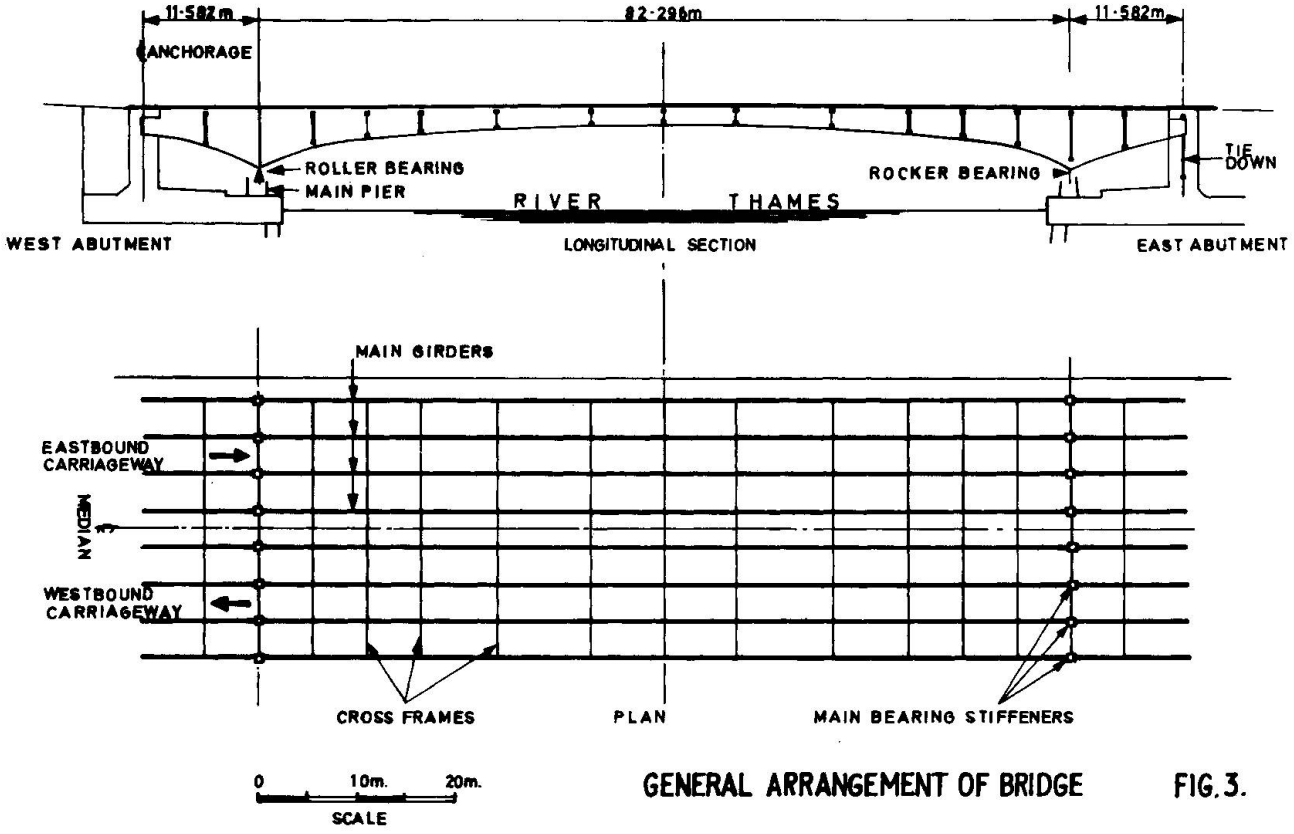

GENERAL ARRANGEMENT OF BRIDGE FIG. 3.

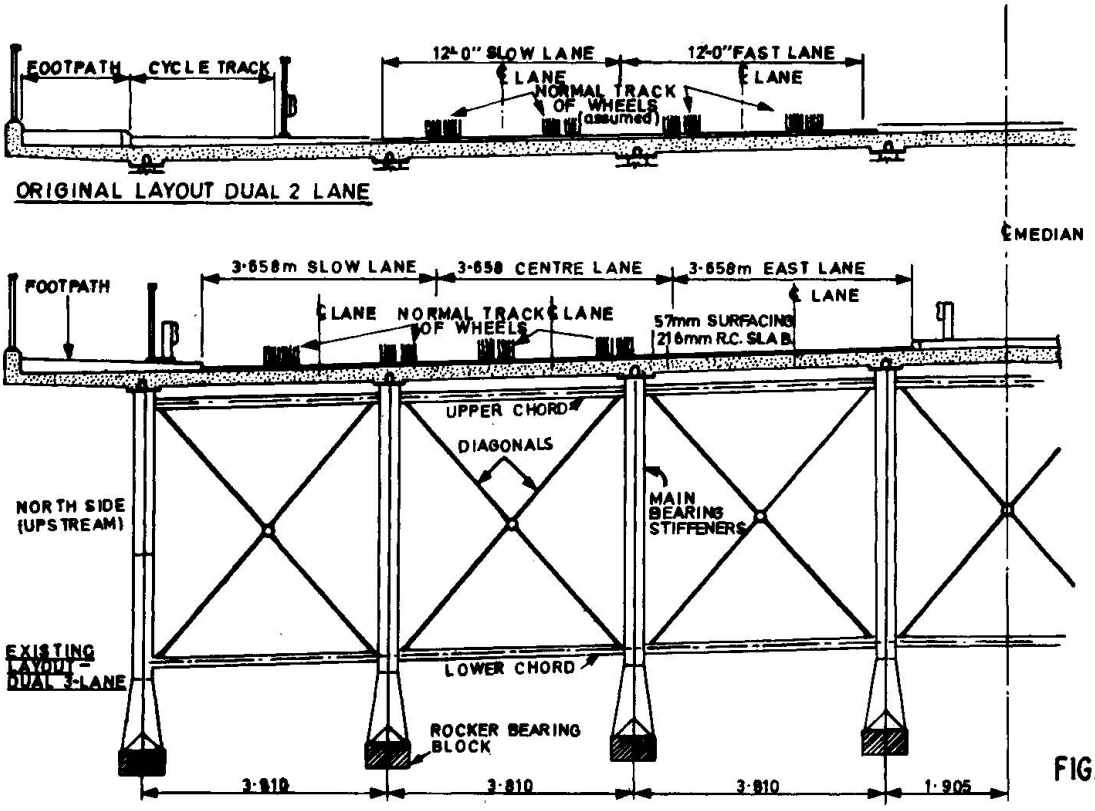

FIG. 4.

CROSS-SECTION THROUGH SUPERSTRUCTURE AT PIER UNDER EASTBOUND CARRIAGEWAY

Design and Retrofit for Fatigue Damage in Web Gap

Calcul et réparation des dégâts dus à la fatigue dans les âmes de poutres

Bemessung und Reparatur von Ermüdungsschäden im Steg von Stahlträgern

THOMAS A. FISHER
Steinman, Boynton, Gronquist and London
New York, NY, USA

JOHN W. FISHER
Prof., Assoc., Dir.
Lehigh University
Bethlehem, PA, USA

CELAL N. KOSTEM
Prof.
Lehigh University
Bethlehem, PA, USA

DENNIS R. MERTZ
Research Assistant
Lehigh University
Bethlehem, PA, USA

SUMMARY
Unanticipated fatigue cracking has resulted because of out-of-plane distortions as a result of the three dimensional behaviour of structures. This paper provides a summary of two separate studies. In one, a recommendation is provided to minimize cracking in the web at diaphragm connection plates in right bridges. The second reviews retrofit procedures for the cracking in longitudinal girder webs at floor beam connection plates.

RESUME
Des fissures imprévues de fatigue ont été constatées à cause des distorsions hors de leur plan des âmes de poutres dues au comportement tridimensionnel des structures. Cet article fournit un résumé de deux études séparées. Dans l'une, une proposition est faite en vue de diminuer le risque de fissuration dans l'âme au droit des raidisseurs pour les ponts. La seconde présente des méthodes de réparation des fissures se produisant à la liaison des âmes de poutres-maîtresses avec les entretoises.

ZUSAMMENFASSUNG
Infolge der räumlichen Tragwirkung stellten sich beim Anschluss der Querträger an die Längsträger unerwartete Ermüdungsrisse ein. Der Beitrag behandelt zusammenfassend zwei verschiedene Untersuchungen. In der ersten Studie wird eine Empfehlung gegeben wie die Ermüdungsrisse beim Anschluss der Querträger an die Stege der Brückenlängsträger auf ein Mindestmass beschränkt werden können. Die zweite Untersuchung bespricht Reparaturmethoden für die Risse in den Stegen der Längsträger.

1. INTRODUCTION

The past ten years have seen much with regard to the development of fatigue design criteria for bridges [1]. Design curves have been established for typical details, and yet fatigue cracking of bridges still occurs. Most frequently, this cracking has resulted because of unanticipated distortions as a result of the three dimensional behavior of the structure. However, cracks have also developed from poor design details and large initial flaws which were not detected nor recognizable as being significant at the time of fabrication. Most bridges are designed for two dimensional behavior with slight provision, if any, listed for consideration of the third dimensional effects on the structure [2].

This paper provides a summary of two separate studies. In one, an analysis and recommendation to minimize cracking in the web at diaphragm connection plates of right bridges is provided. In the second, retrofit procedures are suggested for the cracking that has developed in the longitudinal girder webs at floor beam connection plates.

The diaphragm connection plate is assumed to be welded to the web and compression flange but cut short or tight fit to the tension flange. A comparable condition existed at the floor beam connection plates. A review of a typical floor beam girder bridge is given in Ref. 3, together with the results of an analysis and summary of experimental measurements.

2. DESIGN CRITERIA FOR DIAPHRAGM CONNECTION PLATES

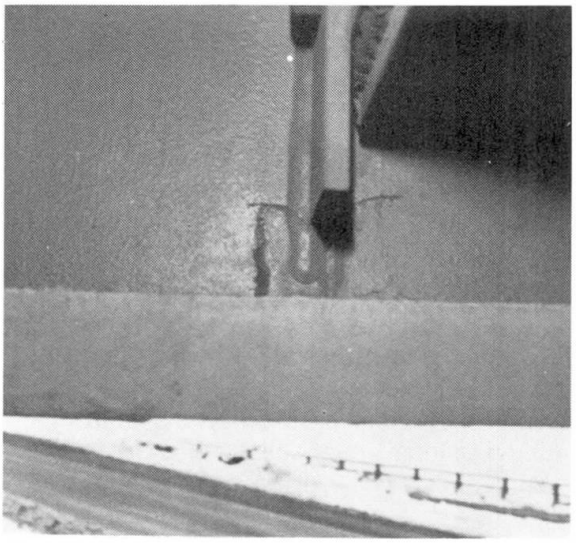

Fig. 1 Cracking at Transverse Diaphragm Web Connection Plate (Skewed Bridge)

Figure 1 shows an example of a detail which developed a fatigue crack. This crack is caused by displacements in the third dimension which occur as a result of interaction between primary (main girders) and secondary members (cross-frames, diaphragms, lateral bracings, etc.). This is the out-of-plane displacement which is not considered in the present design practice [2].

To define the interaction between the primary and secondary members, and to determine the extent of the contribution of various design parameters to the stresses developed in the web gap region (e.g. web thickness, flange thickness, gap length, etc.), an analytical study was undertaken [4]. The scope and results of the study are too extensive to be completely covered in this paper. Thus, only the highlights of this study will be presented. A "typical" bridge was chosen to be the prototype for the investigation (Figs. 2 and 3). All design dimensions and details of the bridge reflect the current design practice in the U.S.A. This structure was modeled using the finite element method and Program SAP IV [5]. The primary finite element model accounted for all structural details. Subsequently, the structural detail region of interest, the web gap region, was substructured using a highly refined finite element mesh. Various design parameters were changed to assess their effects on the stress concentration near the web gap region. Some of these parameters were: different vehicular configurations, placement of the vehicle, stiffness of the cross-bracings, connection details of the cross-bracings, web and flange thickness of main girders, and web gap length.

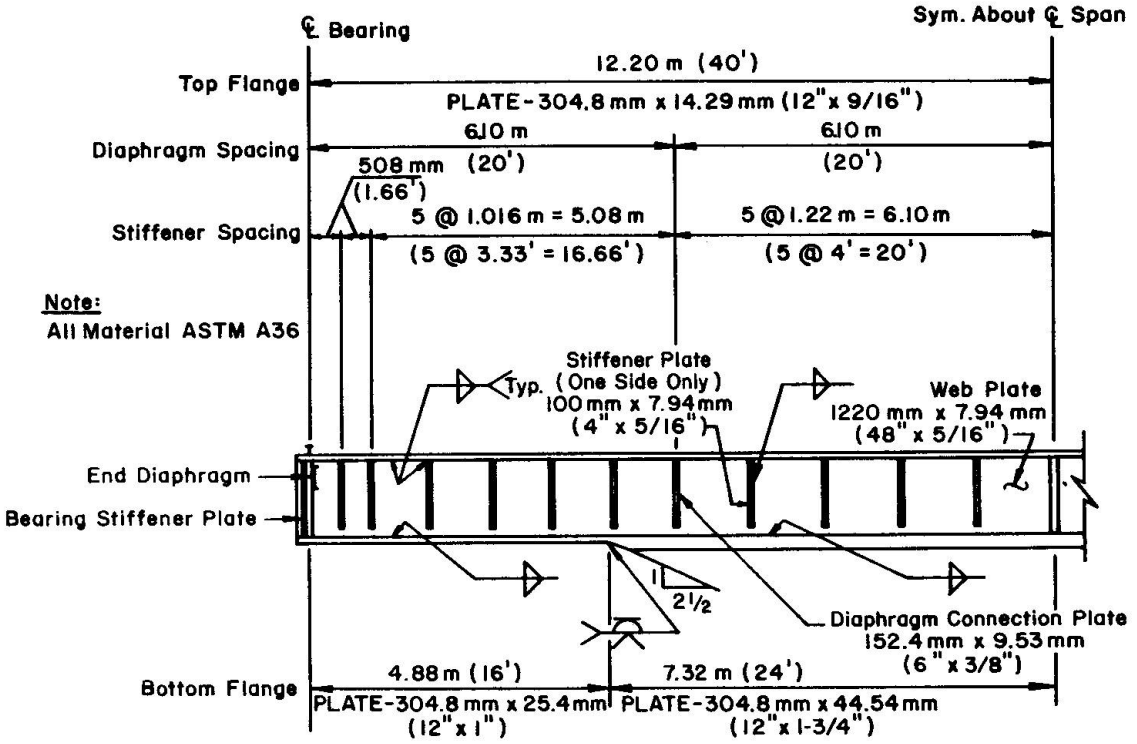

Fig. 2 Elevation of the Bridge Girder

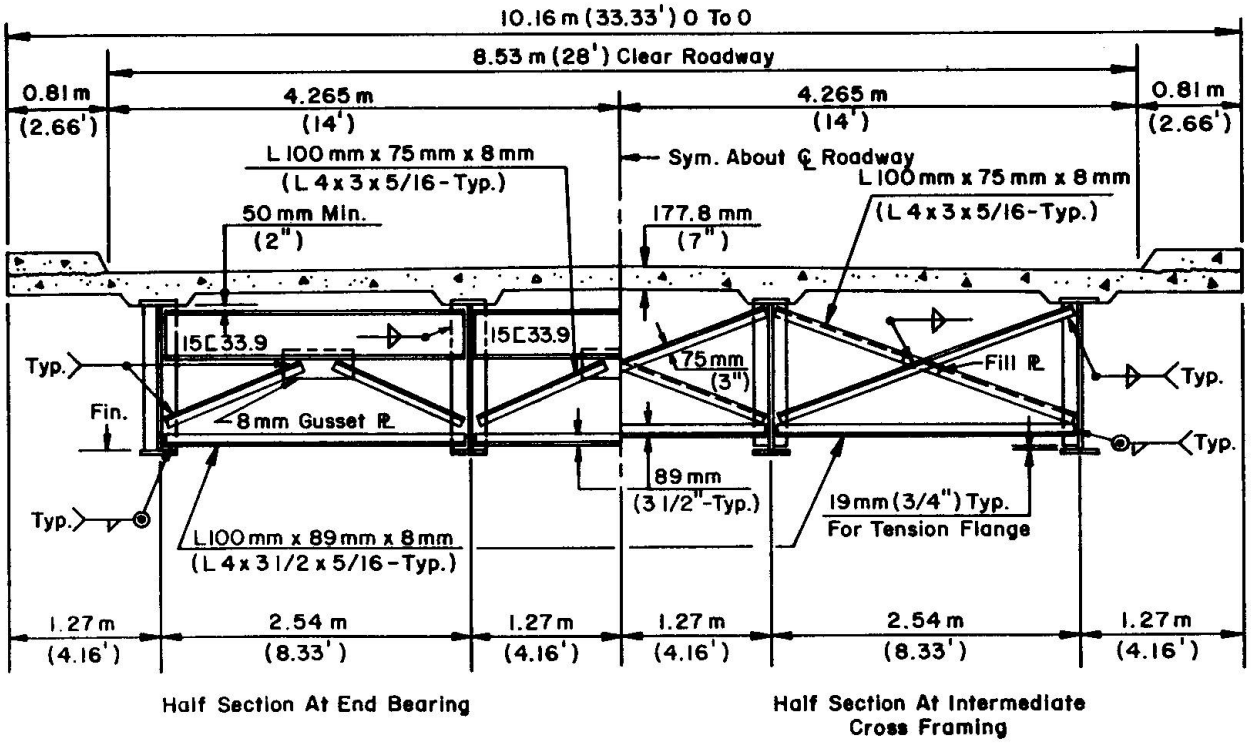

Fig. 3 The Cross-Section of the Bridge

The study indicated that a large stress level exists in the web in the immediate vicinity of the tip of the cut short stiffener. The stress buildup decays rapidly along the length of the girder. The cross-bracing introduces nonnegligible

local deformations in the web of the girders. All common detail connections between the cross-bracings and the main girders were found to be "moment resistant connections." It was also noted that practical changes in the dimensions of the flange thickness do not appreciably change the magnitude of the stress level. It was noted that increased web thicknesses of the girders significantly reduce the secondary stresses, if the gap length is greater than about 51 mm. However, for small gaps (less than 51 mm) the increased thickness of the web adversely affected the web stress.

Observations have disclosed that fitted transverse plate details resulted in the highest web stresses, whereas welded stiffeners produced the lowest stresses (292.3 MPa and 1.0 MPa, respectively). These stresses agreed with observed field data and accentuated the presence of stress concentrations in the detail [1,6]. The distortion of the web gap region at the fitted stiffener focused into a small gap (1.6 mm), resulting in large web stress. This stress buildup was due to the geometry of the region; these stresses do not include effects of residual stress.

The range of stress which occurred in the web gap region was determined to be caused by the relative displacement and rotation between the end of the cut short stiffener and tension flange. A comparison of the theoretical stress ranges to experimental data was then conducted. This was facilitated by using the crack growth relationship:

$$N = \int_{a_i}^{a_f} C \frac{da}{\Delta K^3} = C' S_r^{-3}$$

with an initial crack size of 0.762 mm. A final through thickness crack size of 28.6 mm was also selected, but this value had very little effect on the fatigue life estimates. This final crack size was selected, because it represented the length of a typical crack for the experimental data (Fig. 4) [7]. The deflections used in plotting the theoretical values were the relative displacement between the end of the cut short stiffener and the tension flange. This comparison between experimental and theoretical data is shown in Fig. 4. Figure 4 shows that

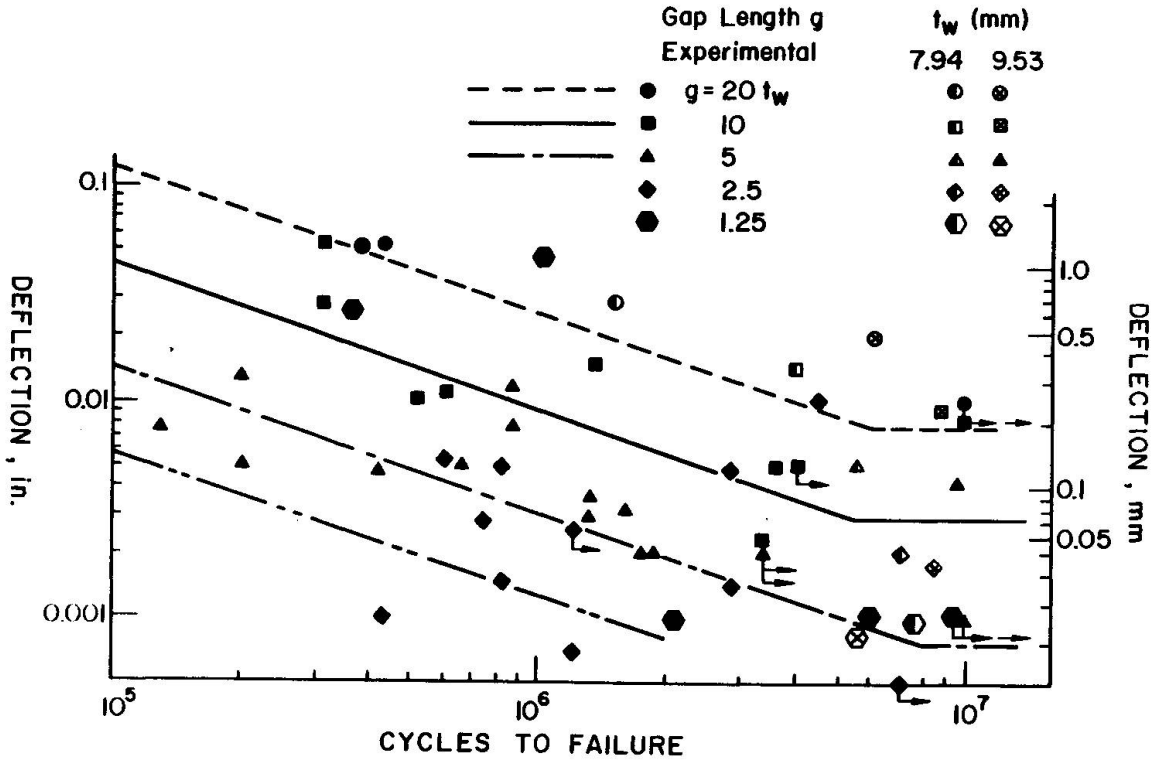

Fig. 4 Experimental and Theoretical Results of Out-of-Plane Displacement

the theoretical data followed the same trends as the experimental data. The theoretical fatigue life estimates generally overestimated the experimental fatigue lives of the details.

Parametric studies were conducted to determine the variation of the maximum web gap stress with varying gap length, web thickness and type of connection of cross-bracing to the transverse connection plate. The results of several studies can be seen in Fig. 4. They correspond to 7.94 mm web with moment connection and a 9.53 mm web with moment connection. The parametric studies permit the following observations and recommendations. The out-of-plane web stresses can be minimized by providing a gap of six to ten times the thickness of the web. They can be effectively eliminated if the transverse connection plate is welded to the tension flange. Welding the transverse connection plate to the tension flange should satisfy the fatigue restrictions of [2], Category "C", with only minor adjustments to the original girder design, because the end of the cut short stiffener is very close to the tension flange and is also classified as a Category "C" detail. If a gap of six to ten times the web thickness is selected, then web buckling under tension field action should be checked.

3. RETROFITTING FLOOR BEAM - GIRDER CONNECTIONS

In many existing structures, high out-of-plane bending and shear stresses in the short, flexible web gaps described in Section 2 for diaphragm connection plates and discussed in Refs. 1 and 3 for floor beam-girder connection plates, are induced by the out-of-plane displacement of the web. This produces fatigue cracking in the web at the weld toe regions of the web-flange welds, the ends of the connection plate-web welds, and/or cracking in the stiffener web weld which originates from the weld root. The problem of out-of-plane displacement-induced fatigue cracking is minimized or eliminated in existing structures by either minimizing or accommodating the displacement. Three techniques have been used to retrofit out-of-plane displacement induced fatigue damaged highway bridges and will be examined in detail in this section. The retrofitting techniques all deal with modification of the flexibility of the short web gap.

Upon the propagation of a fatigue crack in the short web gap, at the junction of the web and flange, and/or at the end of the transverse (vertical) connection plates, the flexibility of the gap relative to out-of-plane displacement has been increased, as the crack provides a horizontal slot. Therefore, when the displacement-induced stress has been reduced sufficiently due to the lengths of the cracks, drilling holes at the crack tips will often constitute a successful retrofit at diaphragm and floor beam connection plates. Figure 5 shows a schematic of the cracks, retrofit holes and resulting displacement.

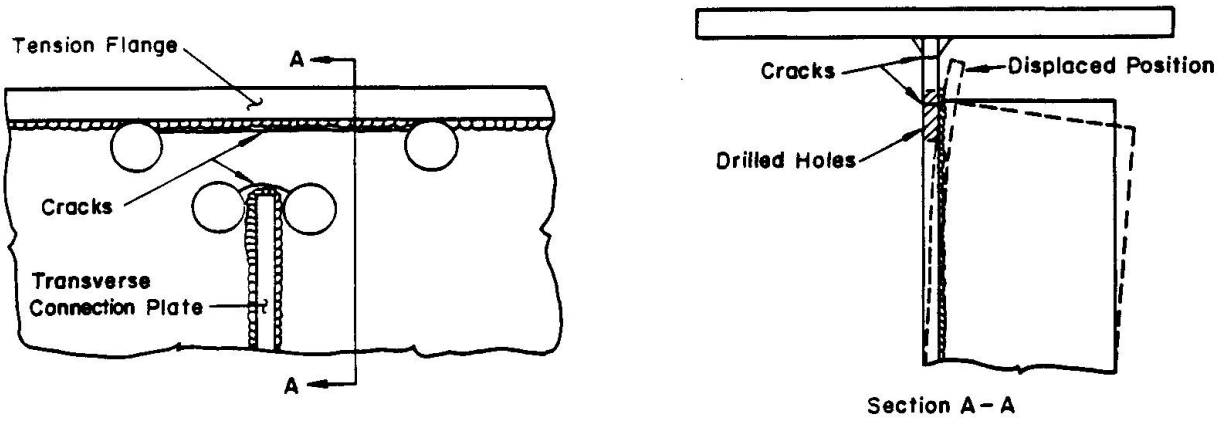

Fig. 5 Schematic of Displacement-Induced Cracks

Several bridge structures have been retrofitted by this procedure for at least eight years and have not shown any evidence of further crack propagation [3,8]. Most of these structures are located on high volume arteries and are subjected to one to two million passages of trucks each year.

In other cases, the cracking itself may not lower the cyclic stress enough, and cracking may eventually reinitiate from the drilled holes. Thus, other more involved retrofitting techniques have been used ir a number of bridge structures where such conditions were thought to exist.

A more reliable method to increase the flexibility of the web gap, and thus better accommodate the out-of-plane displacement, as well as prevent the reinitiation of cracks from the drilled holes, involves the removal of a portion of the connection plate (stiffener) adjacent to the web gap, as illustrated in Fig. 6. Through the removal of this stiffening element, the web gap can be lengthened to accommodate the displacement with a significant reduction in out-of-plane bending stress [1]. This decreases the stress range throughout the web gap between the web-flange fillet weld toe and the end of the connection plate, so that cyclic stresses are below the fatigue limit. This insures that cracks do not reinitiate from the holes drilled at the crack tips.

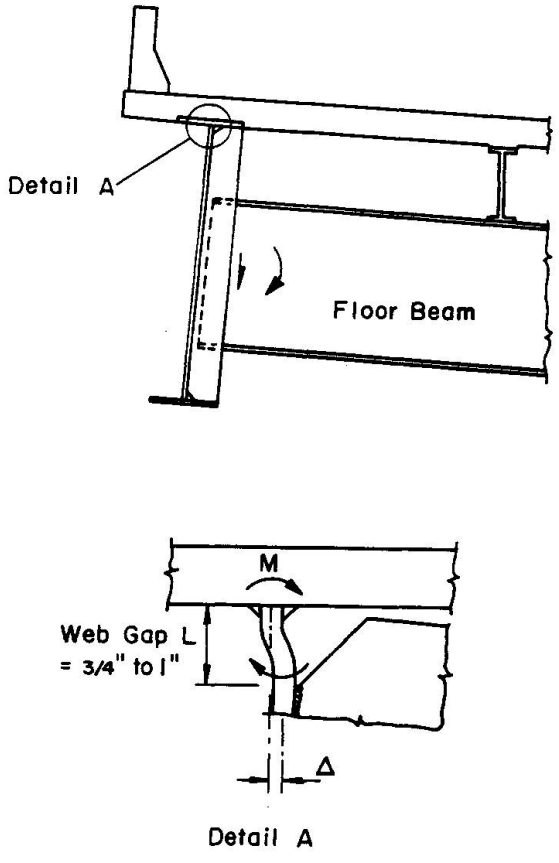

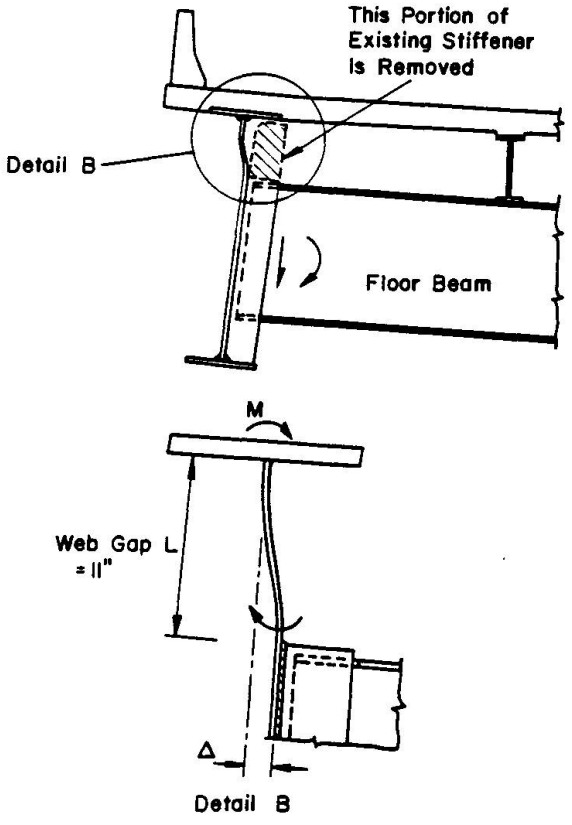

Fig. 6a Distortion of Original Web Gap Fig. 6b Distortion of Retrofitted Web Gap

In order to remove a portion of the connection plate, 50 mm diameter holes are drilled or cut by hole saw in the connection plate tangent to the girder web, as illustrated in Fig. 7. The hole is placed at the depth the stiffener is to be cut back. The connection plate is then removed by cutting vertically along the fillet weld connecting it to the web and horizontally into the hole, as also shown in Fig. 7. The fillet weld and remaining connection plate are ground away from the web, and the horizontal cut edge of the connection plate is also ground smooth. Liquid penetrant inspection identifies any cracks in the web gap or along the web-flange connection.

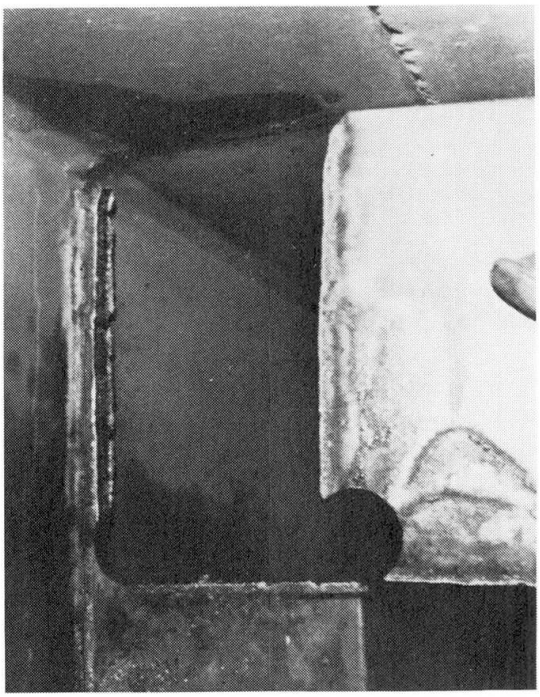

Fig. 7 Removal of a Portion of Connection Plate

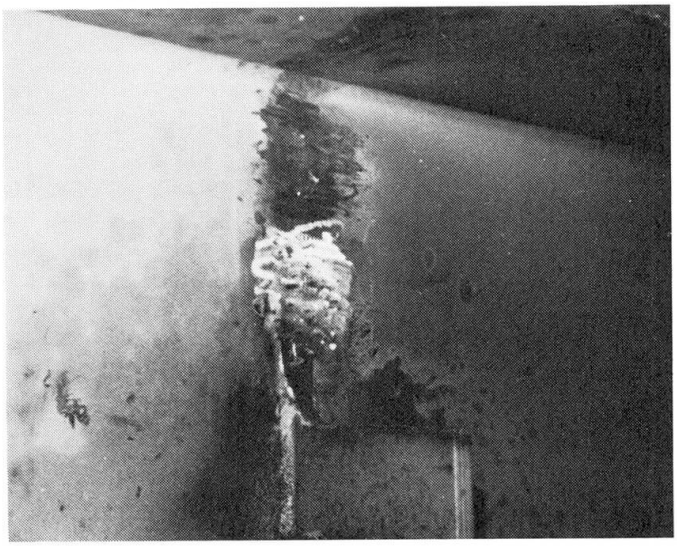

Fig. 8 Ground Surface of Web Gap

Figure 8 shows the surface of the web gap. Holes are then drilled in the web at the crack tip to prevent cracks from further propagation. Figure 9 shows a typical condition in the web gap with drilled holes isolating the cracked areas. High strength bolts are then installed in the holes as shown in Fig. 10 and tightened in order to further enhance the fatigue resistance of the drilled crack tips.

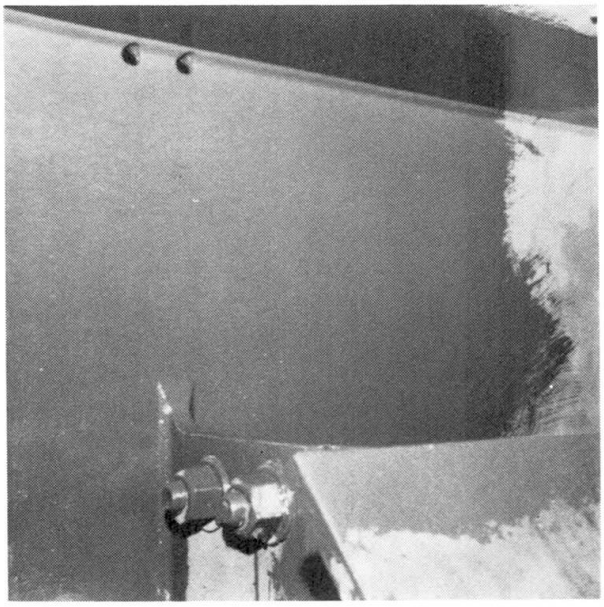

Fig. 9 Web with Drilled Holes Isolating the Cracks

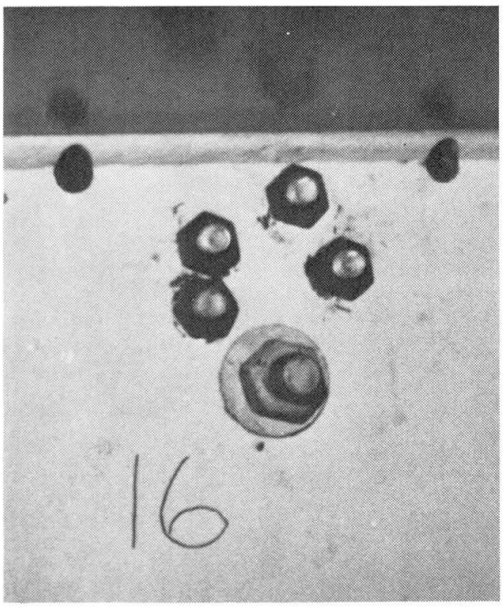

Fig. 10 Bolts Installed in Holes to Enhance Fatigue Resistance

The original short web gap has generally been lengthened to about 30.5 cm in order to accommodate the out-of-plane displacement in the web gap.

The isolated cracks can be checked to insure that fatigue cracks do not reinitiate by evaluating the parameters [9]:

$$\frac{\Delta K}{\sqrt{\rho}} < 10.5 \sqrt{\sigma_y}$$

where ΔK is the stress intensity range in the web between the edges of the retrofit holes in MPa $\sqrt{mm}$, ρ is the hole radius in mm and σ_y is the yield point of the web steel in MPa. The web bending stress due to traffic is generally low in the web, so that most of the retrofit holes are seldom greater than 24 mm.

A more extensive retrofit may be required if the transverse connection plates cannot be removed, because lateral forces are not displacement limited. This may result at piers where lateral forces are transmitted into the reactions. Under these conditions, it is desirable to prevent the movement in the web gap by attaching the transverse connection plate to the tension flange.

This can be accomplished by either welding or bolting the connection plate to the flange in order to provide a positive attachment and prevent the distortion. The alternative of welding the connection plate to the flange is generally not exercised for two reasons. First, there is concern regarding the quality of welds which can be provided under field conditions. Second, in older bridges, the weldability and fracture toughness of the flange material is unknown. Hence, welding the connection plate to the flange is generally not a practical alternative. The web gap distortion can be eliminated by providing a bolted connection between the connection plate and the flange. If the retrofit is carried out with the concrete slab in place, it is necessary to remove a rectangular portion of the slab in order to gain access to the embedded flange, as illustrated in Fig. 11. Bolt holes are then drilled in the flange and connection plate, and splice angles are inserted between the flange and the connection plate, as shown in Fig. 12. The resulting connection prevents distortion in the web gap.

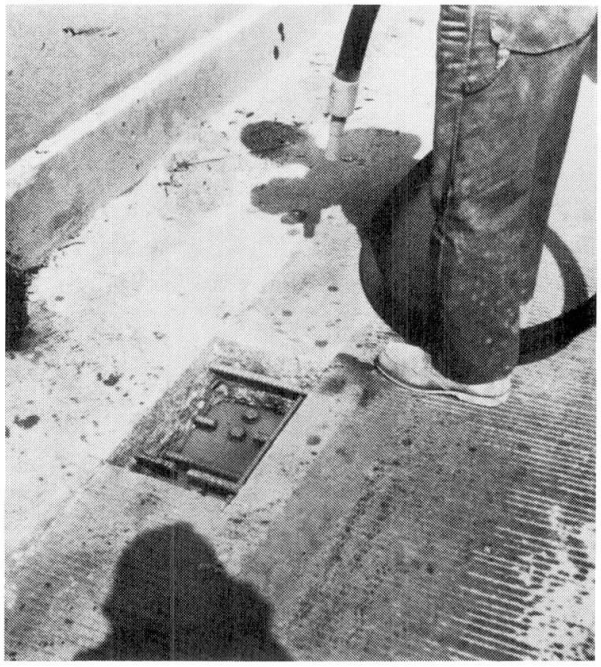

Fig. 11 Portion of Slab Removed to Gain Access to Flange

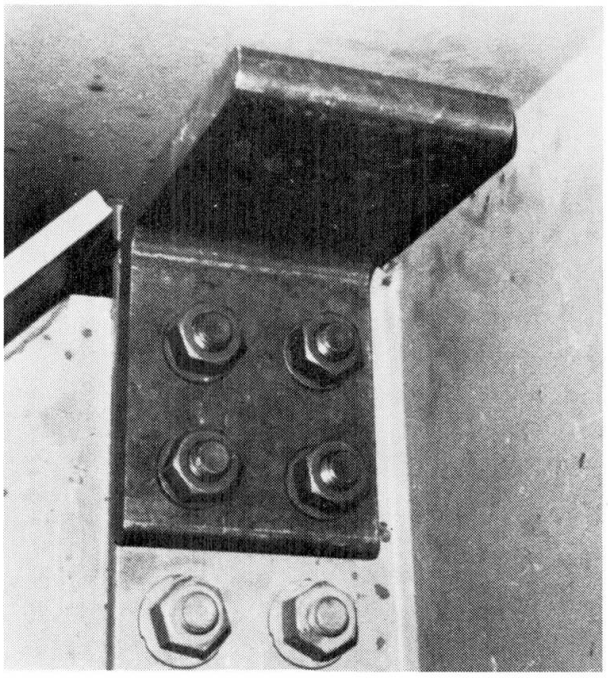

Fig. 12 Splice Angles Inserted Between Flange and Connection Plate

Bolting the connection plate to the flange is much more costly than removing a portion of the connection plate to increase flexibility. Therefore, this option should only be used when increasing web gap flexibility is not adequate to prevent further crack growth.

REFERENCES

1. Fisher, J. W.: BRIDGE FATIGUE GUIDE - DESIGN AND DETAILS, American Institute of Steel Construction, New York City, 1977.

2. American Association of State Highway and Transportation Officials: Standard Specifications for Highway Bridges, Washington, D.C., 1977.

3. Fisher, J. W., Fisher, T. A., and Kostem, C. N.: ENGINEERING STRUCTURES, Vol. 1, IPC Business Piers, October 1979.

4. Fisher, T. A. and Kostem, C. N.: THE INTERACTION OF PRIMARY AND SECONDARY MEMBERS IN MULTI-GIRDER COMPOSITE BRIDGES USING FINITE ELEMENTS, Fritz Engineering Laboratory Report No. 432.5, Lehigh University, Bethlehem, Pennsylvania, June 1979.

5. Bathe, K.-J., Wilson, E. L. and Peterson, F.E.: SAP IV - A STRUCTURAL ANALYSIS PROGRAM FOR STATIC AND DYNAMIC RESPONSE OF LINEAR SYSTEMS. Earthquake Engineering Research Center Report No. 73-11, University of California, Berkeley, California, 1973.

6. Fisher, J. W.: FATIGUE CRACKING IN BRIDGES FROM OUT-OF-PLANE DISPLACEMENTS, Canadian Structural Engineering Conference, 1978.

7. Fisher, J. W., Hausammann, H. and Pense, A. W.: RETROFITTING PROCEDURES FOR FATIGUE DAMAGED FULL-SCALE WELDED BRIDGE BEAMS, Fritz Engineering Laboratory Report No. 417.3, Lehigh University, Bethlehem, Pennsylvania, 1978.

8. Hsiong, W.: REPAIR OF POPLAR STREET COMPLEX BRIDGES IN EAST ST. LOUIS, Bridge Engineering, Vol. 1, Transportation Research Record 664, National Academy of Sciences, Washington, D.C., 1978.

9. Fisher, J. W., Barthelemy, B. M., Mertz, D. R. and Edinger, J. A., FATIGUE BEHAVIOR OF FULL-SCALE WELDED BRIDGE ATTACHMENTS, NCHRP 227, Transportation Research Board, Washington, D.C., 1980.

Leere Seite
Blank page
Page vide

Fatigue and Fracture Analysis of Defects in a Tied Arch Bridge

Fatigue et analyse de la rupture des défauts dans un pont-arc avec tirant

Ermüdungs- und Bruchanalyse von Schäden an einer Stahlbogenbrücke mit Zugband

JOHN W. FISHER
Professor
Lehigh University
Bethlehem, PA, USA

HANS HAUSAMMANN
Research Engineer
ICOM-Construction Métallique
Lausanne, Switzerland

ALAN W. PENSE
Professor
Lehigh University
Bethlehem, PA, USA

SUMMARY
Cracks were detected in the corner weld of the box girders forming the tension members of the tied arch bridge over the Gulf Outlet in Louisiana. A fractographic examination of several cracked corner welds revealed that the cracks extended into the weld metal and heat-affected zone. An analysis of the fatigue and fracture behaviour of the cracks is provided.

RESUME
Des fissures ont été détectées dans la soudure d'angle des poutres en caisson formant la membrure tendue du pont-arc avec tirant sur la „Gulf Outlet" en Louisiane. Un examen fractographique de plusieurs soudures d'angle fissurées a révélé que les fissures se propagent dans le métal de la soudure et dans la zone affectée par l'échauffement. Une analyse du comportement à la fatigue et à la rupture des fissures a été fournie.

ZUSAMMENFASSUNG
In den Ecken der Kastenträger, die das Zugband der Bogenbrücke über den Golf von Outlet in Louisiana bilden, wurden Risse beobachtet. Die fraktographische Untersuchung mehrerer gerissener Eckschweissungen zeigte, dass sich die Risse in das Schweissgut und den durch Hitze beeinflussten Umgebungsbereich fortpflanzten. Eine Untersuchung des Ermüdungs- und Bruchverhaltens der Risse wird präsentiert.

1. INTRODUCTION

The tension members of several tied arch bridges consist of welded built-up sections. These sections are often welded box girders fabricated of single strength steel. High stresses due to the dead load and the live load are carried by these sections. These members are of major structural importance, because a fracture of a tie would likely result in a catastrophic failure of the bridge.

The Mississippi River Gulf Outlet Bridge is located near New Orleans, Louisiana. Figure 1 shows a view of the structure and a tie girder. The tie girders were fabricated of A514 steel. The suspended span is 170.7 m long, and the trusses are spaced 22.86 m apart.

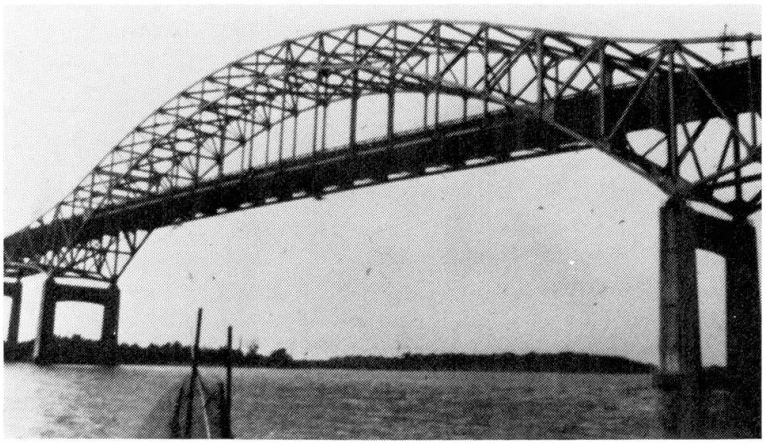

Fig. 1a Overview of Structure

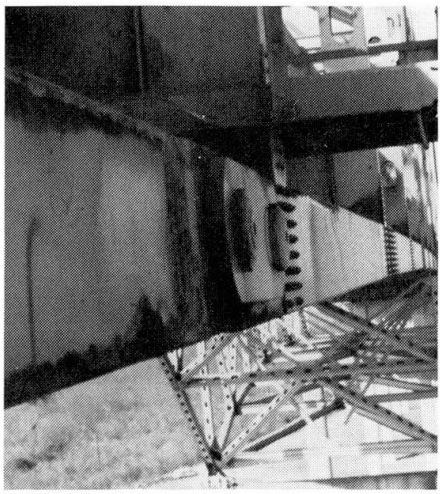

Fig. 1b View of Tie Girder

The tie girders in the Gulf Outlet Bridge are box sections. The web plates are 711 m high and 19 mm thick, the flanges are 635 mm wide and 16 mm thick. The plates are fillet welded at the four box corners. At floor beam connections and at the pinned connection of the tie (see Fig. 1b), additional interior corner welds are used to transfer the forces. The dimensions of the box are shown in Fig. 2.

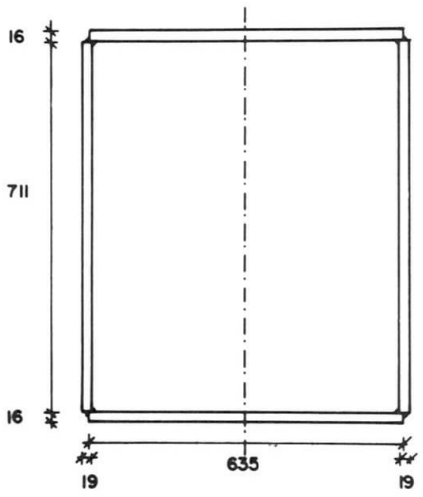

Fig. 2 Dimensions of Tie Girder (mm)

Fig. 3 Crack in Longitudinal Weld

Transverse cracking was inadvertently detected in the box corner fillet welds when the web groove welds at the pinned connection were being checked by radiography. Figure 3 shows one of the interior weld cracks after it was enhanced with liquid penetrant. Some cracks were below the surface and were only visible after slightly grinding the weld surface.

Several of the defects were removed from the box corners by coring (see Fig. 4a), so that detailed metallographic and fractographic studies could be carried out to ascertain the cause of cracking. Figure 4b shows the polished face of the box

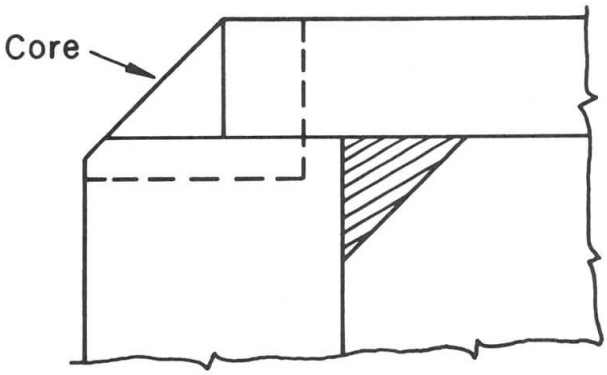

Fig. 4a Schematic Showing Core Sample at Web-Flange Corner Weld

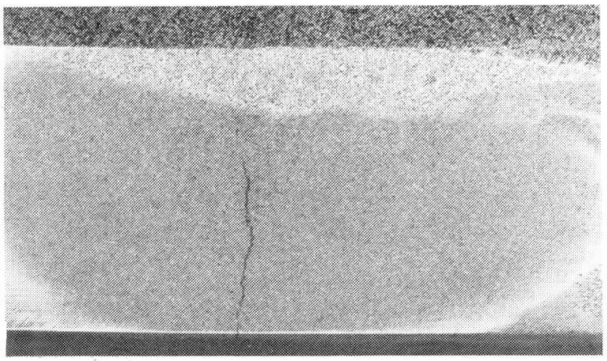

Fig. 4b Ground Surface of Weld Segment Showing Crack

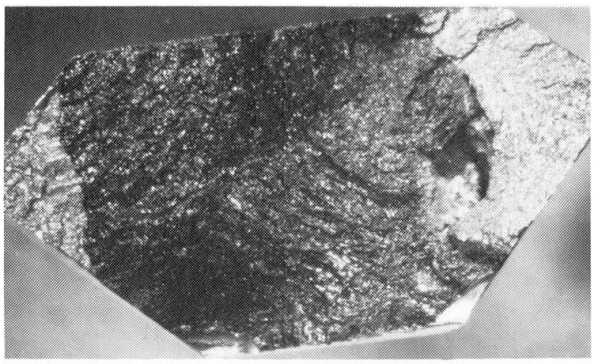

Fig. 4c Exposed Crack Surface

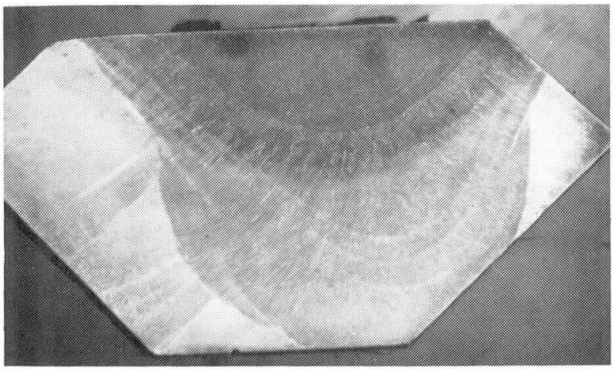

Fig. 4d Polished and Etched Surface Behind Crack

corner weld and the transverse weld crack that was observed. The small segment was broken open to expose the crack surface which is shown in Fig. 4c. A section just behind the crack surface was polished and etched and can be seen in Fig. 4d. This illustrates that multiple weld passes were added to the original submerged arc weld and that the crack extends throughout the corner weld into the heat-affected zone. On the whole, the fractographic examination of the crack surface suggested that the crack was produced during or shortly after welding. Some fatigue crack growth striations were also suggested in a few areas at very low ΔK levels. Similar transverse weld cracking has been reported in groove welds and attributed to hydrogen and residual stresses[1].

Because the cracks at the intersection between the web and the flange are oriented perpendicular to the main stress field due to the dead load and live load, an investigation was made to determine if these cracks could propagate under the cyclic live load stress. Small cracks may sharpen under cyclic load and also initiate brittle fracture, as a result of the high residual tensile stresses due to welding at the box corners.

2. STRESSES AT THE CRITICAL LOCATION

The bottom chord in a tied arch bridge is mainly subjected to high tensile forces due to the dead and live load and to residual stresses. The design calculations indicated a dead load stress of 252 MPa existed in the tie girder box of the Gulf Outlet Bridge. The dead load stress was assumed to be uniformly distributed over the cross-section.

The actual live load stress range was not known. The design live load stress range including an impact factor of 7.5%, is 48 MPa. Based on the design calculation and existing measurements on large bridge structures[2,3], the Miner effective stress range was estimated to be 14 MPa, and the highest regularly encountered live load stress range is 28 MPa.

The residual stress due to welding the box corners was estimated using a procedure outlined in Ref. 4. To predict the residual stresses and strains, a finite discretization at the cross-section was used.

The calculation of the residual stresses assumed an elastic-perfectly plastic stress-strain response and temperature dependent material properties. The variation of the temperature as a function of the time and the location on the cross-section for each weld pass has to be known. It has been shown that the temperature distribution at discrete time intervals must be known in order to minimize the calculation efforts[5].

The determination of the temperature distribution in the web and flange plate due to the heat input of welding is based on the principles of heat transfer in a thin semiinfinite plate. The temperature at a given location in the plate is a function of the heat input, the position of the location relative to the moving heat source (electrode) and various thermal properties of the plate. For the calculation of the temperature in the plates, the following assumptions were made[6]:

- Between 15 and 35% of the heat is lost, due to radiation and melting of the electrode,
- The temperature at some distance from the heat source remains unchanged,
- The heat source is a point source,
- The temperature is dependent on the distance between the heat source and the location of the point for which the temperature has to be predicted, and
- Half the heat produced by welding the web-flange connection goes into the web plate and half into the flange plate, independent of the thickness.

Different weld passes are made during the fabrication of the box girder. First, the plates are temporarily assembled with small tack welds. Then the automatic submerged arc welds at the outside corners are made. Next, longitudinal welds

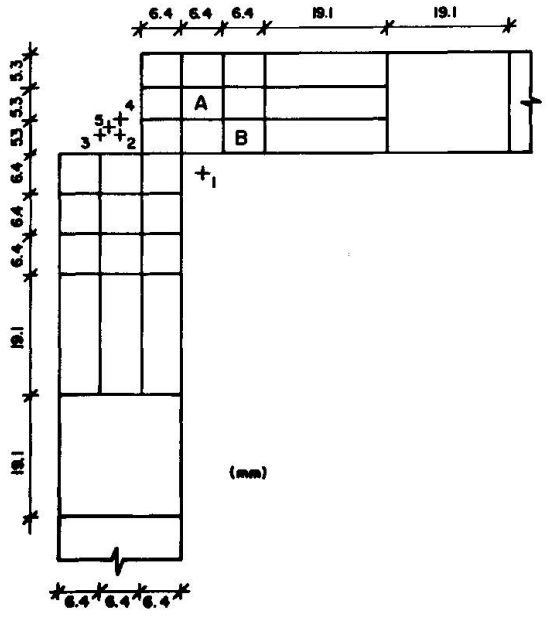

Fig. 5 Weld Sequence and Discretization near Box Corner Weld

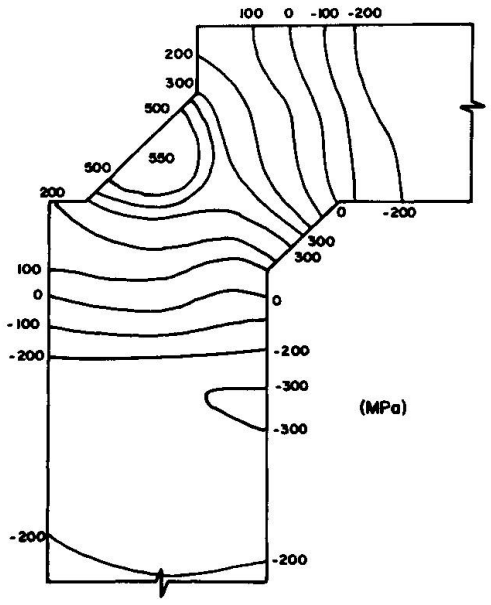

Fig. 6 Residual Stress Distribution near Box Corner Weld, Box Girder

inside the box are made manually, and finally several manual passes are made over the outside submerged arc weld. It is assumed that the total welding at one corner can be simulated with five weld passes.

The residual stresses due to welding were calculated using a computer program developed at the University of Missouri[4]. To calculate the stress distribution, the cross-section was divided into finite elements; part of the discretization is shown in Fig. 5, with the weld passes shown as crosses.

The residual stress distribution was calculated at the end of each weld pass. This distribution was used as the initial condition for the next weld pass. Based on the residual stress at the center of each element, the total distribution was derived using linear interpolation. The final stress distribution is shown in Figs. 6 and 7.

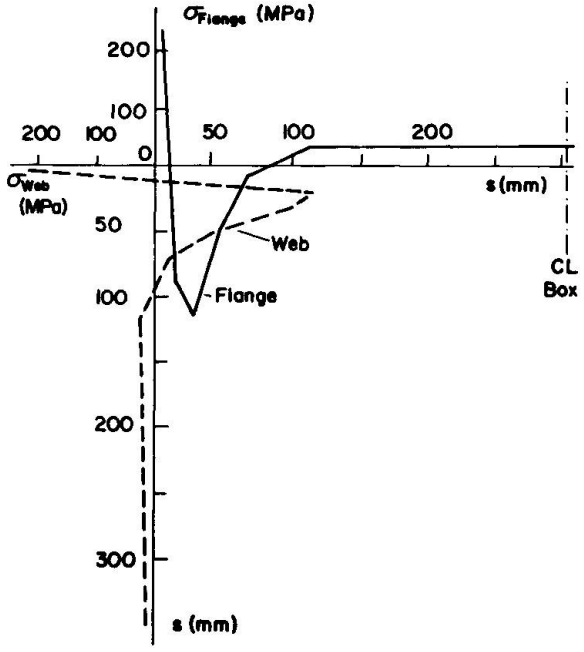

Fig. 7 Residual Stress Distribution due to Corner Welds in Middle Plan of Web and Flange Box Girder

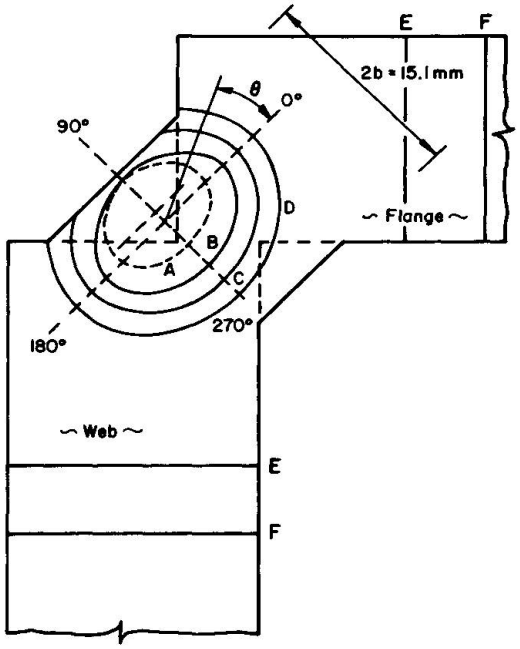

Fig. 8 Investigated Crack Shapes in Corner Weld, Box Girder

3. ANALYSIS OF THE CRACKS AT THE WELD CORNER

The cracks in the corner welds are of different shapes and sizes. Several shapes that were evaluated are shown in Fig. 8. It was assumed that the cracks can be analyzed as elliptical cracks circumscribing the flaw.

The total stress intensity factor is calculated using the principle of superposition. The K-value due to the uniformly applied dead and live load stress is calculated using the solution to an imbedded elliptical plan[7]. The K-value due to the residual stress shown in Fig. 7 was estimated using a procedure described in Ref. 8. The varying stress field is discretized by discrete point loads, and the corresponding K-value is calculated. The total K-value is obtained by an integration over the entire crack surface.

As the cracks are in the material of limited thickness, the K-factor has to be adjusted by the finite width and free surface correction factors.

All the cracks were close to the free surface. The material between the crack front and the weld surface is so thin, that it was easily ground away. This ligament is so small that it plastically deforms without initiating a brittle fracture. The load transmitted through this ligament is so small that it can be neglected. Instead of an internal elliptical crack, a U-shaped surface crack results.

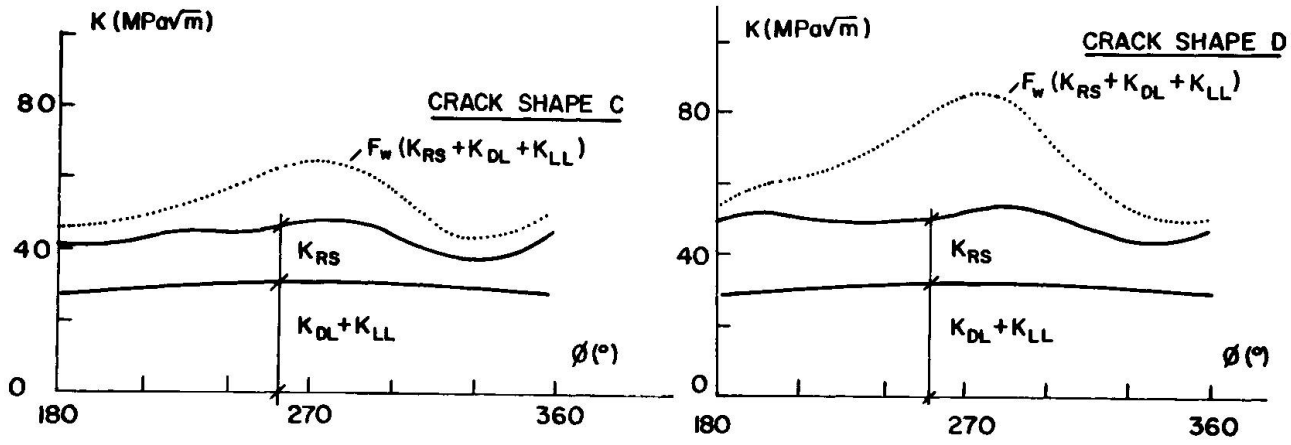

Fig. 9 Stress Intensity Factor for Cracks in Corner Weld

The crack shapes indicated in Fig. 8 were numerically evaluated, and two typical results are summarized in Fig. 9. The stress intensity factor is shown as a function of the phase angle θ (see Fig. 8). The stress intensity factor is shown for the dead and live load stress, as well as the residual stress. The dead and live load K-value is almost constant along the circumference because of the ratio a/c. Superimposed is the K-value resulting from the residual stress field. The stress intensity factors are corrected by the finite width and the free surface correction factor.

The crack front moves into the web and the flange plates as soon as the embedded crack becomes too large to be accommodated in the weld area of the web-flange welded connection. Typical crack stages in the web and flange are shown in Fig. 8 and indicated as E and F. These crack configurations were treated as two independent edge cracks. Both crack fronts (the front in the web and the front in the flange) propagate at the same rate, because the cyclic applied stress is uniform. The total crack opening is almost the same, because the residual stress distribution in the web is almost identical to the stress distribution in the flange. Hence, the crack in the web can be analyzed independent of the crack in the flange.

The analysis of a crack with an irregular crack front and stresses varying over the crack length and plate thickness was made using a numerical procedure. The numerical procedure is based upon the solution of a semiinfinite straight fronted three-dimensional crack. In order to obtain the K-value for different boundary conditions, the solution has to be normalized by $1/\pi$ and integrated between $-\pi/2$ to $\pi/2$ over the entire crack surface[8].

$$K = \frac{1}{\pi} \int_0^a \int_{-\pi/2}^{\pi/2} \sigma\ (a,\ \theta)\ d\theta\ da$$

This equation was evaluated numerically.

The stress intensity factor for the uniformly applied stress (σ_{LL}, σ_{DL}) was estimated using the closed form solution. The stress intensity factor due to residual stress was calculated separately. The stress at the box corner was replaced by a splitting force. Numerical results were obtained for the different crack conditions. The total stress intensity factor was obtained by superposition.

4. PREDICTED FATIGUE BEHAVIOR OF THE CRACKS AT THE WELD CORNER

It is of primary importance to know if fatigue crack propagation under the cyclic applied live load will occur for the crack shapes shown in Fig. 8. If fatigue crack growth under the cyclic applied live load stress is likely, then the cracks will increase in size, and brittle fracture could eventually result. If the crack geometry and the applied stress are small enough, no crack growth will occur. Small cracks may be tolerated if the structure's factor of safety is adequate against fracture throughout its service life. In order to establish the reserve against brittle fracture, the dimensions of the largest crack and the fracture toughness of the material has to be known for the lowest anticipated service temperature.

The cracks at the intersection of the web and flange are in a zone of high tensile residual stress. The R-ratio is close to unity which decreases the threshold stress intensity range to a minimum value of 2.75 MPa $\sqrt{m}$. The usual flaws at the fillet weld root (i.e. pores and slag) have contributed to the formation of transverse cold cracks in the weld. These cracks are irregular in shape, so that locally a higher stress intensity factor may exist. The crack tip is very sharp, because the cracks were caused by cold cracking.

The cyclic applied equivalent Miner stress range was approximated as 14 MPa $\sqrt{m}$ for axial stress and bending. For the crack initiation, the maximum possible stress range under service loads has to be considered. The maximum stress range due to the traffic load was assumed to be 28 MPa.

It was found that the stress intensity range is larger than ΔK_{TH} for all the crack shapes shown in Fig. 8. Crack shapes B, C and D exceed the crack growth threshold when the stress range is 14 MPa. The increase in the total stress intensity factor (due to traffic, dead load and residual stress) is rapid, as the crack approaches the back free surface. Figure 9 shows the stress intensity along the crack front for crack shapes C and D. A material with poor fracture toughness (i.e. 50 to 60 MPa $\sqrt{m}$) will likely fracture with crack propagation between crack shapes C and D. If the material has better fracture toughness, larger crack sizes can develop before crack instability. Fortunately all cracks were detected and retrofitted before this occurred.

5. RETROFITTING PROCEDURES

The examination of the defects and analysis indicated that it was desirable to grind and inspect with liquid penetrant all manually welded box corners. These locations were suspect, as it was likely that inadequate levels of preheat existed when the manual weld passes were made. Except for the pinned connections, these locations were confined to the bolted splices between the end of a member and the first internal diaphragm.

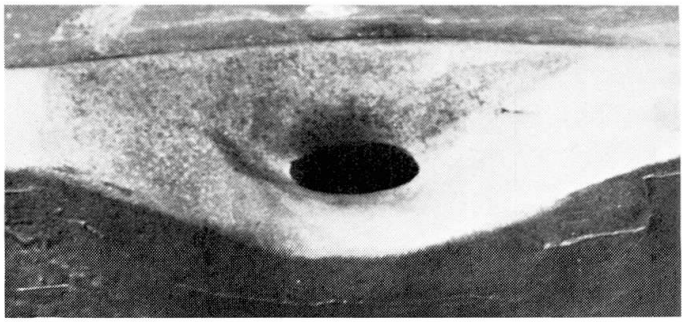

Fig. 10 Photo Showing Retrofit

All cracks in the longitudinal weldments were removed by either grinding, drilling or coring. Figure 10 shows a retrofitted region after removal of a crack. The ground area was checked by liquid penetrant to ensure that no crack tip remained in the structure.

6. CONCLUSIONS

The largest embedded cracks in the web-to-flange connections were found to be susceptible to fatigue crack propagation under the most severe service load conditions. Hence, the cracks in the weldments would enlarge and sharpen with an accumulation of stress cycles if not removed from the structure.

The transverse cracks in the longitudinal web-flange fillet welds were all caused at the time of fabrication. They were all located in manually made sections of the longitudinal weldments. This observation and the fractographic and metallographic examination all suggested these cracks were hydrogen related. All cracks removed from the structure for examination were found to originate at a porosity or entrapped slag and were in a region of high weld shrinkage stress.

The criticality of the transverse cracks were assessed by a fracture mechanics analysis considering the contributions of dead load, live load and welding residual stresses. This permitted the defects to be evaluated and removed in an expeditious manner.

7. REFERENCES

[1] Takahashi, E. and Iwai, K., PREVENTION OF THE TRANSVERSE CRACKS IN HEAVY WELDMENTS OF 2-14/C_r - 1 M_o STEEL THROUGH LOW TEMPERATURE POSTWELD HEAT TREATMENT, Transactions of the Japan Welding Society, Vol. 10, No. 1, April 1979.

[2] Fisher, J. W., et al., FATIGUE AND FRACTURAL RESISTANCE OF LIBERTY BRIDGE MEMBERS, Fritz Engineering Laboratory Report No. 420.2, Lehigh University, Bethlehem, PA, May 1981.

[3] Fisher, J. W., et al., AN EVALUATION OF THE FRACTURE OF THE I79 BACK CHANNEL GIRDER AND THE ELECTROSLAG WELDS IN THE I79 COMPLEX, Fritz Engineering Laboratory Report No. 425-1(80), Lehigh University, Bethlehem, PA, October 1980.

[4] Doi, D. A. and Guell, D. L., A DISCRETE METHOD OF THERMAL STRESS ANALYSIS APPLIED TO SIMPLE BEAMS, Appendix IV, Vol. I, NCHRP 12-1 and 12-6, Transportation Research Board, National Research Council, Washington, D.C., October 1974.

[5] Daniels, J. H. and Batcheler, R. P., FATIGUE OF CURVED STEEL BRIDGE ELEMENTS, EFFECT OF NEXT CURVING ON THE FATIGUE STRENGTH OF PLATE GIRDERS, U. S. Department of Transportation, Federal Highway Administration, DOT-FH-11-8198.5, Washington, D.C., 1972.

[6] Tall, L., RESIDUAL STRESSES IN WELDED PLATES - A THEORETICAL STUDY, Welding Journal, Vol. 43, American Welding Society, New York City, 1964.

[7] Tada, H., Paris, P. and Irwin, G. R., THE STRESS ANALYSIS OF CRACKS HANDBOOK, Del Research Corp., Hellertown, PA, 1973.

[8] Roberts, R., et al., DETERMINATION OF TOLERABLE FLAW SIZE IN FULL SIZE WELDED BRIDGE DETAILS, Report FHWA-RD-77-710, Federal Highway Administration, Office of Research and Development, Washington, D.C., 1977.

Fatigue Problems in Suspension Bridges: A Case Study

Problèmes dus à la fatigue dans les ponts suspendus: un exemple

Dauerfestigkeitsprobleme von Hängebrücken: Ein Beispiel

M.P. BIENIEK
Professor
Columbia University
New York, NY, USA

R.B. TESTA
Professor
Columbia University
New York, NY, USA

R.J. KRATKY
Consulting Eng.
Weidlinger Associates
New York, NY, USA

H.B. ROTHMAN
Consulting Eng.
Weidlinger Associates
New York, NY, USA

SUMMARY
This paper contains an investigation of the fatigue damage in various components of a suspension bridge. An experimental and analytical program leading to the determination of the range and number of cycles of the live-load stresses in the deck system is presented together with estimates of the crack growth rates at certain critical locations. The effect of a stiffening scheme on the torsion-induced fatigue stresses is outlined.

RESUME
Cet article contient une étude des dommages dus à la fatigue dans les différents éléments d'un pont suspendu. Un programme expérimental et analytique permet de déterminer l'amplitude et le nombre de cycles de contraintes dues à des charges mobiles dans le tablier, de même qu'une estimation de la vitesse de propagation des fissures dans certains endroits critiques. L'effet d'une méthode de raidissement sur les différences de contraintes dues à la torsion est indiqué.

ZUSAMMENFASSUNG
Dieser Artikel behandelt die Dauerschwingfestigkeit verschiedener Teile einer Hängebrücke. Ein experimentelles und analytisches Programm für die Bestimmung der Grenzspannungen und die Zahl der Lastspiele für die Fahrbahnkonstruktion unter Verkehrsbeanspruchungen wird beschrieben und die Rissfortpflanzungsrate an gewissen kritischen Stellen abgeschätzt. Der Einfluss eines Versteifungssystems auf die Wechselspannungen infolge Torsion wird angedeutet.

1. INTRODUCTION

Suspension bridges provide a number of unique and difficult problems of fatigue of their components. The main factors which cause fatigue damage in suspension bridges are the following:
-Due to the effectiveness of the cables in supporting the dead loads, the live loads control the stress levels in the stiffening girders or trusses, the deck systems and the bracings, with frequently occurring total stress reversals.
-The relatively high flexibility of suspension bridges leads to much higher secondary stresses than in any other type of bridges.
-The response of a suspension bridge to wind loading is predominantly oscillatory, i.e. of fatigue causing type.
-Simple increase of cross-sectional dimensions of affected elements leads very seldom to improved stress conditions; in fact, the level of secondary stresses is often increased as a result of such a design change.

This paper contains a study of the first two factors, performed for the case of the Manhattan Bridge in New York City. The Manhattan Bridge was completed in 1909, over the East River, as a link between the boroughs of Manhattan and Brooklyn. A general view and cross-section of this bridge are shown in Fig. 1. The bridge carries unusually heavy traffic loads from three roadways (on two levels) and four subway tracks. The flexibility of the system and the asymmetric loads from the pairs of off-center subway tracks produce large torsional deformations, with one side of the bridge deflected up to 8 feet more than the other. Abnormal deterioration of the bridge components, especially of the floor system, and its relation to the twist was observed within a few years of bridge opening and has continued ever since. In a series of reconstruction jobs, the upper lateral bracings were removed, the upper roadways demolished and rebuilt, suspender ropes replaced, tower links altered, fractured chords and lower laterals restored, and innumerable repairs were made to cracked floor members.

The study described in this paper utilizes a number of tools which became only recently available to the bridge engineer. The investigation of the problems of the Manhattan Bridge consists of the following:
-Detailed computer analysis of the entire structure modelled as a three-dimensional system.
-Strain-gage measurements of stresses at several critical locations, performed under static test loads and, with continuous recording, under typical traffic conditions.
-Fatigue and fatigue crack propagation analysis.

2. STRAIN MEASUREMENTS

Since a preliminary analysis, utilizing a simplified model of the bridge, failed to detect abnormally high stresses even in the areas of the deck system with most severe damage histories, a stress measurement program was initiated. Strain gages were placed on the floor beams of the upper and lower roadways (Fig. 1). The strain gage locations were chosen on elements which were free from cracks, close however to suspected stress concentrations. Fig. 2 shows typical arrangements of the strain gages on the upper and the lower floor beams. All the gages were placed symmetrically on both sides of the floor beams in order to be able to monitor the weak-axis bending.

The strain measurements under static loading were performed with the objective of gaining some basic insight into the working of the bridge and providing a

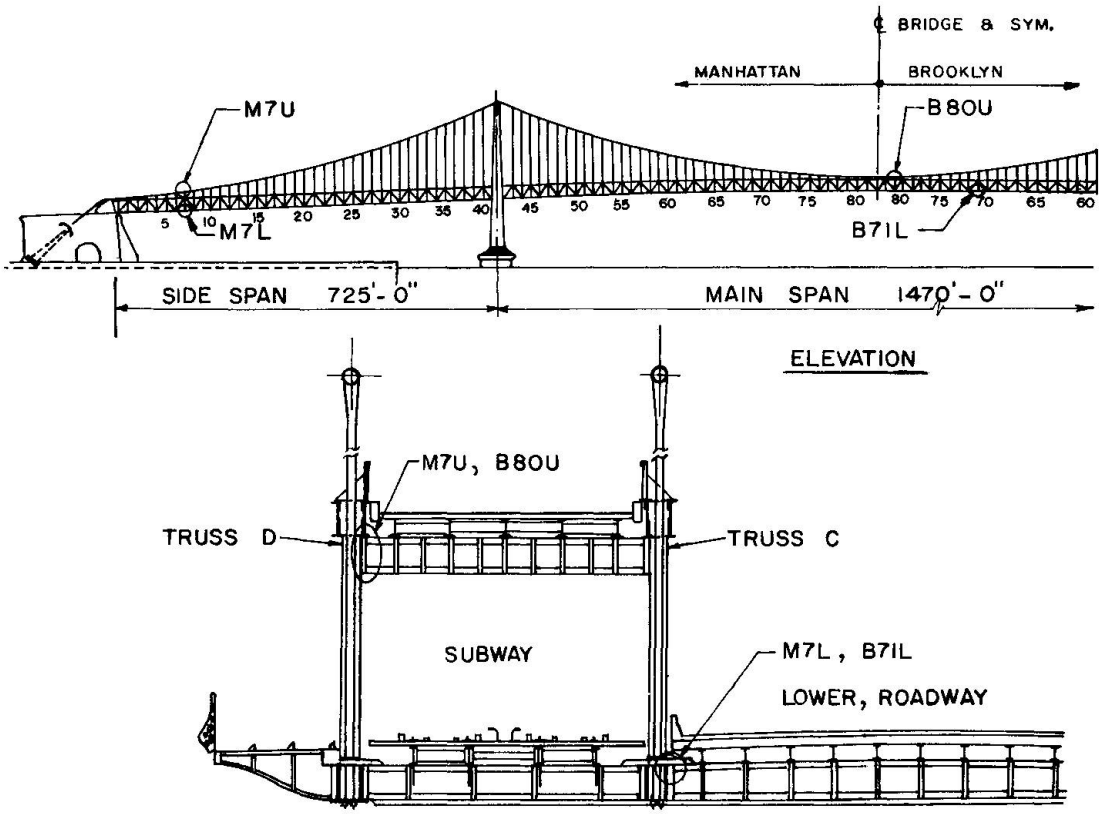

Fig. 1 Manhattan Bridge: Elevation and Typical Cross Section; Strain Gage Locations are Indicated

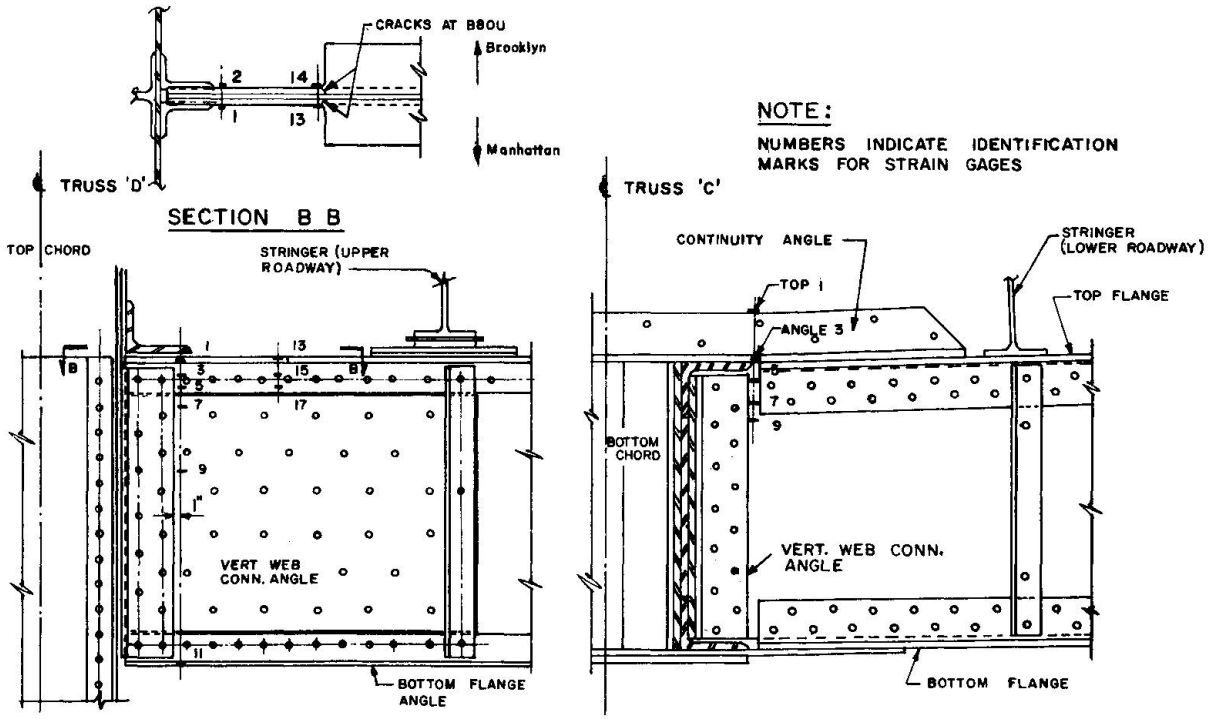

Fig. 2 Strain Gages on Upper (Left) and Lower (Right) Floor Beams

means of verification of future computer modelling of the bridge. The test load consisted of two subway trains (10 empty cars in each train) moving abreast on the tracks between trusses A and B. The trains were stopped at thirteen points along the length of the bridge and the gage readings were taken. Table 1 contains a few representative stress data.

Table 1 Static-load Stresses (psi) in the Upper Floor Beams

Location; Gage No.	Load Position L/2 Manhattan Side Span	L/4 Main Span	L/2 Main Span
M7U; 1	+12,840	-11,370	-4,980
M7U; 2	-11,490	+11,640	+5,190
M7U; 13	- 8,610	+10,230	+2,520
M7U; 14	+11,820	-17,550	-3,480

Since gages 1 and 2, and similarly 13 and 14, are located on opposite sides of the floor beam, the comparison of the stresses at gage 1 and gage 2 (and at 13 and 14) reveals very strong weak-axis bending (Fig. 3). The comparison of gage 1 and gage 13 (and 2 and 14) indicates the bending curvature reversal between the cord of the truss and the first stringer (Fig. 3). This last effect was evidently caused by excessively large friction between the stringer and the floor beam.

In order to obtain data on stresses in the floor beams under normal traffic conditions, continuous recordings of the inputs from several gages were made during normal traffic on the bridge. The recording periods were from 7:30 to 9:30 a.m. (heavy traffic to Manhattan), from 4:30 to 6:30 p.m. (heavy traffic to Brooklyn), and from 11:00 p.m. to 1:00 a.m. (light traffic). Sample traces of strain records are shown in Fig. 4. It was evident that the stresses in the floor beams caused by direct loading by various vehicles were a relatively small fraction of the total stress ranges. The prevailing contributions to the stresses in the floor beams came from the overall deformations of the bridge, with largest peaks generated by coincidental meeting of two or more subway trains at certain locations along the length of the bridge. By counting the stress cycles on the continuous records, stress range histograms were extrapolated to cover a thirty-year period of the bridge life. One of these histograms is shown in Fig. 5, for the gage No. 14 at the location M7U (an upper roadway floor beam).

3. STRESS ANALYSIS

The first-order deflection theory was used for a detailed stress analysis. It was felt that a linearized theory would be sufficiently accurate while allowing use of superposition and taking advantage of the system's symmetry. It was thus possible to model the bridge structure very realistically, as a three-dimensional system. Every panel point was taken into account and the major structural components including the floor beams, were modelled as individual elements. The stringer-floor beam interaction was analyzed on a smaller (local) model for various conditions of the reactions between the stringers and the floor beams. Accuracy of the analysis was confirmed by comparing its stress predictions with the data obtained by the strain-gage measurements.

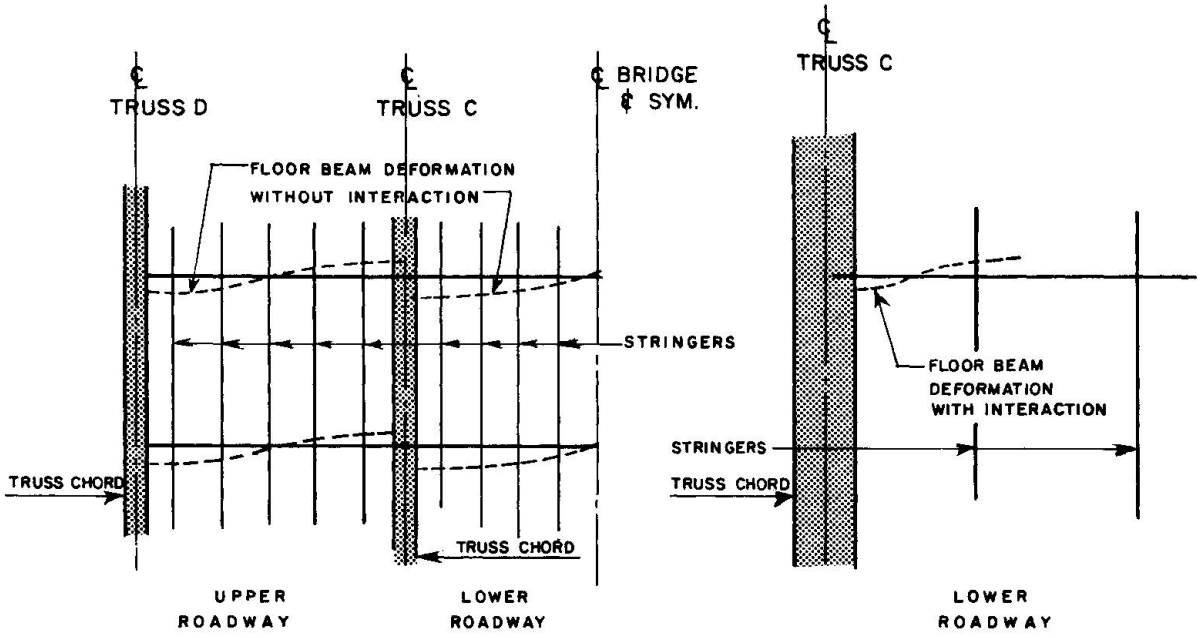

Fig. 3 Weak-axis Bending of the Floor Beams; Figure at Right Shows Aggravated Bending Due to Stringers Interaction

By combining the loads from the four subway tracks and from the roadways, the maximum stresses for strength design and the stress ranges for fatigue design were established. The analysis was performed for the present state of the bridge and for several proposed stiffening schemes. The stress ranges in the upper floor beams determined analytically for the existing configuration and for the proposed stiffening scheme are shown in Fig. 7.

The most important lessons learned from this analysis are the following:
-Three-dimensional modelling of the bridge structure is absolutely necessary if correct determination of stresses and deformations is to be achieved.
-Stresses which may be treated as "secondary" in other types of bridges become often of primary importance in suspension bridges.

4. FATIGUE CRACKING PREDICTIONS

Within the strength of materials methodology, the cumulative fatigue damage in a structure subjected to variable-amplitude cyclic loading can be estimated with the aid of one of the existing rules. Among them, Miner's rule appears to be reasonable and enjoying widespread acceptance. Its use requires the knowledge of the S-N diagram of the material, obtained from constant-amplitude fatigue tests, and the histograms (or "load spectra") of stress ranges imposed on the element to be analyzed. According to Miner's rule, the damage, D, is

$$D = \sum_i n_i/N_i \qquad (1)$$

where n_i = number of actual cycles of stress range S_i;

N_i = number of cycles to failure at stress range S_i.

Failure occurs when D = 1.

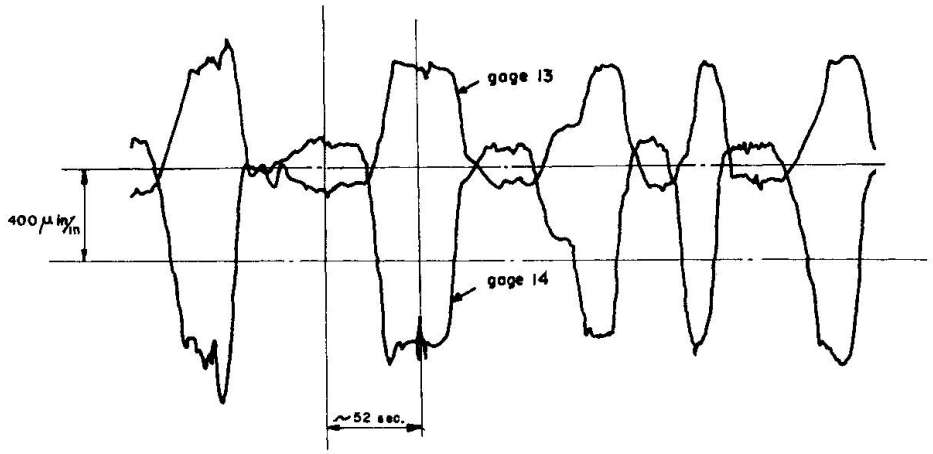

Fig. 4 Samples of Stress Records; Location M7U, Gages 13 and 14

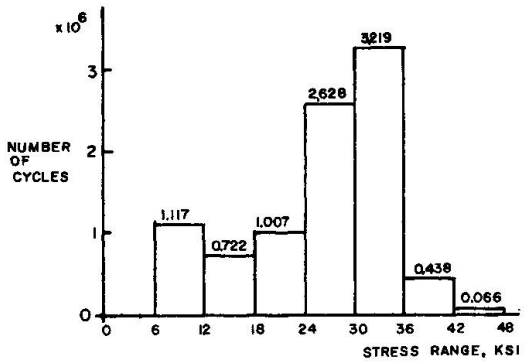

Fig. 5 Histogram of Stress Ranges; Location M7U, Gage 14

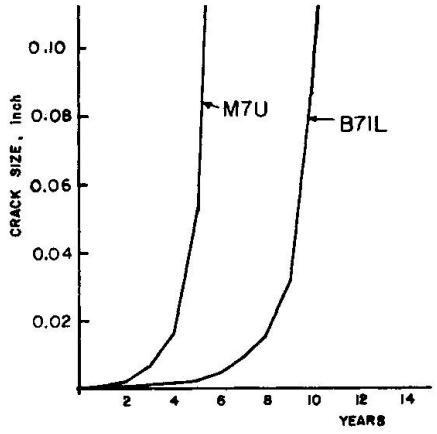

Fig. 6 Crack Growth at Locations M7U and B71L (Initial Crack Length Assumed at 0.001 in.)

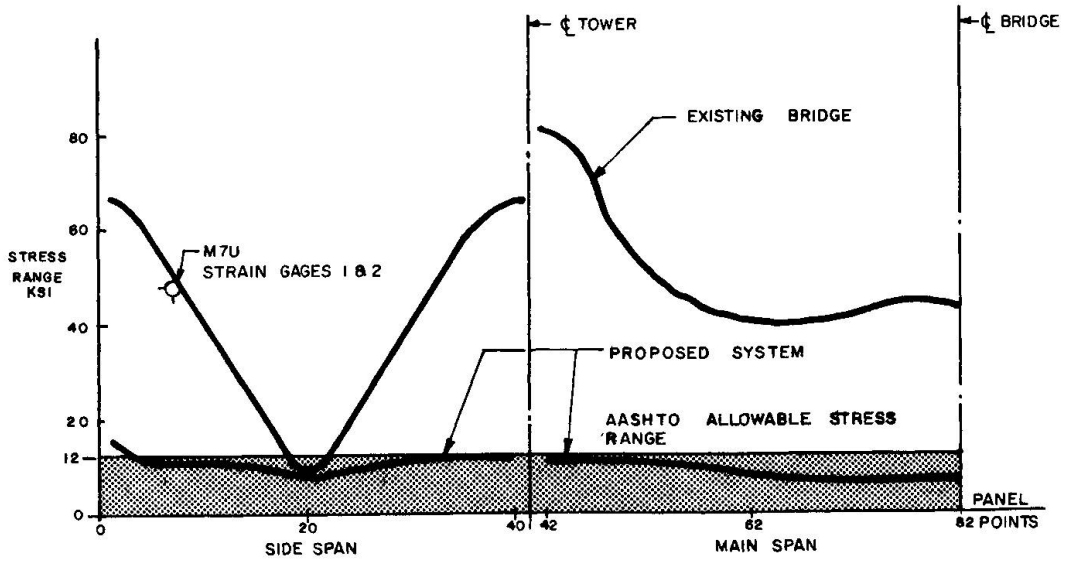

Fig. 7 Stress Ranges at Upper Roadway Floor Beams

Miner's rule has been applied to several locations on the floor beams, for which the experimental stress-range histograms were determined and the S-N curve of rolled A-36 steel was used. The results for 30-year service period are, for example:

Location M7U : D = 0.77
Location B71L : D = 0.14

In reality, cracks in the floor beams in the vicinity of these and other locations were observed after a service period of less than 30 years since the last replacement and rehabilitation work. Thus, the existence of cracks must be attributed to one or a combination of the following factors:
-Initial flaws in the material;
-Initial cracks, notches, and other surface flaws causing local stress concentrations;
-The effects of corrosion;
-The possibility that at some locations the peak stresses were occasionally higher than the levels determined in the present investigation.

The above observations seem to point to the fracture mechanics methods as perhaps the more rational approach to the fatigue cracking problems in bridges. In order to develop an estimate of the rate of growth of hypothetical and, in some instances, existing cracks in the floor beams, the following formula was used ([1], [2])

$$\frac{da}{dN} = C\,(\Delta K)^n \qquad (2)$$

where a = crack length, N = number of cycles, ΔK = range of stress intensity factor, C and n = material constants.

For A-36 structural steel, the values of the two material constants were adopted from Ref. [1] (p. 261) as

$$C = 3.6 \times 10^{-10}, \qquad n = 3$$

The stress intensity factor was determined under the assumption of uniform nominal stress in the analyzed element and small length of the crack as compared to the dimensions of the element. Thus, the expression for ΔK is

$$\Delta K = 1.12\,\Delta\sigma\,\sqrt{\pi a} \qquad (3)$$

where $\Delta\sigma$ is the nominal stress range. The values of $\Delta\sigma$ with the corresponding number of cycles were taken from the strain-gage records described in Section 2. Integration of Eq. (2) was performed with the aid of the Euler method, with the time interval of 0.5 year (i.e. with the update of the value of "a" in the expression for ΔK on the right-hand side of Eq. 2 at half-year intervals). The initial crack length was assumed to be equal to 0.001 in. Typical results of this analysis are shown in Fig. 6. The general trend indicated by these theoretical predictions appears to be in agreement with the actual observation of the crack growth between two consecutive inspections. Given the erratic nature of some of the effects present in the system (among them, notably, the stick-slip contact between the stringers and the floor beams which causes the situation depicted in Fig. 3), the fracture mechanics approach is, in fact, remarkably successful in explaining the progress of damage of the components in question.

5. STIFFENING SCHEME

A number of stiffening schemes were considered. The solution which possesses the advantage of being effective, economical, and not detracting from the appearance of the bridge consists of strengthening the floor beams and restoration of the lateral bracing system at the level of the two upper roadways. The torsional rigidity of the bridge is thus considerably increased; the two pairs of trusses and the lateral bracings from two very effective torque tubes. The stress ranges in the floor beams of the modified system are shown in Fig. 7, where - for reference - the allowable stress range according to the AASHTO Specifications, [3], is also given.

REFERENCES

1. ROLFE, S.T. and BARSOM, J.M.: Fracture and Fatigue Control in Structures, Prentice-Hall, 1977.
2. ROBERTS, R., BARSOM, M.M., FISHER, J.W. and ROLFE, S.T.: "Fracture Mechanics for Bridge Design," Federal Highway Administration, U.S. Department of Transportation, Washington, D.C., 1977.
3. AASHTO STANDARD SPECIFICATION FOR HIGHWAY BRIDGES, 12th edition, The American Association of State Highway and Transportation Officials, Washington, D.C., 1977.

Design of the Steel Gates for the Eastern Scheldt Storm Surge Barrier

Dimensionnement des vannes en acier pour le barrage anti-tempête de l'Escaut oriental

Bemessung der stählernen Schützen des Sturmflutwehres an der Ostschelde

E. YPEY
Chief design engineer
Ministry of Traffic and Waterstaat
Voorburg, the Netherlands

H. v.d. WEIJDE
Senior design engineer
Ministry of Traffic and Waterstaat
Voorburg, the Netherlands

SUMMARY
The steel gates of the barrier have main support structures of tubular steel trusses. Heavy storms will create high stresses in the tubular connections because of stress concentration. As the waves have periods of 6 to 10 seconds, some 15'000 load cycles may be expected in a 24 hour storm. For economic reasons the designers expect and accept fatigue cracks after 30 to 40 years of use and will give special instructions for inspection on that basis.

RESUME
Les vannes en acier du barrage sont constituées d'une structure principale en treillis composé de tubes d'acier. Des contraintes élevées dans les assemblages entre tubes sont dues à des effets de concentration de contraintes, lors de violentes tempêtes. Les vagues ayant une période de 6 à 10 secondes, il peut se produire quelques 15'000 cycles de charge lors d'une tempête de 24 heures. Pour des raisons économiques, les ingénieurs projeteurs prévoient et acceptent l'apparition de fissures de fatigue après une durée d'utilisation de 30 à 40 ans et fournissent des instructions spéciales pour un contrôle des ouvrages.

ZUSAMMENFASSUNG
Die Tragkonstruktion der stählernen Schützen des Sturmflutwehres besteht aus Rohrträgern. Infolge der Spannungskonzentration verursacht ein schwerer Sturm hohe Spannungen in den Verbindungen. Da die Wellen Wiederkehrperioden von 6 bis 10 Sekunden aufweisen, ergeben sich ungefähr 15'000 Belastungszyklen während eines Sturmes von 24 Stunden Dauer. Aus wirtschaftlichen Gründen werden bei einer Nutzungsdauer von 30 bis 40 Jahren Ermüdungsbrüche akzeptiert und spezielle Inspektionsvorschriften erlassen.

General description of the design of the flood barrier

The mouth of the estuary of the Eastern Scheldt has three channels, named Hammen, Schaar and Roompot. Between the channels, totally 3,5 kilometers wide, is shallow water in which islands constructions are made (fig. 1).
In the three channels 66 piers, forming 63 apertures, will be placed on 45 m centre-to-centre distance. The piers are 45 m high and have base plates measuring 25 x 50 m2. The sills between the piers will be increased in height and box-beams will span the piers, thereby achieving the desired effective flow opening of 14.000 m2 between sills and box-beams. The tidal range will still be 77% of what it is today and as a result of that, the salt water tidal environment in the Eastern Scheldt will be kept intact. This will conserve the mussel and oyster cultures and other specific flora and fauna.
A steel gate will be installed between each pair of piers. Under normal conditions the gates are open, allowing seawater to flow in and out the Eastern Scheldt. The existing environment will thus be kept intact. Under storm condtions the gates will be closed. The hydraulic electro-mechanical devices which operate the gates, will be housed in the prestressed concrete bridge elements spanning the piers.

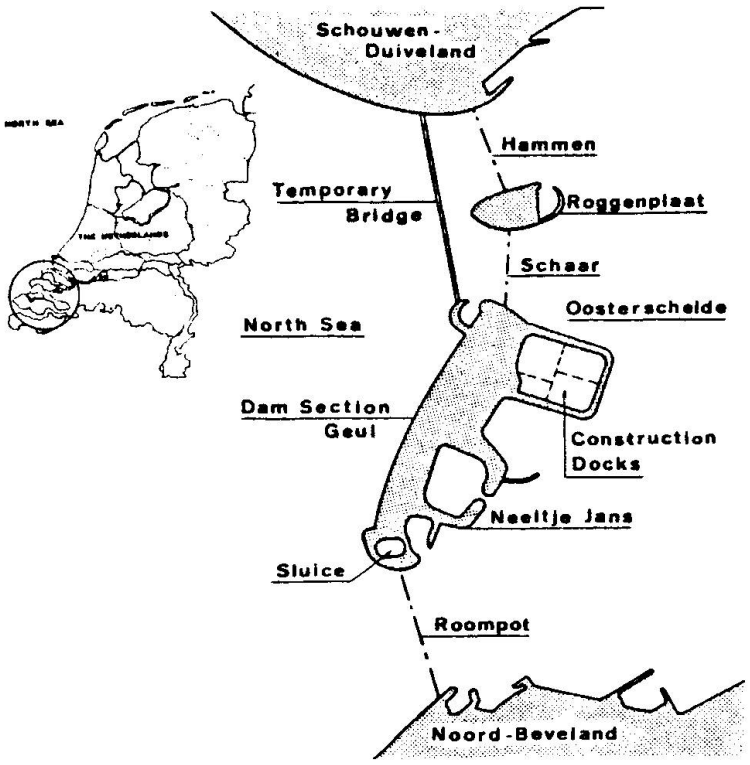

fig. 1 The mouth of the Oosterschelde with trace of stormflood barrier

Steel gates

The closure system of the flood barrier consists of a static part, the sill and box-beam and a mobile part, the steel gates. There are 63 steel gates with a gross flow profile of 18.000 m2. The gross flow profile of 18.000 m2 has an effective profile of 14.000 m2 taking flow contraction and blocking of two gates for maintenance into account. With the effective flow profile of 14.000 m2 a tidal range of 2.70 metres is achieved.

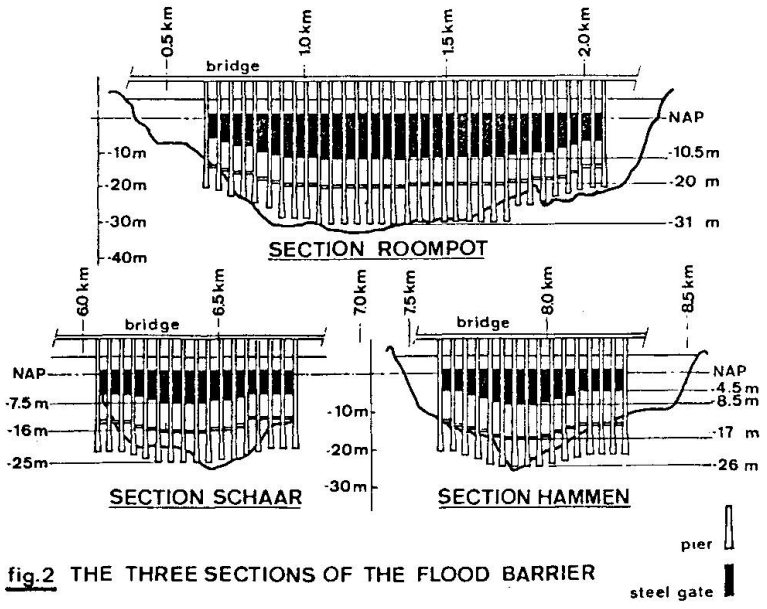

fig.2 THE THREE SECTIONS OF THE FLOOD BARRIER

The 63 steel gates are divided over the three channels as follows:
15 in the Hammen;
16 in the Schaar van Roggenplaat;
32 in the Roompot.
These numbers are determined by the flow volumes in the channels. The height dimension of the steel gates will be determined by the cross-sectional profile of the channel (see also fig. 2) and varies in steps of one metre from 5.90 metres to 11.90 metres; weights vary between 300 and 520 tons. In their closed position the steel gates extend from the concrete sills upwards to Amsterdam Zero + 1.20 metres (the under side of the box-beams). From Amsterdam Zero + 1.20 metres to Amsterdam Zero + 5.80 metres the concrete box-beam acts as a barrier. The thickness of the gates is 5.40 metres. There will be 7 different types of gates, due to the difference in height. Because the piers, between which the steel gates are sliding up and down, are founded independent of each other, positioning tolerances (with respect to centre-to-centre distances and nonparallelity) will have to be

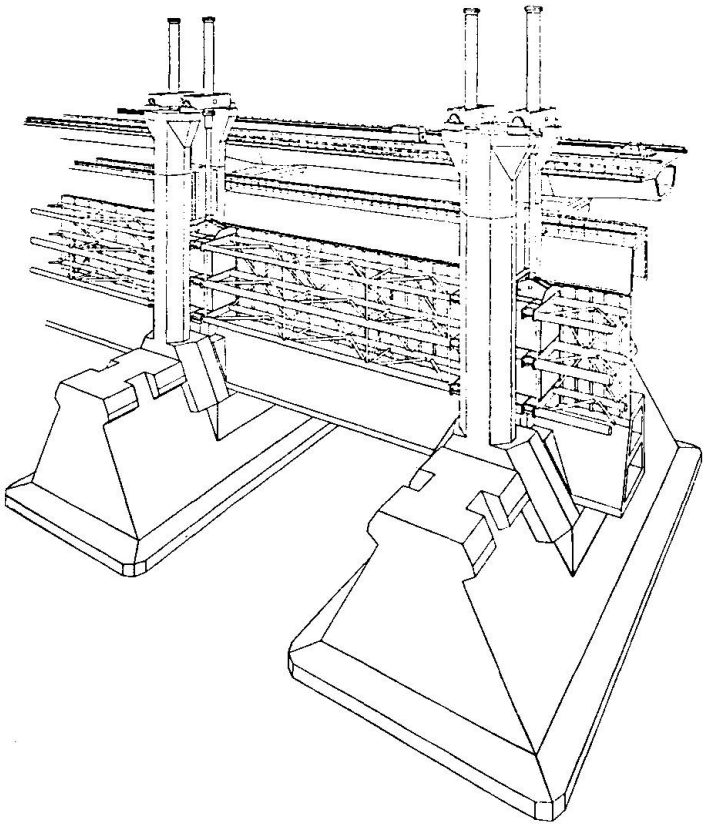

fig. 3 Artist impression of flood barrier

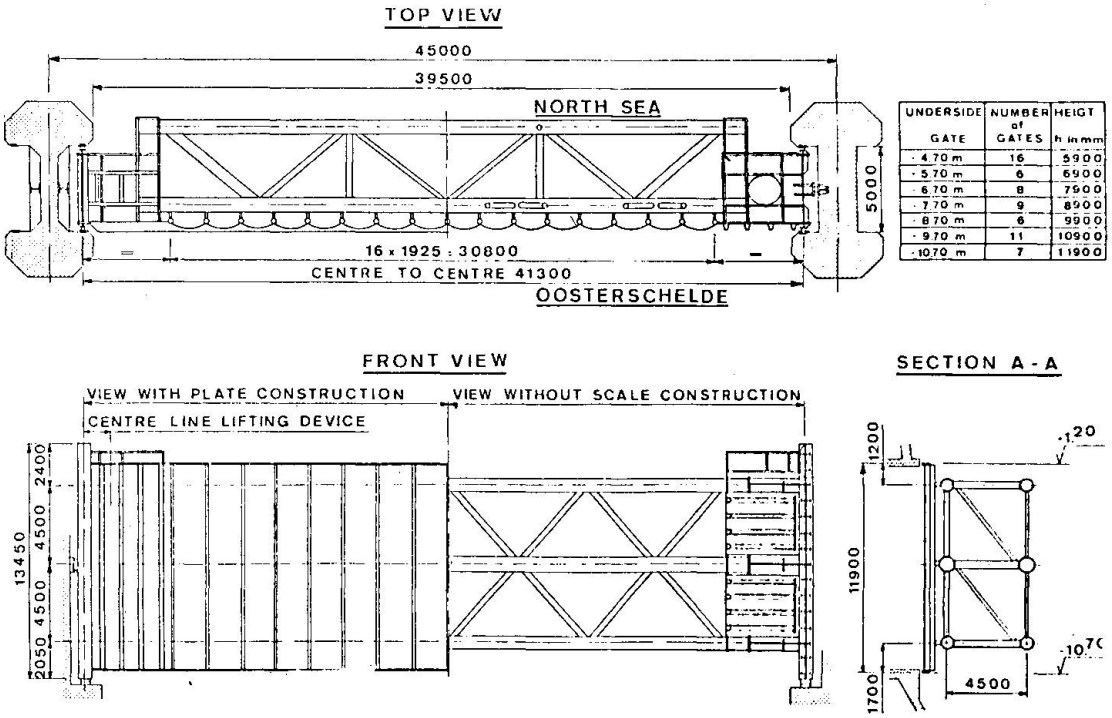

UNDERSIDE GATE	NUMBER of GATES	HEIGT h in mm
-4.70 m	16	5900
-5.70 m	6	6900
-6.70 m	8	7900
-7.70 m	9	8900
-8.70 m	6	9900
-9.70 m	11	10900
-10.70 m	7	11900

fig. 4 Construction of steel gate

taken into account during the designing phase of the gates.
Furthermore, differences in subsidence between the piers occur as a result of the loads on the barrier, which could cause the gates to become jammed. To compensate for these influences, the gates have a variable length and a torsionally weak construction is required.
The correct length of each gate can be determined only after the corresponding piers have been positioned and the sill is constructed between the piers at the location of the gate. Therefore the gate will be assembled in three parts of which one is overlong. The three parts are the two "box type" end constructions and the tube truss constructions, the latter being overlong.

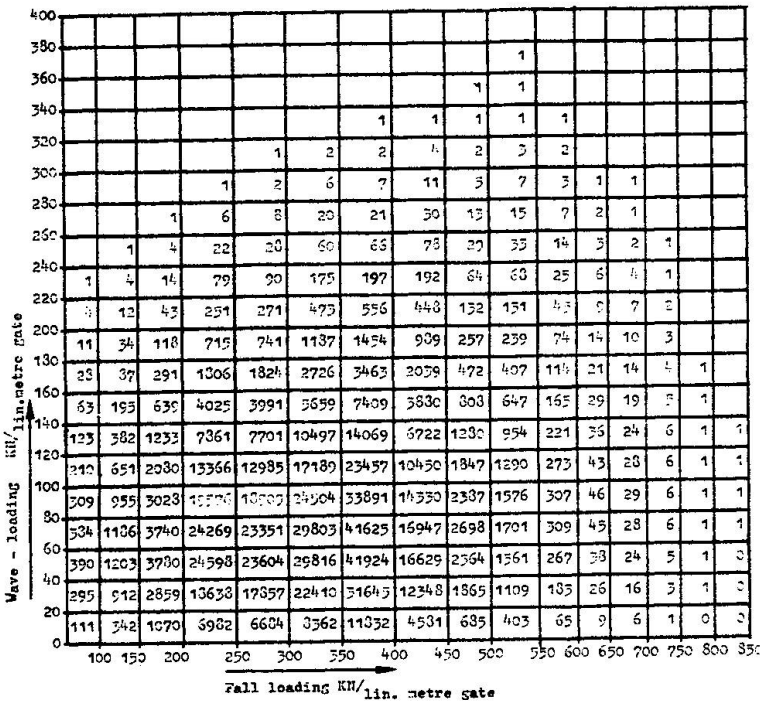

TABLE 1 Number of loading combinations wave loading — fall loading gate 16 Roompot

After the correct span length has been measured, this part is adjusted to the desired length. The three parts are then attached to each other with welded connections.
Since great horizontal loads must be absorbed during closing and opening, a lever gate with slide supports was chosen, whereby loads are transfered throughout the entire height of the gate to the pier.
Worst-case conditions for the strength calculation for the steel gate in closed position are:
a water level on the North Sea side of Amsterdam Zero + 5.5 m and on the Eastern Scheldt side of Amsterdam Zero - 0.7 m. The "significant" wave height then is 3.8 metres (by "significant" wave height is meant the average height of the highest one-third of the waves occurring in a storm).
Consideration must be given to the slamming effects of waves against members of the gate construction.

wave loading KN/lin.m	total number of loadings in 200 years	number of reduced loadings in 200 years
20.	41132.	36.
40.	110165.	1991.
60.	146403.	15627.
80.	146093.	54975.
100.	119856.	119856.
120.	83877.	186405.
140.	51113.	223138.
160.	27534.	215732.
180.	13296.	174508.
200.	5846.	121723.
220.	2383.	75325.
240.	919.	42525.
260.	343.	22536.
280.	126.	11453.
300.	46.	5657.
320.	16.	2610.
340.	6.	1277.
360.	2.	547.
380.	1.	347.
	749157.	1276259.

TABLE 2 Number of wave loadings in 200 years, number of reduced loadings gate # 16 Roompot

Dynamic loading of the gates

For the consideration of the effects of the dynamic loading, a long term distribution of the loading intervals has been made considering a life time of the construction of 200 years. The stress level and stress distribution depends of:

a. the location of the gate in the barrier;
b. the relation of tide and wave height;
c. the "opened periods and the "closed" periods of the gate;
d. the shape of the construction having effect on the transfer;
wave → wave loading → stress in construction.

Extensive calculations have been made to determine the probability of the dynamic loading on each gate. An illustration of the distribution of the dynamic loading of gate number 16 in the Roompot is given in table 1. Since the periods of the loadings due to water level difference are long, their loading effect can be neglected in the calculations of the effects of the dynamic loadings. Resulting, consideration is only given to the wave loading, the total number of loadings in 200 years is given in table 2.

In order to receive a more or less identical safety guarantee for all the gates, the load-spectra of the various main members of the gates have been reduced to a standard load-spectrum. This method is acceptable since the main members are of an identical construction type and therefore the same S-N curve is applicable. For the tube truss constructions this is the X-X line of the Americal Welding Society (fig. 5).

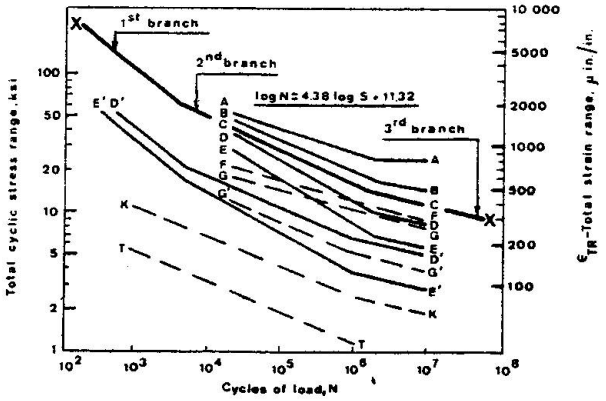

fig.5 Allowable fatigue stress and strain ranges for stress categories (American Welding Society)

For the reduction it is acceptable to use the second branch of the S-N curve. The equation of this branch is approximately:

$\log N = 4.38 \log S + 11.32$ (S in ksi)

$N = C_1 \times S^{4.38}$ (C_1 = constant)

Since the stress S is linear dependent on the loading L, it can also be written:

$N = C_2 \times L^{4.38}$

Taking:

L_r = loading to which actual loading is reduced

L_a = actual loading

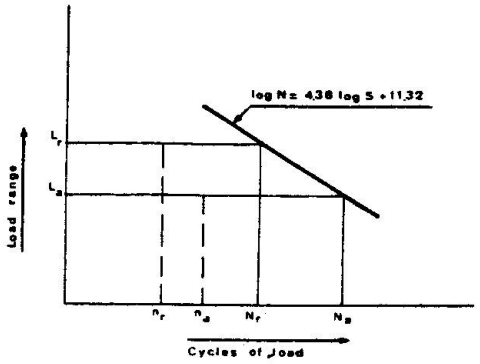

fig.6 S-N curve

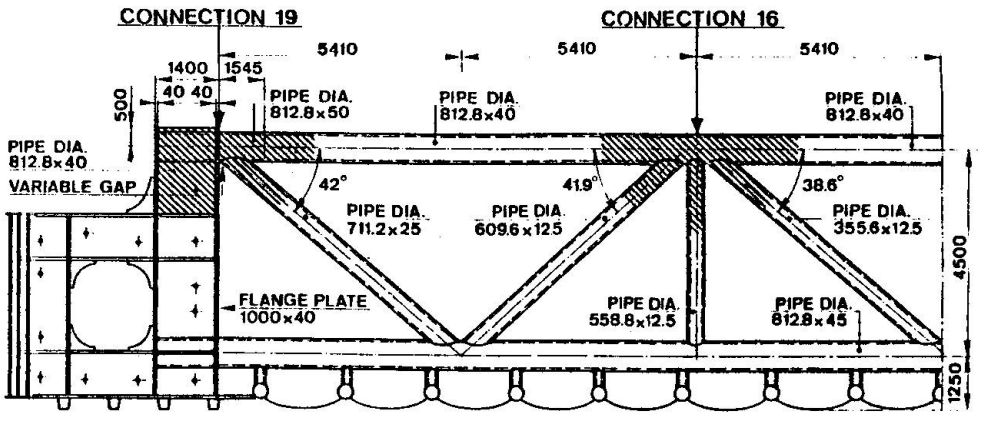

measures in millimetres

fig. 7 LOCATION OF CONNECTIONS VERIFIED IN LABORATORY

n_r = reduced number of cycles
n_a = actual number of cycles
then

$$n_r = n_a \times \left(\frac{L_a}{L_r}\right)^{4.38}$$

This means that n_r cycles of loading L_r give the same result towards fatigue as n_a cycles of loading L_a.
For the gate number 16 in the Roompot this method of reduction results in the number of reduced loadings as given in table 2.
For the reduced loading is taken

$$L = 100 \text{ KN/}_{\text{lin. metre}}$$

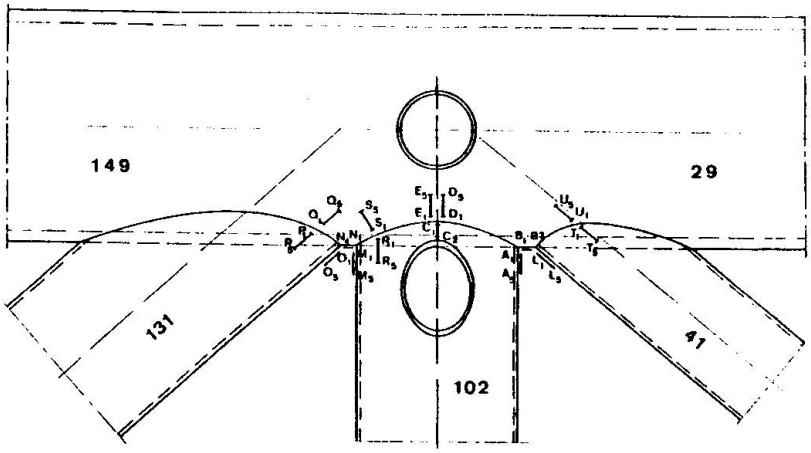

fig.8 LOCATION OF STRAIN GAUGES IN CONNECTION No.16

Stress concentrations, strain concentrations (S.C.F. - S.N.C.F.)

For the less complicated mutual connections of the tubes the calculation method of Kuang, Potvin and Leick [1] for the determination of the stress concentration factor has been applied in the preliminary design phase.
For the more complicated connections the three dimensional effects were too large. For these connections perspex models were tested to verify the S.N.C.F. (see fig. 7). The strain ganges were placed in such positions that the required informations regarding the hot spot stresses would be received (see fig. 8).
In fig. 9 the forces and bending moments acting in the members in the neighbourhood of the connection are illustrated. The forces and moments in the members I and II were small as compared to the other forces and are neglected in the model tests.
The results of the model tests are given in figure 10.
For an easy comparison the results are made dimensionless by dividing the measured strain by the strain due to the axial force in member 41. From fig. 8 and 10 it can be seen that the highest strain appears at the crown position of the connection of member 102 to the chord.

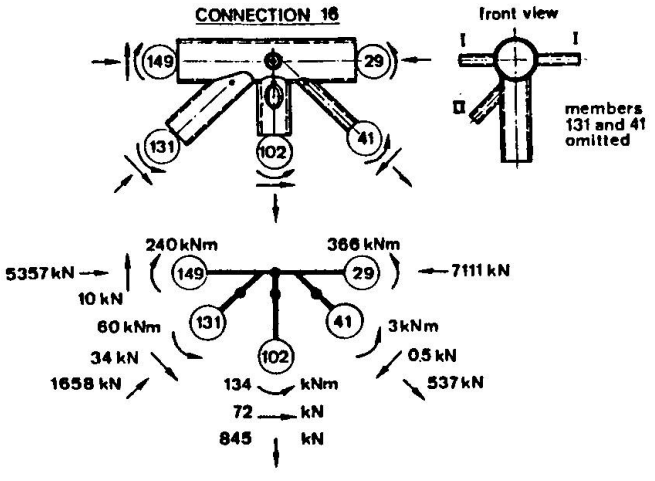

fig. 9 FORCES AND MOMENTS ACTING IN THE MEMBERS OF CONNECTION 16

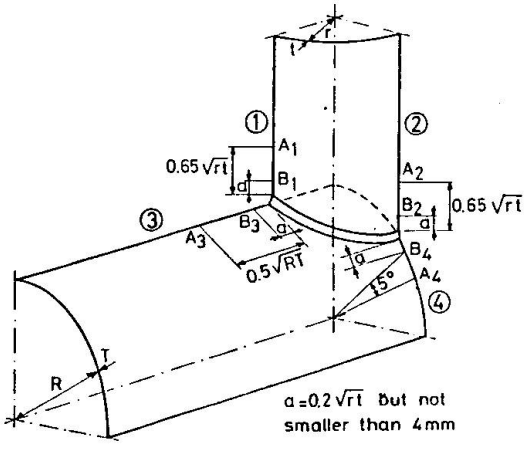

Fig.11 Locations of straingages for linear extrapolation to weldtoe to determine strain concentration factor.

The extrapolation of the measured strains to the weld toe has been carried out according to the procedure outlined by the European Working Group III "Tubular joints", see also fig. 11. This linear extrapolation includes the influence of the geometry of the joint and the geometry of the weld, but not the influence of the condition of the weld toe such as notches, the angle between weld and parent metal etc. These influences must be taken into account by considering the applicable S-N curve.
Due to the difference in height there are 7 different types of gates, which are composed of 2 or 3 trussed girders. As a result of the difference in loading the total number of different types of trussed girders is 13. In order to apply the results of the investigated connection for other geometries the results have been converted in stresses and compared with the calculated stress concentration factors (S.C.F.).

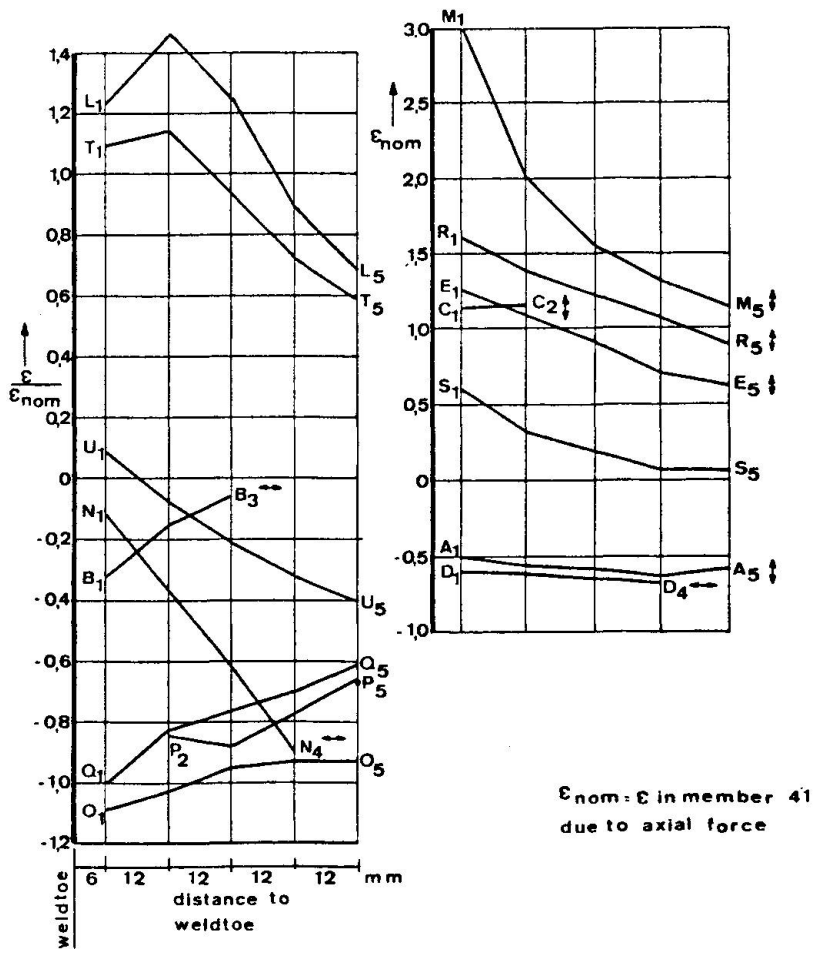

fig 10 $\frac{\varepsilon}{\varepsilon_{norm}}$ in connection 16

For calculating the S.C.F. of a K-T joint with branches of which the diameters and loads are not equal, formulas are not available in the literature, even if the members I and II (see fig. 9) are omitted. Considering the joint as a K-joint, consisting of the branches 131 and 102 (see fig. 9) and all branches having the diameter of member 102, the best agreement is obtained by using the formulas of Wordsworth [2].
The strain in joints with different parameters is calculated by

$$\varepsilon_i = \sigma_{hs} \times \left(\frac{\varepsilon_{measured}}{\sigma_{hs_{calculated}}}\right)_{joint\ 16}$$

From fatigue tests it has appeared that the first visible crack occurs at appr. 25% of the lifetime of the specimen [3].
Since the design lifetime of a gate structure must be 120 years and the adopted AWS X-X curve is based on complete failure of the connection, it means that it is accepted that the first visible crack will occur after approximately 30 years. After every storm-closure the most critical joints of the gates will be inspected. If a crack is not perceived immediately, it would not mean that a gate will fail during the next storm.

The ratio between the number of cycles after which the crack is completely through the wall and the number of cycles required for the first visible crack is greater than 1,5 [3], e.g. for gate number 16 appr. 225.000 load cycles may occur after the first visible crack is in existence, before that crack is completely through and through. The total number of load cycles during a 24-hours storm is approx. 15.000, this means that approx. 15 heavy storms are required after occurrence of the first crack before complete failure of the connections has been reached.
After a crack has been perceived, the crack will be repaired. From fatigue tests on repaired tubular joints it has appeared that the fatigue strength is equal or even greater than the fatigue strenght of the original specimen [3].
All joints are designed as non-overlapped joints to ensure inspection and possibility of reparation of all welds.
In order to carry out a reliable and quick inspection of the critical joints an investigation is started to the application of acoustic or magnetic methods, capable of detecting cracks in uncleaned surfaces.

[1] Kuang, J.G.; Potvin, A.B.; and Leick, R.D.:
"Stress Concentrations in Tubular Joints", paper OTC 2205 presented at the 7th Annual Offshore Technology Conference, Houston, Texas, May 1975
[2] Wordsworth, A.C. "Stress concentration factors at K and KT tubular joints"
[3] Dijkstra, O.D.; De Back, J.:
"Fatigue strength of welded tubular T-and X-joints", paper OTC 3696, presented at 12th Annual OTC in Houston, Texas, May 1980
[4] De Back, J. and Vaessen, G.H.G.:
"Fatigue and corrosion fatigue behaviour of offshore steel structures", ECSC Convention 7210-KB/6/602 (J.7.1 f/76), April 1981

Collapse of a Cantilevered Truss Supporting a Heavy Crane

Rupture d'une poutre-console à treillis supportant un pont-roulant lourd

Bruch eines Fachwerkkragträgers einer Kranbahn

JOHN M. HANSON
President
Wiss, Janney, Elstner & Assoc.
Northbrook, IL, USA

SUMMARY
After three years of operation, a cantilevered steel stuss supporting a heavy 1070-kN crane collapsed as a result of fatigue in the anchor bolts resisting the tensile reaction. The tensile reaction was taken by then 51-mm diameter anchor bolts. It was estimated that these bolts were sujected to approximately 370 000 cycles of loading producing an average nominal stress range of 55 MPa. The failure was attributed to uneven fluctuating tension in the bolts.

RESUME
Après trois ans d'utilisation, une poutre-console à treillis métallique supportant un important pont-roulant de 1070 kN s'est effondrée par suite d'une rupture de fatigue des boulons d'ancrage reprenant la réaction de traction. La réaction de traction était reprise par dix boulons de 51 mm de diamètre. On a estimé que ces boulons furent soumis à environ 370 000 cycles de charge produisant une différence moyenne de contrainte nominale de 55 MPa. La rupture fut attribuée à une distribution non uniforme de la tension dans les boulons.

ZUSAMMENFASSUNG
Nach dreijähriger Betriebszeit brach der auskragende Fachwerkträger eines 1070 kN-Krans infolge Ermüdung der Verankerungsschrauben. Die Zugspannung wurde durch zehn Schrauben mit einem Druckmesser von 51 mm aufgenommen. Eine Schätzung ergab, dass die Schrauben ungefähr 370 000 Lastwechsel mit einer nominellen durchschnittlichen Spannungsdifferenz von 55 MPa erfuhren. Der Unfall wurde einer ungleichen Spannungsverbreitung in den Schrauben zugeschrieben.

1. SITE INVESTIGATION

The site of the collapse of a very large cantilevered truss supporting a heavy 1070-kN crane is shown in Fig. 1. At the time of the collapse, about 10:30 A.M., the crane was at the end of the truss, removing oyster shells from a barge. The operator of the crane was killed, and another man working near the barge was severely injured.

The position of the collapsed truss and markings on the debris clearly established that the failure occurred as a result of loss of the tensile reaction. When this occurred, the truss began to rotate about the compressive reaction. This rotation was resisted by the crane rail, which exerted a horizontal pull, causing the pier taking the compressive reaction to fail in lateral bending at its base. As a result, the truss also moved backward and inward, and finally collapsed.

The tensile reaction was resisted by ten 51-mm diameter anchor bolts, arranged in two rows. The picture in Fig. 2 shows how the bolts protruded through a heavy weldment at the support of the truss that did not collapse. A view of the pier where the failure occurred is shown in Fig. 3. Seven bolts may be observed protruding from the pier. The bolts were bent by the impact of the truss, which occurred after the pier failed that was taking the compressive reaction, and the truss began to fall. Two bolts on the near side of the pier were broken below the top surface, apparently from the truss rolling off of the pier. One bolt, on the far side near the column extending above the top of the pier, was fractured in the region where grout had been placed between the weldment and the top of the pier. The surface of this bolt, as well as other bolts, was corroded in this region. There was no evidence of deformation or slip of any part of the anchor bolts embedded in the pier.

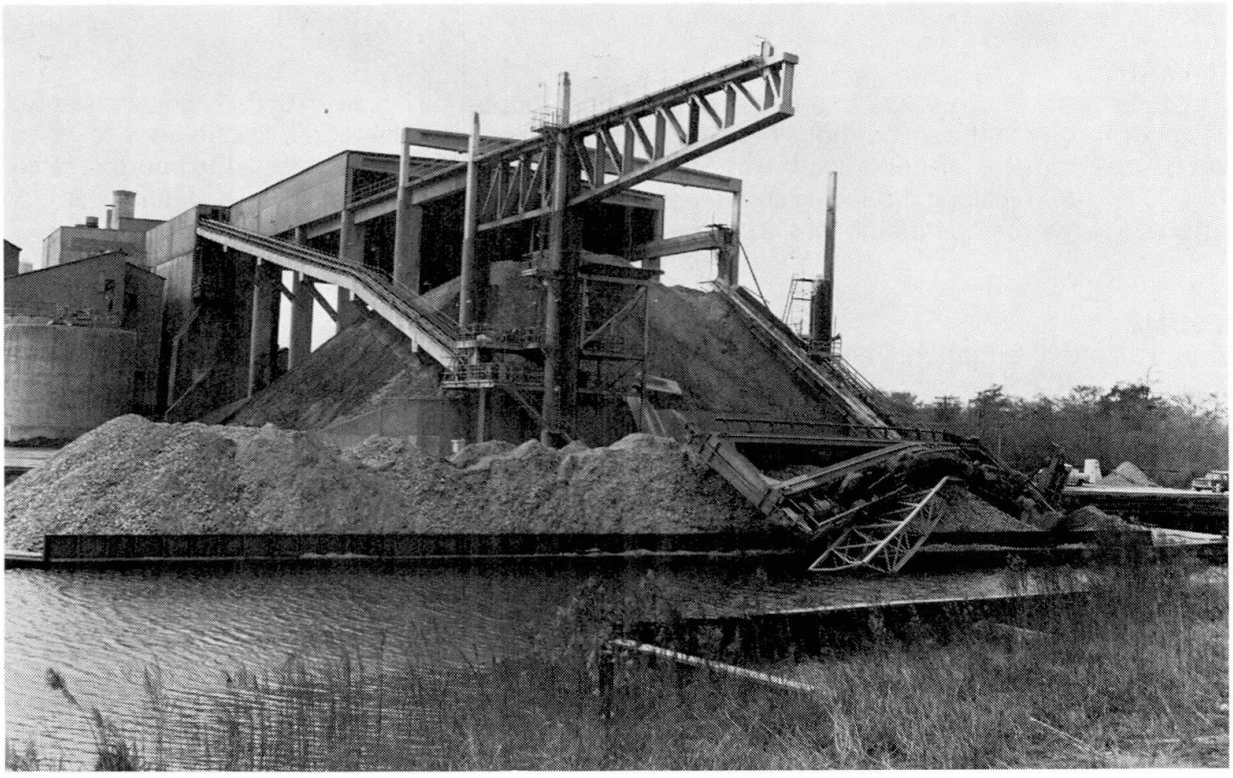

Fig. 1 View of Collapsed Truss and Crane

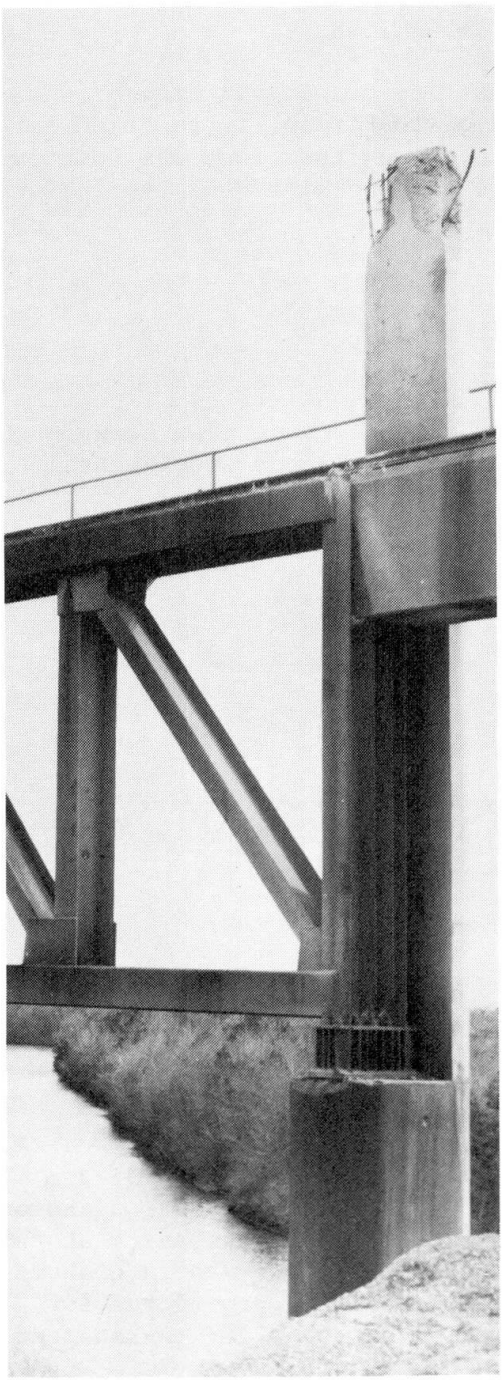

Fig. 2 Weldment of Tensile Reaction

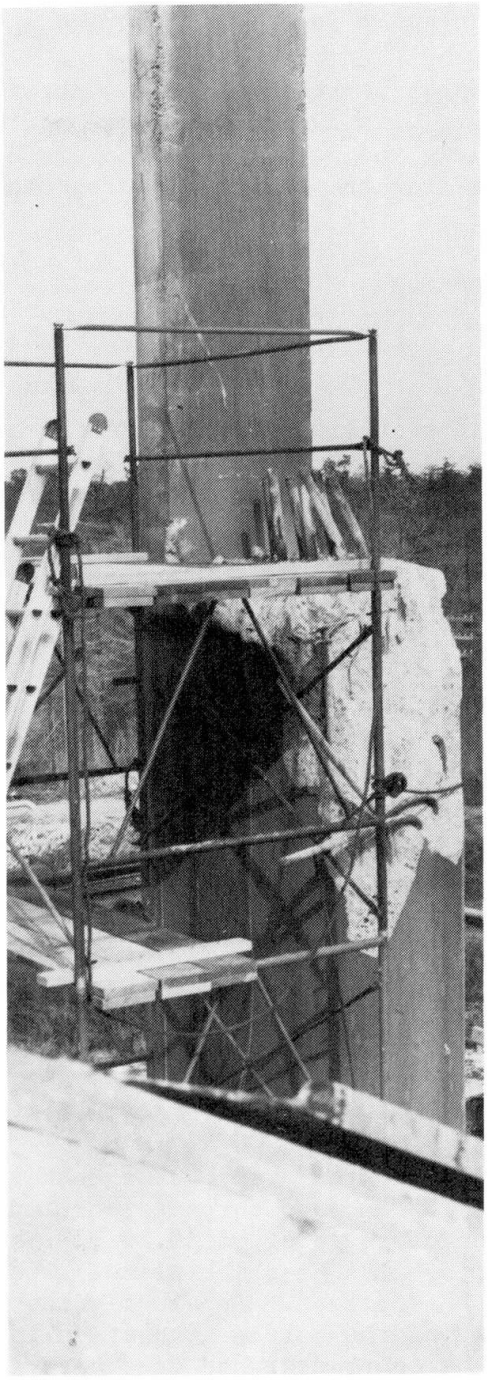

Fig. 3 Failed Anchor Bolts

The tops of five anchor bolts with nuts were eventually recovered. These bolts were fractured near the base of the nuts. It was established that fractures occurred in the threaded portions of all of the bolts.

Discussion with the manager of the plant indicated that the crane generally unloaded one barge of oyster shells each day. Since the crane had an 8 m^3 bucket, and the barge supplied about 2600 m^3 of shells, it was estimated that the crane made approximately 400 daily trips out to the end of the trusses. Furthermore, the crane was generally in use seven days a week, except for three or four times a year when the plant was temporarily shut down. Since the plant had been in operation for three years, it was estimated that the anchor bolts had resisted approximately 370,000 cycles of repeated loading prior to the collapse.

2. REVIEW OF AVAILABLE DRAWINGS AND SPECIFICATIONS

The length of the trusses, as shown in the line drawing in Fig. 4, was 35.9 m. With the crane bridge at the end of the truss, in position for unloading the barge, the load of the crane, P, on the truss was located 15.2 m from the compressive reaction. The load consisted of the following:

Crane bridge	764 kN
Trolley	262 kN
Bucket	44 kN
$8m^3$ of oysters	62 kN

Lateral stability was provided by a welded channel connection between the top chord of the trusses and the concrete columns, and a supplemental truss between the ends of the cantilevers.

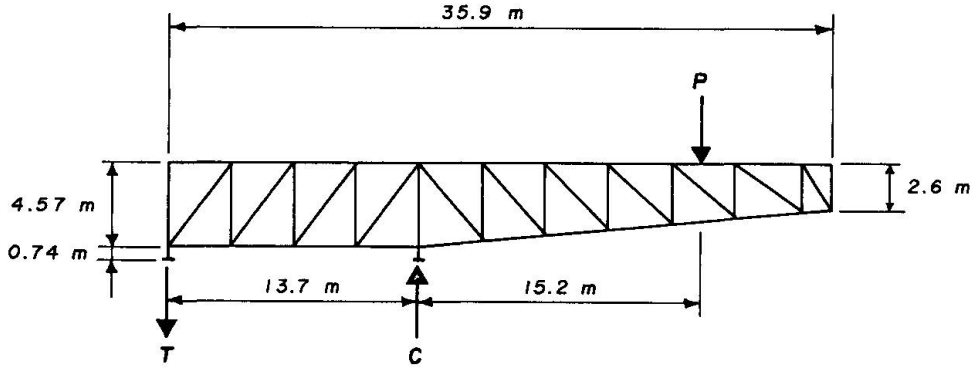

Fig. 4 Elevation of Truss

According to the drawings, the anchor bolts had a total length of 3 m with a 152-mm long threaded portion at both ends. The projection above the top of the pier was 0.59 m. The bolts were anchored in pairs at their bottom by a 32-mm-thick plate. The surface of the bolts was in contact with the concrete. Apparently there were no specified procedures for tightening the bolted connection to the truss, although it was reported that the contractor had used a torque wrench.

3. EXAMINATIONS OF THE BOLTS

Extensive metallurgical examinations of the bolts were carried out by several parties. There was general agreement that fatigue cracking and fracture had occurred in the threaded portion of all of the bolts. Views of the cracked and fractured surfaces in four of the bolts are shown in Fig. 5. The fatigue cracking appeared to have advanced across the bolts in an intermittent manner. Final ruptures appeared to be due to overloading.

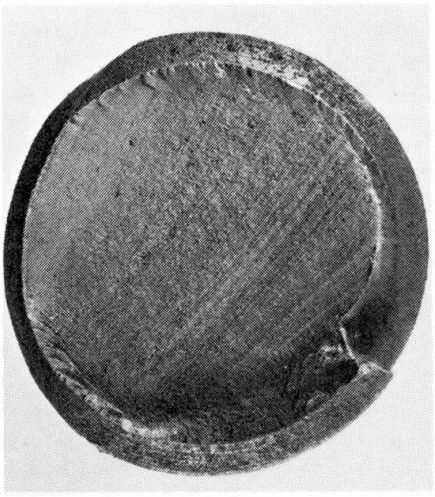

Bolt A

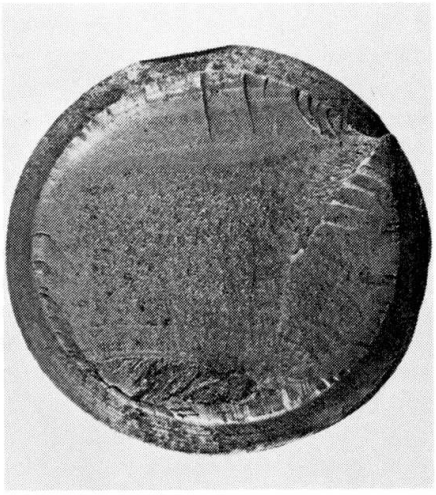

Bolt B

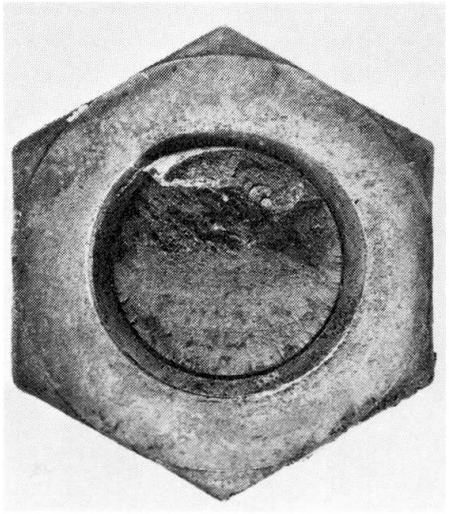

Bolt F

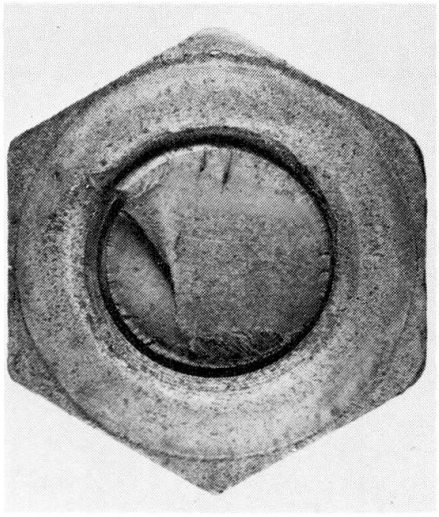

Bolt G

Fig. 5 Fracture Surfaces

A chemical analysis was made on samples obtained from eight bolts. The results were as follows:

	Minimum	Maximum	Average
Carbon	.39	.44	.42
Manganese	.79	.84	.83
Phosphorous	.009	.014	.010
Sulfur	.011	.016	.013
Silicon	.25	.30	.29
Nickel	.10	.19	.12
Chromium	.96	1.03	1.00
Molybdenum	.19	.23	.21
Copper	.04	.14	.11
Aluminum	.01	.04	.03

Physical tests on three samples taken from the bolts indicated that the yield strength, obtained as 0.2 percent offset from the elastic part of the stress-strain relationship, ranged from 268 to 340 MPa, while the tensile strength ranged from 616 to 656 MPa. Charpy V-notch impact test results on three specimens tested at 10 deg C ranged from 33 to 36 Nm.

4. ANALYSIS OF THE CRANE LOADING

The results of an analysis of the compressive, C, and tensile, T, reactions at the points of support of the collapsed truss are presented in Table 1. Three static loading conditions were investigated. It may be seen that the tensile reaction, T, which failed and caused the collapse of the crane varies from approximately 360 kN, when the crane is not on the truss, to 1170 kN when the crane bridge is at the end of the trusses and the trolley is adjacent to the truss. Based on a stress area of 1480 mm^2 through the root of the threads of the anchor bolts, and on the assumption that the load is distributed uniformly to all ten anchor bolts, the preceding values correspond to tensile stresses of 24 and 78 MPa, respectively.

TABLE 1 - STATIC LOAD REACTIONS FOR THE COLLAPSED TRUSS

Load	Compressive reaction (kN)	Tensile reaction (kN)	Nominal stress per bolt at tensile reaction (MPa)
Weight of truss	1125	360	24
Crane bridge at end of truss, trolley in center, and full load of oysters in bucket	2340	990	69
Crane bridge at end of truss, trolley adjacent to truss and full load of oysters in bucket	2700	1170	78

It was estimated that the truss reactions may be magnified approximately 30 percent by dynamic effects. Accordingly, the average tensile reaction that may be imparted to the system of anchor bolts was estimated to be 360 + 1.3 (990 - 360) or approximately 1180 kN. This corresponds to a nominal stress per bolt of 79 MPa.

There may have been further potential for a small amount of magnification of the stresses in the anchor bolts due to lateral forces creating a moment perpendicular to the truss. This moment would be expected to have the greatest effect on the most remote pairs of anchor bolts. However, the primary mechanism for resisting lateral forces was provided by the channel connection welded between the top of the truss and the adjacent higher part of the column.

5. EVALUATION OF FATIGUE STRENGTH

Fatigue test data on threaded parts is limited, at least in North America. However, early tests by Moore and Henwood [1] clearly indicated the importance of stress and the characteristics of the threads. Zero-to-maximum axial tension tests on medium-carbon 9.5 mm studs with die-cut threads had an endurance limit as low as 90 MPa. Low cycle tests on bolts have also been reported by Snow and Langer [2].

More recently (subsequent to the collapse described in this paper) Frank [3] reported on an experimental investigation of anchor bolts that included the following variables: steel type, thread pitch, bolt diameter, method of forming thread, galvanizing and double nuts. Frank concluded that the type of steel, thread size, and bar diameter do not significantly influence the fatigue strength of anchor bolts. The fatigue strength of double-nutted bolts subjected to bending or tension, tightened to one-third of a turn past snug, exceeded the strength of single-nut anchor bolts. According to Frank, the present AASHTO [4] Category E design stress range provides a suitable lower bound design relationship for single-nut anchor bolts and double-nutted anchor bolts tightened to less than one-third of a turn.

The AASHTO Category E design stress range is shown in Fig. 6. Superimposed on the plot is a point representing a nominal stress range of 55 MPa and 370,000 cycles at which the truss is estimated to have collapsed. The failure occurred well below the Category E design range.

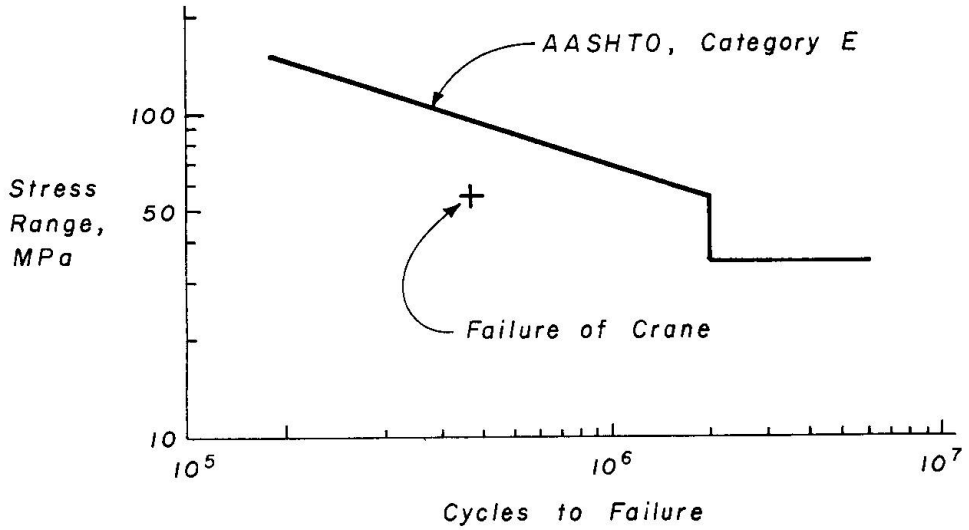

Fig. 6 Comparison of Failure Condition to AASHTO Category E Design Criteria

It should be noted that the AASHTO Category E design stress range is established on the basis that there is a 95 percent level of confidence that 95 percent of the failures will exceed the design condition. There were also a number of uncertainties in the determination of the stress range and cycles causing the failure. However, the most plausible reason for the failure occurring below the Category E design range is lack of uniformity of stress in the anchor bolts. The method of construction apparently did not insure that the stress was uniform when the system was placed in operation. With time, there may have been considerable variation in the bond between the surface of the bolts and the concrete, which may

also have had a significant influence on the stress conditions, irrespective of their adequate end anchorage. Consequently, it is likely that stress ranges as high as 150 to 200 MPa may have occurred in some of the bolts. As noted earlier, the examination of the fracture surfaces indicated that the fatigue cracks advanced across the bolts in a variable manner.

6. FINDINGS

The collapse of the crane occurred as a result of fatigue failures of the anchor bolts. Considering the potential for unequal stresses in the bolts, it was not surprising that the number of cycles to failure was less than the fatigue life indicated by tests on single bolts. More importantly, a structural connection should have been used for the tensile reaction which would not have allowed fluctuating tension in the anchor bolts.

REFERENCES

1. Moore, H. F. and Henwood, P.E.: The Strength of Screw Threads Under Repeated Tension, Bulletin 264, Engineering Experiment Station, University of Illinois, March 1931.

2. Snow, A. L, and Langer, B. F.: Low Cycle Fatigue Strength of Large Diameter Bolts, Journal of Engineers for Industry, American Society of Mechanical Engineers, Vol. 89, Series B, No. 1, February 1967.

3. Frank, K. H.: Fatigue Strength of Anchor Bolts, Journal of the Structural Division, American Society of Civil Engineers, Vol. 106 No. ST6, June 1980.

4. American Association of State Highway and Transportation Officials: Standard Specifications for Highway Bridges, Twelfth Edition, Washington, D. C., 1977.

Fatigue Research on Welded Crane Runway Girders

Recherches de fatigue sur les poutres-supports soudées des ponts roulants

Ermüdungsversuche an geschweissten Kranbahnträgern

S. UMINO
Prof.
Tokyo Denki University
Tokyo and Saitama, Japan

H. MIMURA
Associate Prof.
Tokyo Denki University
Tokyo and Saitama, Japan

SUMMARY
This report presents the results of fatigue tests on welded crane runway girders. They indicate that weld cracks in the vicinity of the upper flange are affected by the local stresses caused by the eccentricity of the crane rail from the centre line of the girder.

RESUME
Cet exposé présente les résultats d'essais de fatigue sur des poutres-supports soudées de ponts roulants. Ils indiquent que les fissures dans les soudures des ailes supérieures des poutres sont affectées par les contraintes locales dues à l'excentricité du rail du pont par rapport au centre de la poutre.

ZUSAMMENFASSUNG
Der Artikel beschreibt die Resultate von Ermüdungsversuchen an geschweissten Kranbahnträgern. Es zeigte sich, dass die Risse in der Nähe des oberen Flansches von den örtlichen Spannungen beeinflusst werden, welche infolge der Exzentrizität der Kranschiene bezüglich der Mittellinie des Trägers auftreten.

1. INTRODUCTION

A welded craneway girder under high wheel loads and high loading cycles usually develops cracks in these places;(1)the fillet welds between the web plate and upper flange;(2)the fillet welds between the rib plate and horizontal stiffener ;(3)the fillet welds between the web plate and rib plate, or the fillet welds between the upper flange and vertical stiffener. These weld fractures occur only in the vicinity of the upper flange of welded craneway girder. One of the possible reasons for these weld fructure is the effect of the local stresses caused by the eccentricity of the crane rail from the center line of girder.

A craneway girder is designed in accordance with the generally accepted procedure, based on static loads and in accordance with the Japanese Standard-Specification for the Design of Steel Structures.

Impact factors are usually introduced in this procedure to represent the effect of dynamic loadings, while the horizontal force acting in the transverse direction is defined as 10% of the wheel load. However, the local stresses caused by the eccentricity of the crane rail are not taken into consideration yet.

The present study is intended to discuss the weld fractures in the vicinity of the upper flange of the craneway girder, based on the fatigue test results carried out at Tokyo Denki University.

2. TYPES OF FATIGUE CRACK IN THE WELDED CRANEWAY GIRDER

An example of the relation between the location of the fatigue crack initiated and the eccentricity of crane rail is shown in Fig.1 of craneway girders in a mill building. These craneway girders are simply supported beams of 12M span supporting 2 cranes of 39M span. The cross section of these girders is built-up

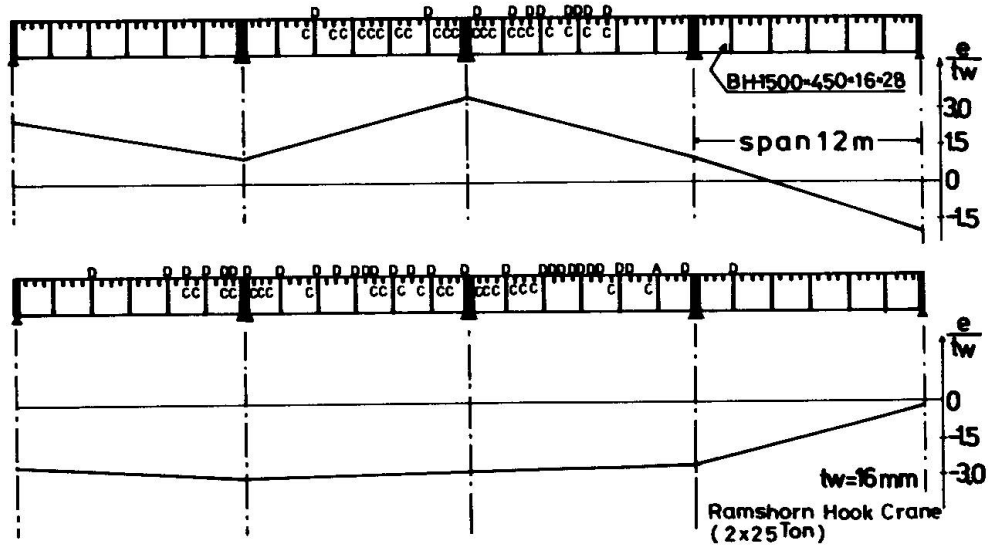

Fig.1 An example of the relation between the location of fatigue crack initiated and the eccentricity of crane rail

H shape of 1500mm depth, 450mm width of flange, 16mm thickness of web and 28mm thickness of flange, and vertical ribs are attached at the web plate beneath the upper flange. The crane rail, with a thick resilient pad laid under it, is a 74 Kgf/M(JIS E 1103) laid on the craneway girder. The serviced cranes are two overhead travelling cranes with 4 wheels per rail respectively. The rated loads of the cranes are 25Tonf. Maximum wheel loads of the cranes are 35Tonf respectively.

The fatigue cracks which were initiated in these girders were observed after a service period of only 7 years. The estimated number of the cycles of loading is about 5×10^5.

The cracks which will occur in the vicinity of the upper flange where e/tw are more then about 3 are shown in Fig.1. (e: eccentricity of crane rail from the center line of girder, tw: thickness of web plate)

Fig.2 shows typical patterns of fatigue crack initiated in a welded craneway girder. For the sake of convenience in this report, the types of cracks which will be dealt with are identified as follows.

Type A crack; crack in the fillet welds between the web and the upper flange

Type B crack; crack in the fillet welds between the rib and the horizontal stiffener

Type C crack; crack in the welds between the rib and the web plate

Type D crack; crack in the welds between the upper flange and the vertical stiffener

Type E crack; crack in the lower flange

(the Type E crack is not dealt with in this report.)

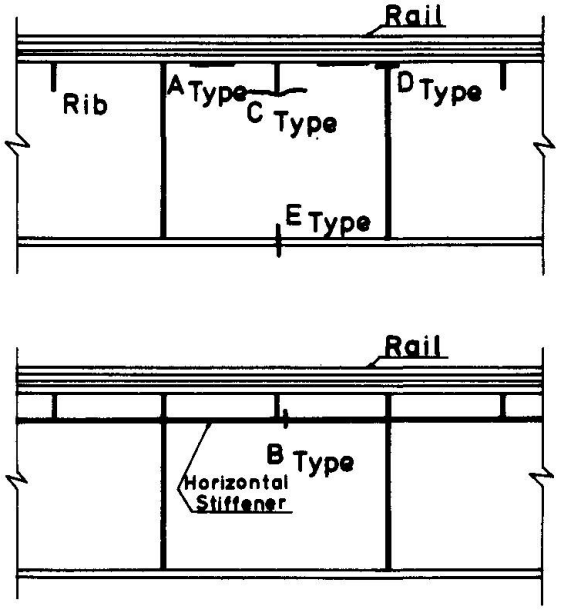

Fig.2 Types of fatigue cracks

3. TEST SPECIMENS AND EXPERIMENTAL METHOD

The details of the tested specimens are shown in Fig.3, and the dimensions of the specimens are shown in Table 1. The kind of steel used in these specimens is JIS-SS41 (structural cabon steel with minimum specified tensile strength of 41 Kgf/mm^2).

These specimens were fabricated by a submerged-arc weld at the fillet weld connection of flange to web, and by a manual weld at the fillet weld connection of the rib to the web and the stiffener to the web. All of these specimens were tested under as welded condition.

The mechanical properties and chemical compositions of the steel used are summarized in Table 2.

The tested girder was simply supported and concentrated load was applied midspan of it though the crane rail (37 Kgf/M) as shown in Fig.4.
A repeated load was applied with 1∿3 Hz in one direction by 50Tonf electro -hydraulic fatigue testing machine.

The initiation and propagation of fatigue cracks were observed using a dye penetrant inspection.

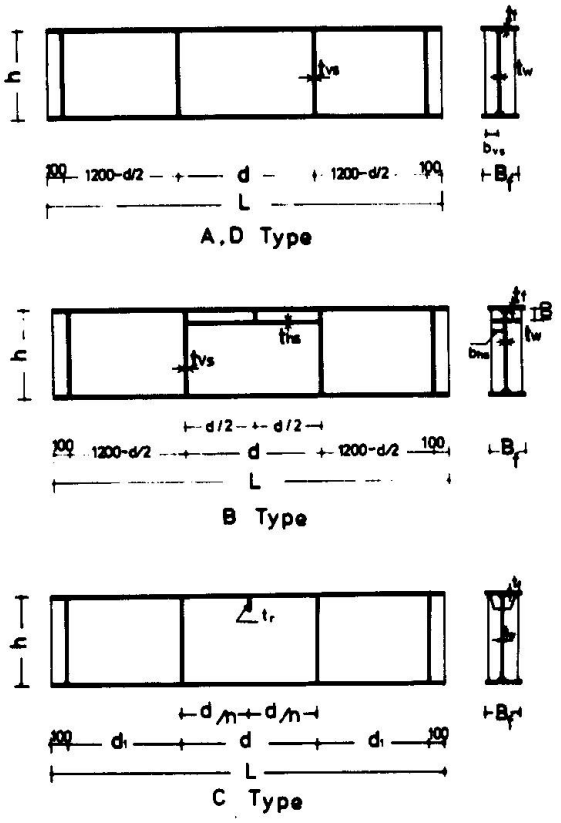

Fig.3 Tested specimens

Table 1 Dimensions of specimens

specimens	Lcm	hcm	dcm	Bfcm	tfmm	twmm	bvscm	tvsmm	bhscm	thsmm	brcm	trmm
BG16- 9- 900/2(9)	240	59.8	90.0	24.1	15.61	8.88	9.1	8.79	10.2	8.69	10.0	8.76
BG16- 9- 900/2(9)	240	59.6	90.0	24.1	15.96	8.87	9.1	8.79	10.0	8.73	10.0	8.76
BG19- 9- 900/2(12)	240	58.0	90.0	24.0	18.99	8.80	10.0	8.80	10.0	11.78	10.0	8.80
BG16- 9- 900/2(9)	240	59.7	90.0	24.1	15.99	8.96	9.1	8.79	10.2	8.74	10.0	8.76
BG16- 6- 600/2(6)	239	57.8	59.8	24.0	15.74	5.80	10.0	5.81	10.0	5.81	10.0	5.82
CG16- 9- 900/2(9)	240	60.0	90.0	24.0	15.66	8.66	9.0	8.85			9.0	8.85
CG16- 9- 900/2(9)	240	59.7	90.2	24.1	15.65	8.85	9.0	8.85			9.0	8.86
CG16- 9- 900/2(9)	240	59.7	90.1	24.1	15.67	8.85	9.0	8.85			9.0	8.85
CG16- 9- 900/2(9)	240	59.8	89.8	24.0	15.62	8.86	9.0	8.86			9.0	8.86
CG16- 9- 900/2(9)	240	60.0	89.9	24.0	16.64	8.84	9.0	8.85			9.0	8.84
CG16- 9- 900/2(9)	240	59.9	90.1	24.1	15.66	8.86	9.0	8.86			9.0	8.86
DG16- 6- 600(6)	239	57.8	59.8	24.0	15.74	5.80	10.0	5.81				
DG22-12- 800(9)	240	57.8	80.0	24.1	21.77	11.79	9.1	9.02				
DG19- 6- 600(6)	240	57.9	90.0	24.0	18.92	5.66	10.1	5.73				
DG16- 9- 900(9)	240	59.8	90.1	24.1	15.64	8.86	9.0	8.80				
DGH19-9- 800(12)	240	40.0	79.8	23.9	18.73	8.76	10.5	11.65				

Table 2 Mechanical properties and chemical composition

specimens	plate(mm)	σ_y(t/cm^2)	σ_B(t/cm^2)	Elon.(%)	Cx100	Six100	Mnx100	Px1000	Sx1000	
B-Type	6	3.34	4.64	25.64	12	25	77	22	7	SH
	9	3.10	4.29	29.03	12	19	77	21	14	
	12	2.91	4.26	29.61	10	20	67	20	12	
C-Type	9	2.40	4.04	32.65	12	19	77	21	14	W
$\frac{A}{D}$-Type	6	3.34	4.64	25.64	12	25	77	22	7	Sv
	9	3.10	4.29	29.03	12	19	77	21	14	
	12	2.80	4.28	30.33	10	30	67	20	12	

SH; Horizontal Stiffener, W; Web, Sv; Vertical Stiffener,

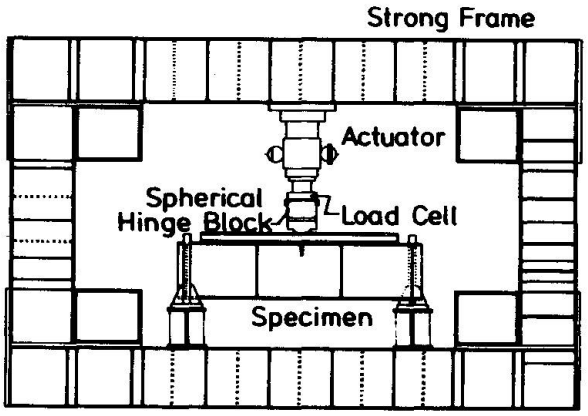

Fig.4 Test set-up

4 TEST RESULTS AND DISCUSSIONS

The fatigue test results are summarized in Table 3 and are illustrated in Fig.5 to Fig.8. In Table 3, ε_1 and ε_2 are the measured strains at the maximum load in the vicinity of the crack initiated on the eccentric side of rail and the opposite side respectively.

Nc represents the number of cycles up to cracks initiated and Nf represents the number of failures.

Nf of these specimens were defined at the number of cycles when the crack developped across the width of stiffener of the Type B and Type D specimens and when the crack in the web plate developped about 80mm in length of the Type C specimens. No Type A crack was observed in these tests.

The fatigue test results for the Type B crack are shown in Fig.5. In this figure, hollow circles represent Nc while solid circles represent Nf.

All of the Type B cracks initiated at the toe of the fillet welds between the rib and the horizontal stiffener. The fatigue crack-growth rate of Type B is about 0.9mm/10^4 cycles until the crack runs though the thickness of horizontal stiffener plate. After that, the crack-growth rate increases to 6mm/10^4 cycles. The crack-growth stopped when it reached the web plate.

Table 3 Results of test

specimens	$\varepsilon_1(\varepsilon_2)\times10^{-6}$	Nc$\times10^4$	Nf$\times10^4$	Pmax-Pmin(t)	Remarks
BG16- 9- 900/2(9)	1560(440)	14.5	42	20-2	
BG16- 9- 900/2(9)	960(270)	48	82	30-2	
BG19- 9- 900/2(12)	800(260)	52	120	30-2	
BG16- 9- 900/2(9)	580(160)	100	170	25-2	
BG16- 6- 600/2(6)	420(150)	—	240	25-2	
CG16- 9- 900/2(9)	2550(-2830)	(3)	6.8	25-2	
	2130(-2160)	4	10.5		
	1450(-2040)	10.6	26.5		
	1000(-1300)	46	64.5		
	450(-1000)	42	75		
	160(- 840)	75	200+		εt (εc)
DG16- 6- 600(6)	1300(- 645)	52	82	25-2	———
DG22-12- 800(9)	1050(- 80)	83	94	30-2	945(-1620)
DG19- 6- 600(6)	820(60)	115	135	30-2	665(- 870)
DG16- 9- 900(9)	600(- 145)	110	128	30-2	580(- 630)
DG22-12- 800(9)	450(- 40)	—	230+	25-2	400(-1250)
DGH19-9- 800(9)	350(- 135)	—	270+	20-2	450(-1235)

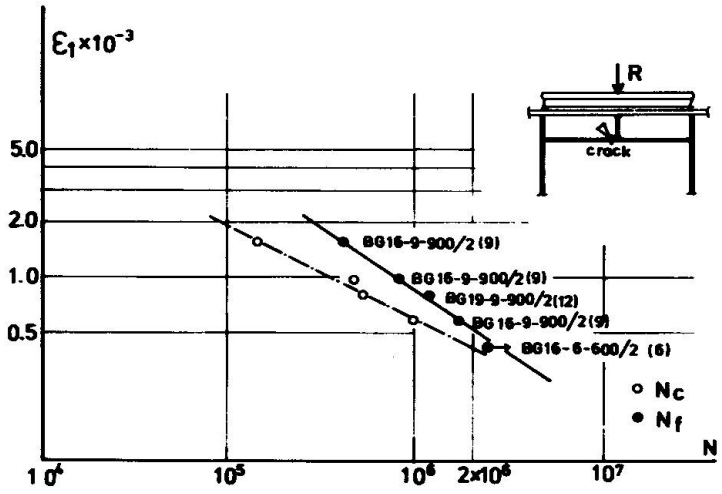

Fig.5 Fatigue test results of the Type B crack

The test results for the Type C crack are shown in Fig.6. All of the Type C cracks initiated at the toe of fillet welds between the rib and web plate at the end of rib. These tests show that the Type C crack appears at a very early loading cycle, even when the eccentricity of crane rail is not so great (e=0.5 tw). In this case, the value of normal stress of the flange is 0.56t/cm^2, and the value of mean shearing stress of the web is 0.24t/cm^2 at the maximum load (25Tonf).

The test results for the Type D crack are shown in Fig.7. In these tests, Type A and/or Type D cracks were expected to occur, however, the tests results showed the initiation of no Type A cracks. εc and εt, shown in remarks of Table 3, are the measured strains of the web beneath upper flange at the loading point on the eccentric side of rail and the opposite side respectively at the maximum load. All of the Type D cracks initiated at the toe of fillet welds between upper flange and vertical stiffener. The cracks developped along the toe of fillet weld. The crack-growth stopped when it reached the web plate.

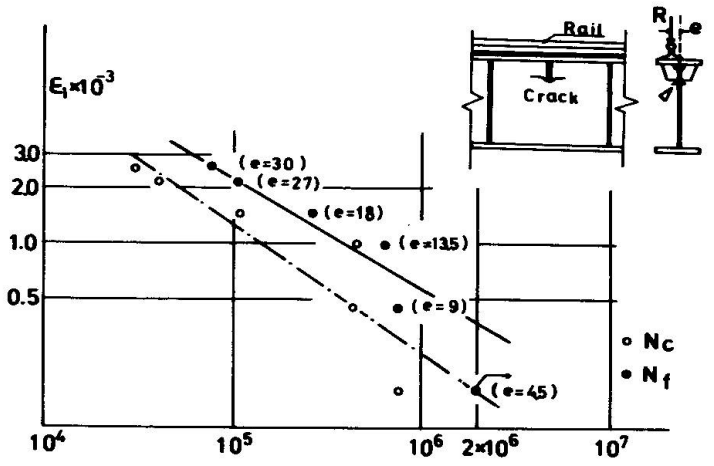

Fig.6 Fatigue test results of the Type C crack

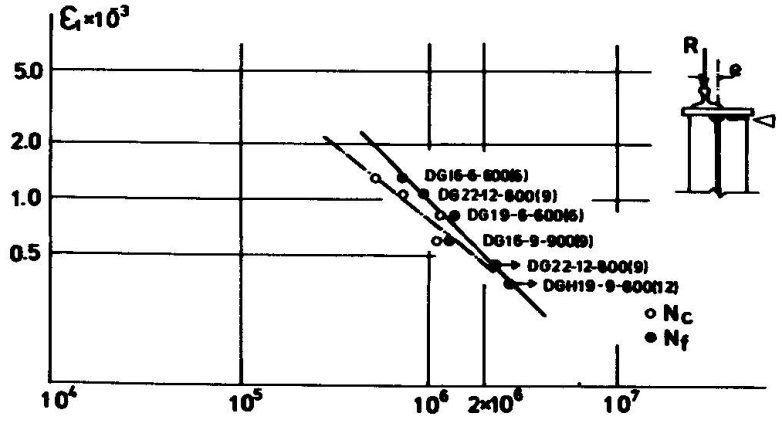

Fig.7 Fatigue test results of the Type D crack

Fig.8 shows the relation among magnitude of eccentricity of the crane rail from the center line of girder, e web plate thickness, tw wheel load, R girder depth, h distance between vertical stiffeners, d torsional rigidity of upper flange and crane rail, JG and fatigue life N obtained from test results. This figure shows that the fatigue lives of the Type B and Type D cracks are nearly equal for the magnitude of eccentricity of the crane rail while the effect of the eccentricity of crane rail is larger for Type C crack then for the Type B and Type D cracks.

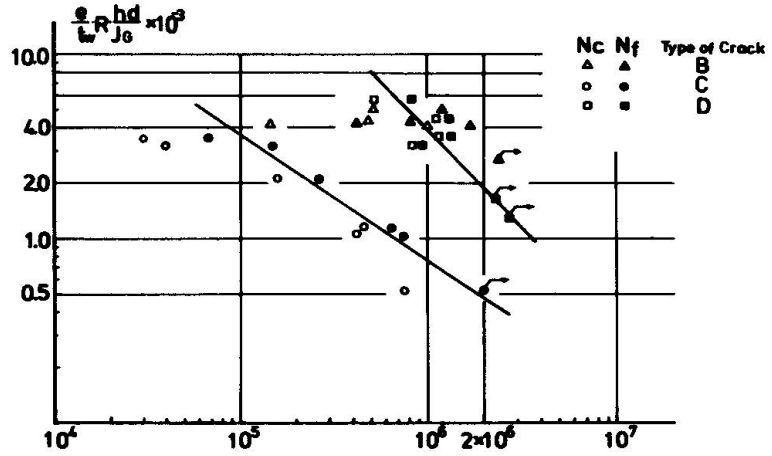

Fig.8 Relation between magnitude of eccentricity of crane rail from center line of girder and fatigue lives

5. CONCLUSION

It is concluded that the fractures in the vicinity of the upper flange of the welded craneway girder are caused by the eccentricity of the crane rail from the center line of craneway girder. Especially, Type C fatigue crack is more affected by the eccentricity of the crane rail. The fatigue lives of the Type B and Type D crack are nearly equal for the magnitude of eccentricity of the crane rail.

REFERENCES

(1) AIJ. Specification for Design of Steel Structures, 1970
(2) S.Umino, et al; Report on Fatigue Failure of Crane Girders, JSSC Vol.12 No.128 1976 (in Japanese)
(3) J.K.Oxfort; Zur Beanspruchung der Obergurte vollwandiger Kranbahnträber durch Torsionsnomente und durch Querkraftbiegung unter dem örtlichen Radlastangriff, Der Stahlbau 12/1963
(4) G.Mass; Investigations Concerning Craneway Girders, Iron and Steel Engineer 3/1972
(5) DIN 4132. Kranbahnen Stahltragwerke, 1980
(6) JIS B8821. Specification for the Design of Crane Structures 1976 (in Japanese)

Lebensdauervorhersage für geschweisste Kranbauteile

Design Life Estimation of Welded Crane Girders

Estimation de la durée de vie d'éléments soudés de ponts-roulants

U. MÜLLER
Dr. -Ing.
Verein Deutscher Eisenhüttenleute
Düsseldorf, BRD

W. UNGERER
Dr. -Ing.
Verein Deutscher Eisenhüttenleute
Düsseldorf, BRD

ZUSAMMENFASSUNG
Ein Dimensionierungsverfahren zur quantitativen Ermittlung und Erhöhung der Anlagenzuverlässigkeit wird vorgestellt. Die Ermüdungsschäden an den Schweissverbindungen von Kran- und Kranbahnträgern wurden ausgewertet. Das Beanspruchungskollektiv im anrissgefährdeten Querschnitt von Schweissverbindungen wurde ermittelt und die Bauteilwöhlerlinie für geschweisste Grossbauteile abgeschätzt. Die rechnerische Lebensdauerschätzung und ein Vergleich der betrieblichen mit den berechneten Bruchlastspielzahlen werden diskutiert.

SUMMARY
A design procedure is presented for evaluating and improving the reliability of installations. This includes a fatigue life calculation and an evaluation of fatigue damage to welded joints in both the crane and its runway girders. In particular, the combination and application of loads is considered in zones of welded joints susceptible to crack initiation. The estimation of S-N curves for large welded elements is discussed and a comparison made between the calculated and measured number of cycles to fracture.

RESUME
Il s'agit d'un procédé de calcul pour l'estimation quantitative et l'augmentation de la sécurité des installations. On effectue le calcul de la résistance sous sollicitations de service et on exploite les dommages dus à la fatigue aux assemblages soudés de ponts-roulants et poutres de roulement. Les courbes de Wöhler d'éléments de construction soudés importants sont estimées et l'on compare les durées de vie calculées avec celles effectives mesurées sous les charges de service.

1. INSTANDHALTUNGSKOSTEN, BAUTEILZUVERLÄSSIGKEIT, DIMENSIONIERUNGSKONZEPT

Im Bereich der deutschen Stahlindustrie werden die Anlagenkosten in hohem Maße durch die Instandhaltungskosten bestimmt. Eine nachhaltige Senkung der Instandhaltungskosten setzt bei dem hohen Niveau der Instandhaltungstechnik in den Hüttenwerken eine Erhöhung der Anlagenzuverlässigkeit durch weiterentwickelte Dimensionierungsverfahren und -maßnahmen voraus. Die Anlagenbetreiber fordern daher von den Anlagenherstellern zunehmend Nachweise für die erreichte Gesamtzuverlässigkeit der gelieferten Anlage. Diese Forderung ist jedoch nur bedingt zu erfüllen, weil es bisher keine allgemein anwendbaren Zuverlässigkeitsmodelle für komplexe Anlagen gibt. Man versucht deshalb heute, hohe Anlagenzuverlässigkeit über eine Vereinheitlichung und Anhebung des Zuverlässigkeitsniveaus aller Einzelbauteile zu verwirklichen und den erreichten Wert durch Zuverlässigkeitsangaben für die Einzelbauteile zu charakterisieren [1]. Diese Aufgabe, die über den Rahmen der bisher in Regelwerken geforderten Nachweise hinausgeht, erfordert ein umfassendes Dimensionierungskonzept, wie es in Bild 1 dargestellt ist. Die Ermittlung der Bauteilzuverlässigkeit kann mit der Betriebsfestigkeitsrechnung erfolgen. Dabei wird durch den Vergleich von auftretenden und ertragbaren Beanspruchungen die Bauteil-Lebensdauerverteilung F(t) ermittelt. Komplement dieser Verteilung ist die Zuverlässigkeitsfunktion R(t).

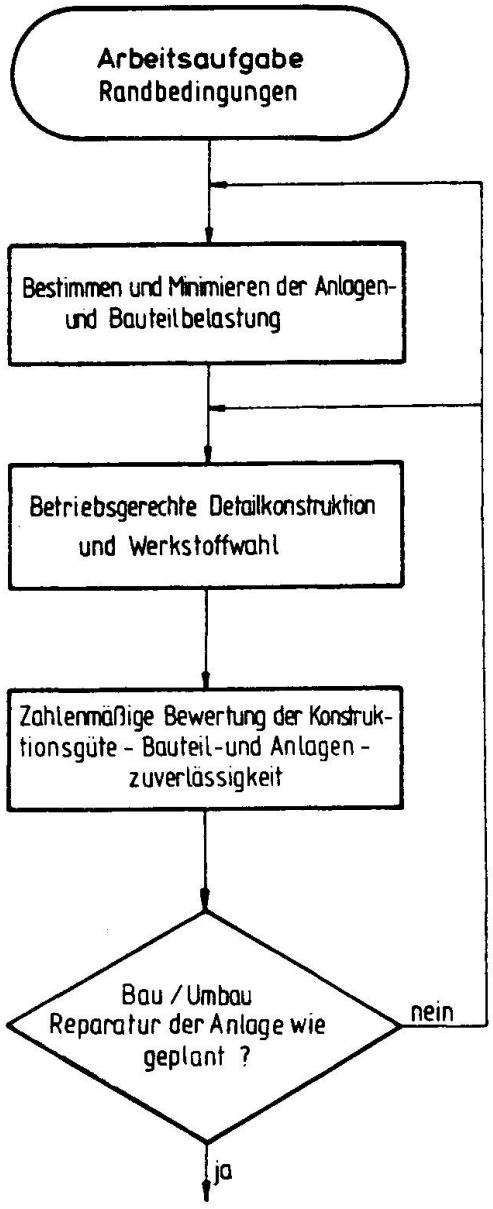

Bild 1: Konzept einer betriebsgerechten Dimensionierung
Fig. 1: Design procedure for service loading conditions

2. BETRIEBSFESTIGKEITSRECHNUNG NACH DEM KONZEPT DER ARBEITSGEMEINSCHAFT BETRIEBSFESTIGKEIT DES VDEh

Die von der Arbeitsgemeinschaft Betriebsfestigkeit empfohlene Vorgehensweise

ist in Bild 2 dargestellt [2].
Die Bauteilbeanspruchungen werden durch das auf die vorgesehenen Nutzungsdauer extrapolierte Kollektiv der Spannungsschwankungen gekennzeichnet, dem im allgemeinen eine Auftretenswahrscheinlichkeit von 50% zugeordnet wird. Die ertragbaren Beanspruchungen werden durch die Bauteil-Wöhlerlinie, die für die Ausfallwahrscheinlichkeit von 50% abzusichern ist, gekennzeichnet. Die Schadensakkumulationsrechnung liefert dann einen Schätzwert für die zu erwartende Lebensdauer bei einer Ausfallwahrscheinlichkeit von 50%.
Der gesuchte Lebensdauerwert für eine geforderte Ausfallwahrscheinlichkeit oder auch Bauteilzuverlässigkeit wird über eine Hilfsgröße i_L gefunden. Sie ist unter Annahme log-normal verteilter Lebensdauern in Abhängigkeit von der Ausfallwahrscheinlichkeit und der Streuspanne $T_{90\%} = L_{10\%} : L_{90\%}$ tabelliert. Der mögliche Bereich dieser Streuspanne wird für Bauteile von Hüttenwerksanlagen in [2] mit 1:5 abgeschätzt.

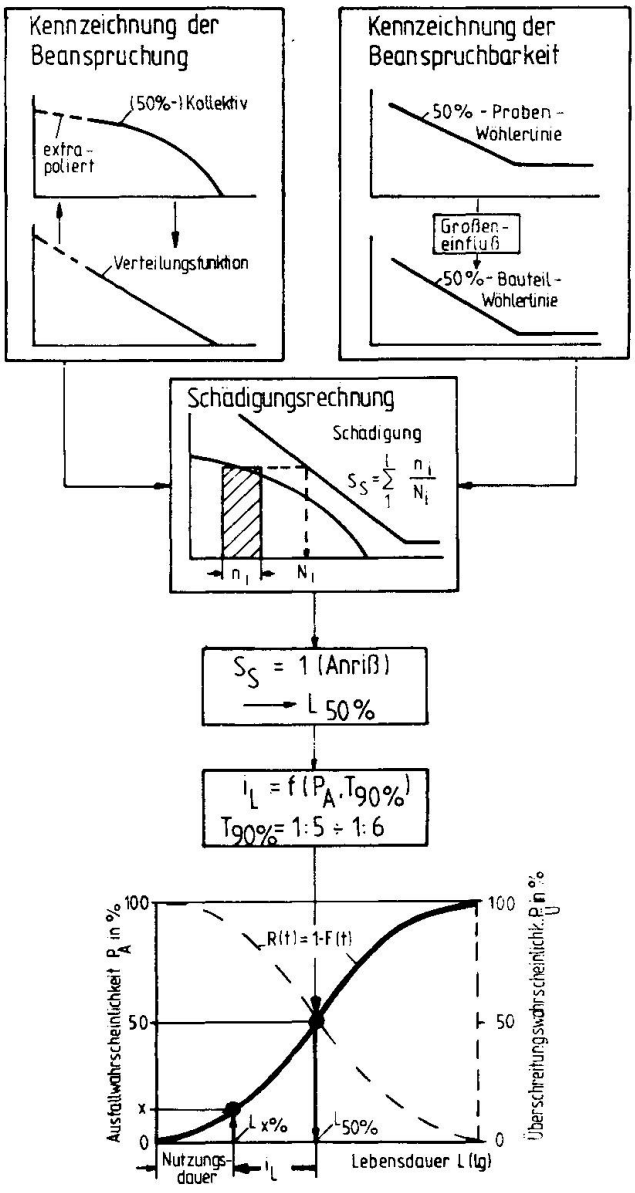

Bild 2: Lebensdauervorhersage für eine vorgebbare Ausfallwahrscheinlichkeit
Fig. 2: Calculation of the life for a required probability of failure

3. BETRIEBSUNTERSUCHUNGEN AN GESCHWEISSTEN KRANTRÄGERN

Im folgenden wird über Untersuchungen berichtet, die das Ziel verfolgten, die Anwendbarkeit des genannten Konzeptes auf Stahlbauteile zu überprüfen. Dazu wurden exemplarisch Ermüdungsschäden an geschweißten Verbindungen im Bereich der befahrenen Obergurte von Kran- und Kranbahnträgern ausgewertet [3].

3.1 Ermüdungsschäden an den Schweißverbindungen im Bereich der befahrenen Obergurte von Krantragwerken

Die Raddruckbeanspruchungen in den geschweißten Verbindungen zwischen dem befahrenen Obergurt und dem Stegblech setzen sich aus der Grundbeanspruchung in-

folge der fiktiv zentrisch eingeleiteten Radlast und Zusatzbeanspruchungen aus exzentrischen Radlasten zusammen. Diese Zusatzbeanspruchungen werden im wesentlichen beeinflußt durch

- die Exzentrizität der Radlast und Seitenkräfte aus der Schrägfahrt von Kran und Katze,
- die Verdrehsteifigkeit von Obergurt, Schiene und Stegblech,
- die Druckverteilung über die Schienenfußbreite,
- den Verschleißzustand von Schienenkopf und Laufrad und
- den fertigungsbedingten Versatz zwischen Schiene und Stegblech.

Sie bewirken Querbiegungen mit örtlichen Spannungskonzentrationen im Bereich der Schweißverbindungen. Ein rechnerisches Verfahren zur Ermittlung der statistischen Verteilung der betrieblichen Beanspruchungsschwankungen unter Berücksichtigung der genannten Einflußgrößen ist bisher nicht bekannt. Im Rahmen der Untersuchung wurden deshalb die betrieblichen Beanspruchungsschwankungen im Bereich des anrißgefährdeten Querschnitts der Schweißverbindungen zwischen Obergurt und Stegblech mit Dehnungsmeßstreifen (DMS) ermittelt. Bild 3 zeigt beispielhaft eine Übersicht über die Meßstellen an einem Kranträger.

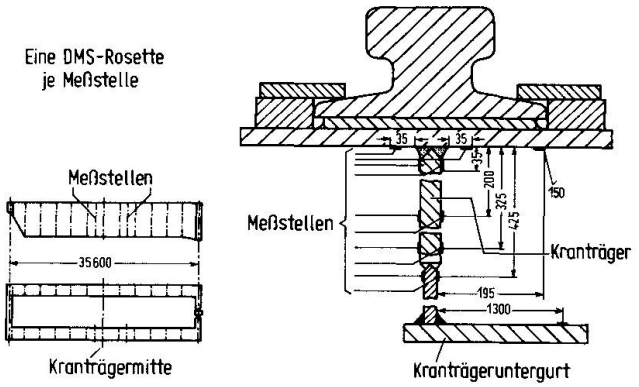

Bild 3: Meßstellenanordnung an einem 100-t Brammentransportkran
Fig. 3: Measuring point arrangement on a 100-t slab conveying crane

3.2 Betriebliche Beanspruchungen

Die umfangreichen Meßergebnisse sind in einem Bericht [3] dargelegt. Deshalb sollen an dieser Stelle nur einige kennzeichnende Teilergebnisse vorgestellt werden. Bild 4 zeigt die aus den gemessenen Dehnungen berechneten Spannungs-Zeit-Verläufe im Stegblech eines Kranträgers. Im Bild sind die Verläufe der Schub- und Normalspannungen sowie die daraus berechneten Vergleichsspannungen nach der Normalspannungs- und Gestaltänderungsenergiehypothese dargestellt. Die in vertikaler Richtung wirkende Normalspannung σ_y wird durch das Spannungsfeld der örtlich eingeleiteten Radlast bestimmt. Sie ist gleich Null, solange keines der beiden Katzräder in unmittelbarer Nähe des Meßquerschnittes steht.
Die Druckspannung σ_y steigt steil an und erreicht einen Höchstwert, wenn ein Katzrad den Meßquerschnitt überrollt. Dieser Verlauf wird hinsichtlich der

Größe der Spannungsschwankungen auf beiden Seiten des Stegbleches beobachtet. Der Einfluß einer überlagerten Stegblechquerbiegung infolge exzentrischer Radlasten verursacht eine geringe Mittelspannungsverschiebung. Die Schubspannung τ im Stegblech setzt sich aus zwei Anteilen zusammen, die der Querkraft und dem Spannungsfeld der örtlichen Radlasteinleitung zugeordnet werden können. Der Verlauf der Normalspannung σ_x , die in Trägerlängsrichtung wirkt, setzt sich aus einem Biegespannungsanteil, der dem Verlauf der Zuggurtbeanspruchungen proportional ist, und einem Anteil aus der Einleitung der Radlasten zusammen. Der ebene Spannungszustand im Stegblech wird im wesentlichen von der Überlagerung der Trägerbiegespannungen, der Schubspannungen aus den Querkräften und dem Spannungsfeld aus der Einleitung der Radlast bestimmt. Die größten Spannungsschwankungen hat die Druckspannung σ_y . Die Verläufe der Vergleichsspannungen sind gleichartig. Sie ähneln im Grundverlauf der Biegespannung σ_x , und haben ähnlich hohe Spannungsspitzen wie die vertikale Druckspannung.

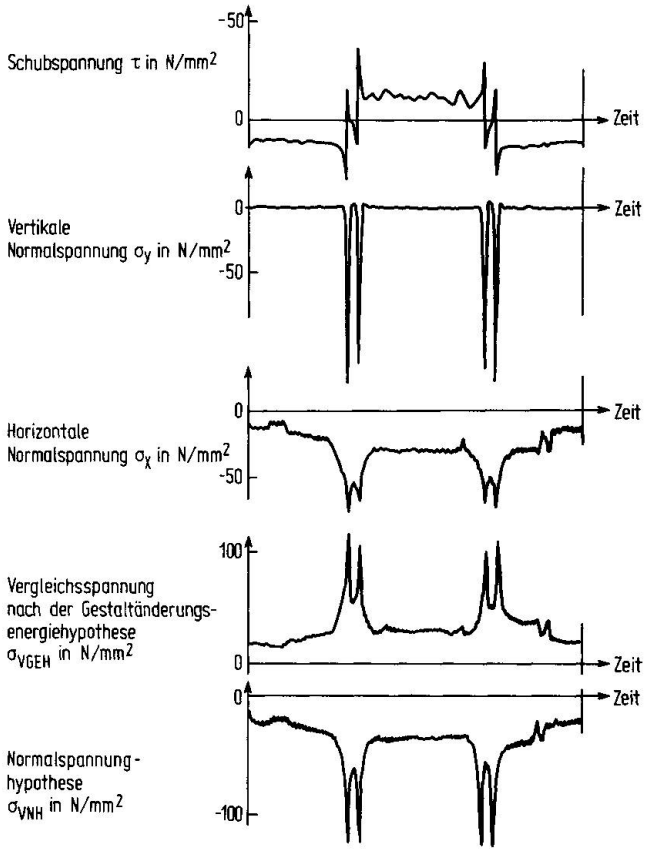

Bild 4: Gemessene Spannungen und berechnete Vergleichsspannungen im Stegblech eines 32-t Stripperkranes für zwei Katzfahrten

Fig. 4: Measured stresses and computed comparision stresses in the web plate of a 32-t stripping crane for two trolley travels

3.3 Kollektiv der gemessenen Spannungsschwankungen

Aus den gemessenen Spannungs-Zeit-Verläufen wurden mit Hilfe der Überschreitungszählung von Klassengrenzen und der Extremwertanalyse Spannungskollektive abgeschätzt. Diesen Auswertungen lagen Beanspruchungsmessungen über drei bis fünf Schichten mit einem repräsentativen Arbeitsprogramm der Anlagen zugrunde. Bild 5 zeigt schematisch das Beanspruchungskollektiv im Katzschienenbereich eines Kranträgers. Die Normalspannung σ_y schwankt bei jeder Katzradüberrollung zwischen einer Oberspannung σ_{yO} im Zugbereich und einer Unterspannung σ_{yU} im Druckbereich. Der Kollektivumfang ist gleich der Zahl der Katzradüberrollungen. Die Unterspannung σ_{yUmin} , die bei jeder Katzradüberrollung erreicht oder überschritten wird, ist näherungsweise berechenbar, wenn die kleinste Rad-

last der Katze zentrisch am Schienenkopf angenommen wird.

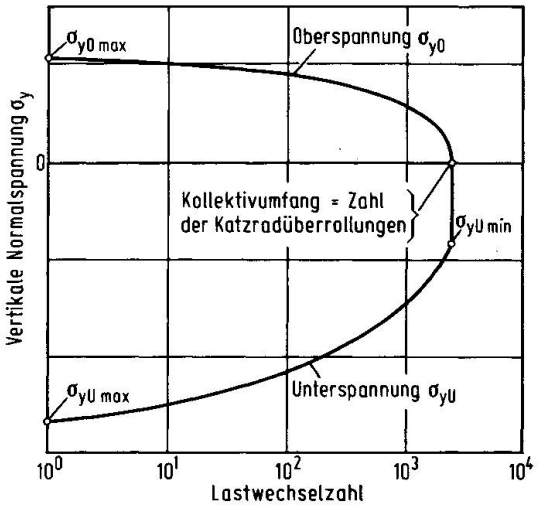

Bild 5: Kollektiv der Überschreitungshäufigkeit von Klassengrenzen für die Normalspannung σ_y im Stegblech eines Krankastenträgers (schematisch)
Fig. 5: Collective of a exceeding frequency of class limits for the normal stress σ_y in the web plate of a crane box girder (schematic)

3.4 Bauteil-Wöhlerlinie für geschweißte Großbauteile

Die benötigten Bauteilwöhlerlinien wurden für die untersuchten Verbindungen konstruiert. Dabei wurde angenommen, daß das normierte Wöhlerlinienstreuband, das aus Versuchen mit geschweißten Kleinproben abgeleitet worden ist, grundsätzlich auch zur Beschreibung der Schwingfestigkeit geschweißter Großbauteile geeignet ist. Damit wird als Schwingfestigkeitskennwert lediglich die mittlere, dauerhaft ertragbare Spannungsamplitude zur Kennzeichnung der Schwingfestigkeit im Bereich $> 10^4$ Lastwechsel benötigt. Ausgehend von den Versuchsergebnissen für geschweißte Kleinproben [4], wurden die Einflußgrößen auf den Schwingfestigkeitskennwert von geschweißten Großbauteilen diskutiert. Die wesentlichen Einflußgrößen sind

- die Fertigungsqualität,
- der statistische Größeneinfluß,
- der geometrische Größeneinfluß und
- der Einfluß von Schweißeigenspannungen [5,6].

Eine differenzierte, quantitative Gewichtung jeder einzelnen Einflußgröße ist heute noch nicht möglich. Die Schrifttumsdurchsicht zeigte jedoch, daß bislang der Einfluß von Schweißeigenspannungen auf den Schwingfestigkeitskennwert zu günstig bewertet wird. Es ist vielmehr davon auszugehen, daß die dauerfest ertragbare Spannungsamplitude einer Verbindung mit Eigenspannungen im Bereich der Streckgrenze bei nur etwa 60 % der ertragbaren Spannungsamplitude einer vergleichbaren, eigenspannungsfreien Verbindung liegen kann. Diese Abminderung wurde auch in dieser Untersuchung berücksichtigt, weil Eigenspannungsmessungen an Wrackteilen von geschweißten Kranträgern und an geschweißten Großproben mit DMS-Bohrlochrosetten die Existenz solcher hohen Eigenspannungen bestätigten. Der Schwingfestigkeitskennwert der untersuchten Verbindungen wurde mit Versuchsergebnissen für geometrisch ähnliche geschweißte Kleinproben unter Berücksichtigung der genannten Einflußgrößen abgeschätzt.

Diese abgeschätzten Schwingfestigkeitskennwerte liegen für den Kerbfall K3 (nach DIN 15018) um 23% und für den Kerbfall K4 um 47% unter den mittleren, dauerfest ertragbaren Spannungsamplituden, die den zulässigen Spannungen nach DIN 15018 zugrunde gelegt sind. Die durchgeführte Abschätzung zeigt eine befriedigende Übereinstimmung mit Vorschlägen von T. Gurney und A. Granström [5,7]. Daraus wird jedoch auch deutlich, daß weitere systematische Untersuchungen zur Schwingfestigkeit geschweißter Großbauteile, insbesondere auch mit betriebsähnlichen, mehrachsigen Beanspruchungsschwankungen, notwendig sind.

3.5 Lebensdauerabschätzung

Mit den konstruierten Bauteilwöhlerlinien und den ermittelten Amplitudenkollektiven der Beanspruchungen im anrißgefährdeten Querschnitt von Schweißverbindungen wurden Schädigungsrechnungen nach der modifizierten, linearen Schädigungshypothese durchgeführt. Die berechneten Bruchlastspielzahlen wurden mit den betrieblich festgelegten Bruchlastspielzahlen verglichen. Dazu wurde, vergleichbar einem statistischen Mittelwerttest, eine Kenngröße M ermittelt. Dabei wird der Abstand zwischen der betrieblichen und der mittleren berechneten Bruchlastspielzahl ins Verhältnis gesetzt zum Abstand der berechneten Bruchlastspielzahlen für die Überlebenswahrscheinlichkeiten $P_Ü$ = 10% und $P_Ü$ = 90%. Die Verteilungsfunktion der ermittelten Kennwerte M für die untersuchten Schadensfälle ist im Wahrscheinlichkeitsnetz (Bild 6) dargestellt. Daraus geht hervor, daß die berechneten und die betrieblichen Bruchlastspielzahlen im Mittel übereinstimmen, weil der Mittelwert der Verteilungsfunktion bei Null liegt. Für den größten Teil der Schadensfälle liegen die betrieblichen Bruchlastspielzahlen innerhalb des berechneten Streubereiches für die Überlebenswahrscheinlichkeiten $P_Ü$ = 10% und $P_Ü$ = 90%, das heißt, M liegt im Bereich $-0{,}5 \leq M \leq 0{,}5$.

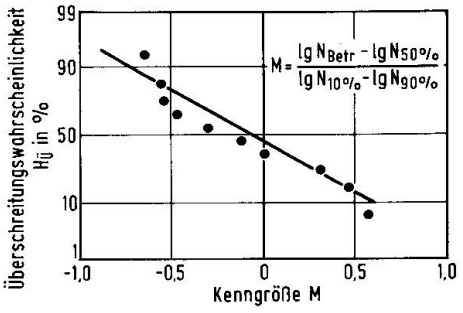

Bild 6 : Verteilungsfunktion der Kenngröße M für die untersuchten Schadensfälle
Fig. 6 : Distribution function of the parameter M for the investigated cases damage

4. ZUSAMMENFASSUNG

Auf der Grundlage dieser Ergebnisse scheint es möglich, die Bauteillebensdauer in der Konstruktionsphase wirklichkeitsnah abschätzen zu können, wenn das Kollektiv der Ermüdungsbeanspruchungen im anrißgefährdeten Querschnitt und die Bauteilwöhlerlinie miteinander verknüpft werden. Mit Hilfe alternativer Schädigungsrechnungen für verschiedene Verbindungsformen kann eine betriebsfeste Bauteilgestaltung mit noch zulässiger Ausfallwahrscheinlichkeit erreicht werden. Die Treffsicherheit solcher Abschätzungen kann durch weitere Schwingfestigkeitsuntersuchungen mit mehrachsigen Beanspruchungsschwankungen verbessert werden.

Die Untersuchung leistet damit einen Beitrag zum eingangs erläuterten Dimensionierungskonzept für Stahltragwerke, das es dem Konstrukteur ermöglichen soll, die Bauteilzuverlässigkeit in der Konstruktionsphase als Maß für die Konstruktionsgüte nachzuweisen.

5. SCHRIFTTUM

1. Ungerer, W.: Betriebsfestigkeitsbetrachtung als Mittel zur Erhöhung der Zuverlässigkeit und Verfügbarkeit ermüdungsgefährdeter Produktionsanlagen der Stahlindustrie, VDI-Berichte Nr. 395 (1981) S. 33/44

2. Leitfaden für eine Betriebsfestigkeitsrechnung. Bericht der Arbeitsgemeinschaft Betriebsfestigkeit ABF 01, Düsseldorf 1977

3. Müller, U.: Beitrag zum Ermüdungsverhalten geschweißter Krantragwerke. Diss. TU Clausthal 1979

4. Gaßner, E., Griese, F.W. u. E. Haibach: Ertragbare Spannungen und Lebensdauer einer Schweißverbindung aus Stahl St 37 bei verschiedenen Formen des Beanspruchungskollektivs. Archiv Eisenhüttenwesen 35 (1964) H. 3, S. 255/67

5. Gurney, T.R.: Fatigue design rules for welded steel jonits. Welding Institut Research Bulletin May 1976

6. Haibach, E.: Schwingfestigkeitsverhalten von Schweißverbindungen. VDI-Berichte Nr. 268 (1976) S. 179/192

7. Granström, A.: The Fatigue Behavior Of Crane Girders. IIW Doc. XIII - 894 - 78